FACULTY OF SCIENCE
UNIVERSITY OF COPENHAGEN

Properties and Transport Characteristics of Majorana Fermions in Nanowires

by Filip Anselm Rasmussen

Thesis submitted for partial fulfillment of the requirements for the Degree of

Master of Science

at University of Copenhagen

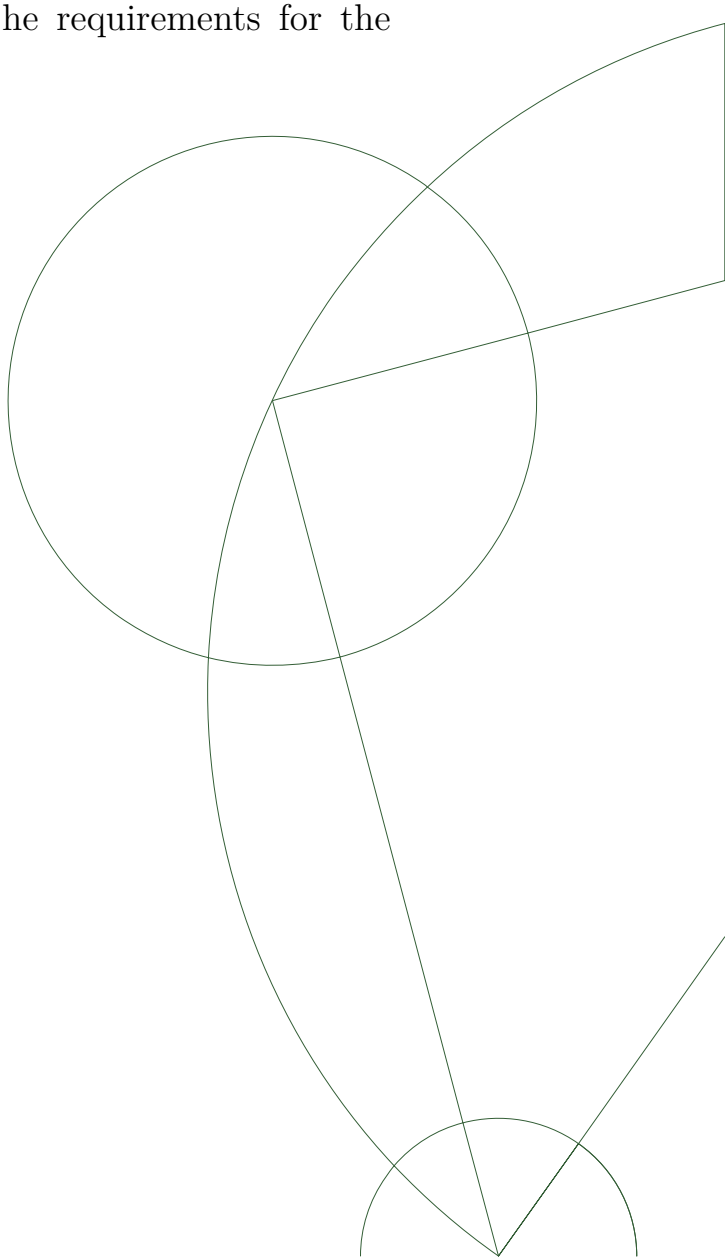

Academic Advisor: Prof. Karsten Flensberg
Niels Bohr Institute
University of Copenhagen
September 7, 2012

Abstract

Majorana fermions are quasiparticle excitations which are features of a two-dimensional quantum system in a so-called topological phase. Majorana fermions are non-Abelian anyons and the system therefore has a degenerate groundstate protected by a gap to the other excitations. It has been proposed that a system with Majorana fermions can be utilized for performing fault-tolerant quantum computations and their existence in solid state systems is thus of big general interest. In this thesis it is shown how Majorana fermions may be used to realize a quantum computer and how they can occur in solid state systems. Specifically we consider a system of a semiconducting nanowire with strong spin-orbit coupling in proximity to a conventional superconductor and show that this system should indeed have a so-called topological phase with Majorana fermions localized at each end of the wire. Properties such as spectrum, wavefunctions and gap size are investigated analytically as well as numerically. Lastly the tunnelling conductance characteristics of a wire with Majorana fermions are calculated and we find a robust zero-bias conductance peak as a characteristic feature.

Resumé

Majorana fermioner er kvasipartikelexcitationer, der er specielle træk ved todimensionelle kvantesystemer i en såkaldt topologisk fase. Majorana fermioner er ikke-Abelske anyoner og systemet har derfor en degenereret grundtilstand adskildt fra andre excitationer af et gap i spektret. Det er blevet foreslået at et system med Majorana fermioner can benyttes til at udføre fejlsikre kvanteberegninger og deres eksistens i faststofsystemer er derfor af stor interesse. I denne afhandling vises hvordan Majorana fermioner kan anvendes til at realisere en kvantecomputer og hvordan de kan opstå i faststofsystemer. Specifikt betragter vi et system bestående af en halvleder nanowire med kraftig spin-orbit kobling i umiddelbar nærhed til en konventionel superleder og viser at dette system rent faktisk har en topologisk fase med Majorana fermioner lokaliseret ved hver ende a nanowiren. Egenskaber såsom spektrum, bølgefunktioner og størrelsen af excitationsgappet undersøges analytisk såvel som numerisk. Til sidst beregnes tunnelleringskonduktansen for en nanowire med Majorana fermioner og vi finder at en top ved nul bias-spænding er en robust karakteristisk egenskab af Majorana fermioner.

Contents

Chapter 1

Quantum Computation

The research in the field of topologically protected non-abelian modes in condensed matter systems has become very active within the last couple of years. While the fundamental nature of topological states of matter is interesting in its own right, the observation that systems with non-Abelian topological order can be used to construct a quantum computer that is naturally immune to errors has focused much more attention on this field. To see how topological quantum computer can be realized and why it is considered "better" than other proposals, we will in this chapter first review the basics of normal quantum computing. Though the rest of this thesis will mainly not be concerned with quantum computation, there may be drawn references to specific aspects of this subject. Therefore I have chosen to include this section which will serve as a short overview of the main principles of quantum computation. Some parts of what is going to be described will not be completely necessary for understanding the main subject of this thesis but have however been included to give a coherent picture of quantum computation.

1.1 Classical Computation

The electronic computers that nowadays are present in everything from telephones to cars are all implementations of a *classical* binary digital computer. As the name implies this type of computer operates on information which can be represented by an array of binary digits, i.e. a number which can only take one of two values: 0 or 1. Formally a classical computer is a function f that takes an input register of n bits, each having the value either 0 or 1, and returns an output register of m bits, i.e.

$$f : \{0,1\}^n = \{0,1\}^m. \tag{1.1}$$

The value of the output register is uniquely determined by the value of the input and thus we say that the classical digital computer is a *deterministic computer* [35], since running the computer again and again with the same input always yield the same result. In an electronic computer the input and ouput registers consists of metallic leads and their binary value is represented by the voltage of the lead. The computation of the desired function f is implemented by an electronic circuit consisting of various electronic

components such as resistors, diodes and transistors, that connects the input leads with the output leads. With many input bits one can imagine that the wiring needed to implement the function correctly would be pretty complicated. However any function can in fact be decomposed into a series of elementary operations, called logic gates, acting on a small number of bits. One of these gates is the single bit NOT ($\neg$) gate that simply evaluates to the opposite value of the input bit, which in binary arithmetic (where x is a binary number) can be stated as

$$\text{NOT}: \quad \neg x = 1 - x. \tag{1.2}$$

Examples of two bit gates are the AND ($\wedge$), that evaluates to 1 if both inputs are 1 and 0 otherwise, and OR ($\vee$), that evaluates to 1 if just one (or both) of the input are 1 and 0 otherwise. In binary arithmetic these are written as

$$\text{AND}: \quad x \wedge y = x \cdot y \tag{1.3}$$

$$\text{OR}: \quad x \vee y = x + y - x \cdot y. \tag{1.4}$$

All of the mentioned gates possibly changes the values of the input bits, but in some calculations we might need to save the input values for some other part of the calculation later on. This can be acheived by copying the bit with the COPY gate that simply output two bits of the same value as the input. The COPY gate is however not always considered a logic gate, and instead one just assumed that it is always possible to copy a bit. With these gates on can construct a variety of different functions - in fact on can show than *any* function can be implemented by a series of these gates, thus we call this a *universal gate set*. However these gates are not unique and one can construct other gates like NAND, NOR, XOR, etc., and also find universal sets among these and from one universal set all other gates can be constructed. The exact combination of the gates that evaluates the function is called the circuit and it is often useful to visualize it by a diagram in witch the bits are represented by lines and the gates as various symbols with in- and outgoing connections. For example the AND-gate can be visualized as

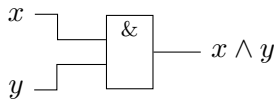

and a more complex function combining different gates is for example

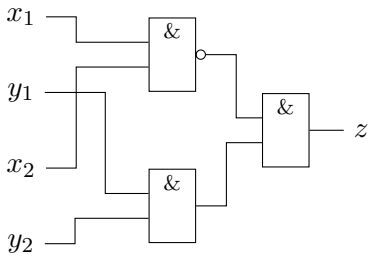

In this way it is possible to build all computational operation off a few elementary gates and vizualize it in simple diagrams as above.

1.2 Qubits and Quantum Parallelism

The basic principle of a quantum computer and what is essentially what seperates it from a classical computer is its use of quantum bits or qubits as inputs and output. In a classical computer the bit takes a value of either 0 or 1 for instance represensted by two different voltages as in an electronic computer. In a quantum computer however, the basic building block is the qubit, which can be represented by any physically realizable two-state system. For instance one might represent a qubit system by the ground state and an excited state of an atom, the two spin states of an electron or atom or two polarization directions of a photon. If we let $|0\rangle$ and $|1\rangle$ denote the two basis states of a single qubit system then the basic principles of quantum mechanics states that the actual state of the system can be in any superposition of these two states. Mathematically we define the two states $|0\rangle$ ad $|1\rangle$ as basis vectors (they need to be orthorgonal) in a 2-dimensional vector space, the Hilbert space, and the state $|\psi\rangle$ of the system can then be written as the vector

$$|\psi\rangle = \alpha|0\rangle + \beta|1\rangle, \tag{1.5}$$

where α and β are complex coefficients satisfying the normalization condition $|\alpha|^2+|\beta|^2 = 1$. Like the case for classical bits we can use a system of several qubits to represents binary strings, e.g. $|x\rangle = |01101\ldots101\rangle$. With a system of several qubits the system can be in any superposition of the multi-qubit basis states, also called the *computational basis*, given by

$$\{|0,0,\ldots,0\rangle, |1,0,\ldots,0\rangle, \ldots, |1,1,\ldots,1\rangle\}. \tag{1.6}$$

The state of an N qubit system can thus be represented as a normalized vector in the 2^N-dimensional Hilbert space, i.e. it can be expanded in the computational basis as

$$|\psi\rangle = \sum_{0}^{2^N-1} \alpha_x|x\rangle, \tag{1.7}$$

where x denotes the binary string corresponding to the given state. In the case of the classical computer we can only evaluate an input corresponding to *one* of the basis states a time. A quantum computer, however, can take any superposition of the basis states as an input, and in this way evaluate the function for several values at the same time. This is what is called *quantum parallelism* [9] and one of the reasons why quantum computers are believed to be able to perform certain tasks faster than classical computers. As already mentioned the classical computer is deterministic which always ensures the same outcome for a given input. A quantum computer on the other hand is probabilistic, meaning that a calculation based on some input x may result in any of all possible outcomes y_i, each with a certain probability $p_i(x)$. For instance if the result of a quantum computation is the single qubit state $|\psi\rangle$ given by Eq. (1.5) and measure in the basis $|0\rangle$ and $|1\rangle$ we get 0 with probability $|\alpha|^2$ and 1 with probability $|\beta|^2$. In fact it is the probabilities of the outcomes that encode the result of the computation.

1.3 Quantum Gates

So now we have introduced the quantum equivalent of the classical bit, the qubit, and we have seen hints of how we possibly can make use of the quantum feature of superposition to exploit massive quantum parallelism, but we still haven't seen how we actually do computations with the qubits. Actually we haven't really made clear exactly what is understood with a quantum computation, so let's do that now. If we consider an N-qubit system we can prepare it in som known initial state $|\psi_0\rangle$, e.g. $|00\ldots0\rangle$, then a quantum computation is some operation f that takes the initial state to some final state,

$$|\psi_0\rangle \xrightarrow{\text{quantum computation}} |f(\psi_0)\rangle, \tag{1.8}$$

which is then understood as the result. We can read out the result by performing measurements on the qubits that project them onto the $|0\rangle$ or $|1\rangle$ states and a given outcome will come with some probability. Thus in general a single measurement will typically not be enough to get the result with a certain accuracy and one then has to do the computation several times until the desired accuracy is reached.

However not any final state is possible, there are some natural constraints on what the operation f can do. First of all qubits cannot be added or removed from the system during the operation, so the Hilbert space is preserved. Secondly, the overall probability is preserved such that the final state is still normalized to one. These two constraints are only satisfied if f is a linear unitary operation, and it can therefore be represented by a unitary operator (or matrix) $\mathbf{U}_f$. Thus the result of the computation of the function f of the input state $|\psi_0\rangle$ is the state given by

$$|f(\psi_0)\rangle = \mathbf{U}_f|\psi_0\rangle. \tag{1.9}$$

Even though mathematically we are able to construct an infinite number of different unitary operators, the qubits follow the laws of nature and we therefore have to do some physical actions in orde to carry out a specific operation. In the Schrödinger picture the state of the qubit system evolves in time as if subject to a unitary transformation $U(t)$, which satisfies the Schrödinger equation

$$\frac{dU}{dt} = \frac{i}{\hbar}H(t), \tag{1.10}$$

where $H(t)$ is the Hamiltonian of the system. Thus by cleverly modifying the system and therefore the Hamiltonian we can effectively implement a specific unitary operator that carries out the desired computation.

For classical computers we can divide any computation into a series of one- or two-bit logic gates so we might look for equivalent *quantum gates*. For instance the quantum equivalent of the single bit NOT gate works as

$$a|0\rangle + b|1\rangle \xrightarrow{\text{NOT}} a|1\rangle + b|1\rangle, \tag{1.11}$$

where $|0\rangle$ and $|1\rangle$ simply has been exchanged. If we represent the state as the vector (a, b) then we see that the unitary matrix corresponding to the NOT gate is the Pauli matrix $\sigma_x = \left(\begin{smallmatrix} 0 & 1 \\ 1 & 0 \end{smallmatrix}\right)$,

$$\begin{pmatrix} a \\ b \end{pmatrix} \xrightarrow{\text{NOT}} \begin{pmatrix} 0 & 1 \\ 1 & 0 \end{pmatrix} \begin{pmatrix} a \\ b \end{pmatrix} = \begin{pmatrix} b \\ a \end{pmatrix}. \tag{1.12}$$

However, contrary to the case for classical computers this is not the only single qubit gate, for instance we may simply apply a phase factor $\mathrm{e}^{(}\mathrm{i}\theta)$ to the state, an operation which does not make sense for a classical bit. In fact the group of single qubit operators $U(2)$ is infinite, and while this certainly gives us some possibilities it can also give us some problems as we will see in the next section.

To generalize the tools from classical computation we also need quantum equivalents of the two-bit logic gates like NAND and XOR. NAND and XOR and any other useful two-bit gate takes two bits as input but only outputs a single bit and single bit of information is therefore lost in the process, making the gate *irreversible*, meaning that we cannot reconstruct the input bits from the output bit. Another way to say it is that the function it implements is not one-to-one but many-to-one and therefore cannot be inverted or reversed. Qubit operations, however, has to be unitary and since a unitary transformation is guaranteed to have an inverse, quantum computation is guarenteed to be *reversible*. In fact classical computation can also be made reversible [4, 35], typically by introducing an extra so-called *ancilla* bit that ends up storing the result of the gate. An example of a reversible gate is the reversible XOR gate given by

$$\text{XOR:} \quad (x, y) \Rightarrow (x, x \oplus y) \tag{1.13}$$

which can be visualized in circuit diagram as

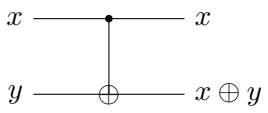

The reversible XOR gate flips the seconds bit if the first is 1 and does nothing otherwise and of this reason it is also called the controlled-NOT or CNOT gate, since the first bit controls whether a NOT operation should be carried out on the seconds bit or not. The cost of a reversible computer is that it needs more bits, the gain however, is that it in principle can run without any energy consumption, a feature the traditional irreversible computer does not have since the erasure of one bit of information inevitably requires a minimum work of $kT \ln 2$, as given by the famous Landauer's Principle [20].

The same way we constructed a quantum equivalent of the NOT gate we can find a qunatum equivalent of the CNOT gate. If we let $|\psi\rangle = a|00\rangle + b|01\rangle + c|10\rangle + d|11\rangle$ denote a general two-qubit state then we see that the CNOT gate acts on the state as

$$\text{CNOT:} \quad a|00\rangle + b|01\rangle + c|10\rangle + d|11\rangle \longrightarrow a|00\rangle + b|01\rangle + d|10\rangle + c|11\rangle. \tag{1.14}$$

Representing the state by the vector (a, b, c, d) we note that this is equivalently stated as

$$\text{CNOT} : \begin{pmatrix} a \\ b \\ c \\ d \end{pmatrix} \Rightarrow \mathbf{U}_{\text{CNOT}} \begin{pmatrix} a \\ b \\ c \\ d \end{pmatrix} = \begin{pmatrix} a \\ b \\ d \\ c \end{pmatrix} \tag{1.15}$$

where the transformation matrix is given by

$$\mathbf{U}_{\text{CNOT}} = \begin{pmatrix} 1 & 0 & 0 & 0 \\ 0 & 1 & 0 & 0 \\ 0 & 0 & 0 & 1 \\ 0 & 0 & 1 & 0 \end{pmatrix}. \tag{1.16}$$

There are only a finite number of n-bit reversible classical gates and one can find quantum equivalents to all of them, but this is however not all quantum gates, since these span the continuum of the unitary operators of $U(2^n)$. But as for classical computers we do not need all of them to perform a general computation, with a limited *universal set of quantum gates* one can construct any unitary transformation.

1.4 Errors and Error Correction

In theory both the classical and quantum computer would function fine as described above, but unfortunately the real world does not always behave as well as we want and both classical and quantum computers can suffer from computational errors. In a classical electronic computer electronic noise in the circuit could "flip" a bit or make it unreadable. To avoid this kind of problem one could simply increase the voltage between the two bit values so that it is much bigger than the typical fluctuations. However this might not be wanted because it could lead to a bigger power consumption which again leads to heating and then perhaps more errors. Instead one can use an *error correction code* that via some method correct the typical errors. The simplest way to do this is to store each bit of information in a redundant way, so that we do not rely on a single physical bit. We might for instance encode each logical bit in three physical bits:

$$0 \to (000), \quad 1 \to (111) \tag{1.17}$$

Then if an error occurs that flips e.g. the third bit so that

$$(000) \to (001), \quad (111) \to (110), \tag{1.18}$$

then to correct the error we can just set the value of all the physical bits to that of the majority. In the case of a three-bit encoding this works if only one bit flips at a time - if two bits flip the correction code fails to correct the error. We can improve this method to any desired reliability by just encoding the logical bit in enough physical bits. In practice this works quite well as we all know, since our everyday computers seem pretty reliable.

In quantum computers the thread from errors is more serious. First of all the typical physical realizations of qubit systems we can think of tend to be of very small size and the treshhold between the two qubit states can be hard to control so that natural fluctuations might be a bigger problem. Secondly, the errors may be more subtle, since the information is stored in the superposition of basis states of the qubit.

Errors in quantum system occur because we cannot construct a truly isolated qubit system. It is therefore inevitable that the environment will interact with the qubit in some way that we may not be able to determine and therefore may cause some of the information stored in the qubit system to be lost - a process called *decoherence*. To see how this happen we let $|\psi\rangle = a|0\rangle + b|1\rangle$ be the state of the qubit and consider the environment as some auxillary system which initially is in the state $|\mathrm{e_i}\rangle$. Then the total system $|\psi\rangle|\mathrm{e_i}\rangle$ evolves in time under some unitary transformation given by the total Hamiltonian $\mathcal{H}$ such that

$$(a|0\rangle + b|1\rangle)|e_\mathrm{i}\rangle \longrightarrow a(u_{00}|0\rangle|\mathrm{e}_{00}\rangle + u_{01}|1\rangle\mathrm{e}_{01}) + b(u_{10}|1\rangle|\mathrm{e}_{10}\rangle + u_{11}|1\rangle|\mathrm{e}_{11}\rangle), \tag{1.19}$$

where u_{ij} is the matrix elements of the transformation and $|\mathrm{e}_{ij}\rangle$ denotes different states of the environment. From Eq. (1.19) it is clear that the resulting state of the qubit is entangled with the environment an thus we can no longer write it as pure superposition of its basis states but it is said to be in a mixed state. The effect of this is that when we measure the state of the qubit by projecting it onto its basis it seems like random transformations has been applied. We note that Eq. (1.19) may be written in the form

$$|\mathrm{e_i}\rangle \longrightarrow (|\mathrm{e}_I\rangle I + |\mathrm{e}_X\rangle)X + |\mathrm{e}_Y\rangle Y + |\mathrm{e}_Z\rangle Z)|\psi\rangle, \tag{1.20}$$

where $|\mathrm{e}_I\rangle = u_{00}|\mathrm{e}_{00}\rangle + u_{10}|\mathrm{e}_{10}\rangle$, $|\mathrm{e}_X\rangle = u_{01}|\mathrm{e}_{01}\rangle + u_{11}|\mathrm{e}_{11}\rangle$ and so on. I, X, Y, Z are operators acting on the qubit states, where I is the identity and X, Y and $Z = XY$ correspond to three types of errors that can occur to the qubit. The errors are *bit flip* errors (X), *phase* errors (Y) and both ($Z = XY$). Besides errors that occur due to the environment even when we do nothing there is also the possibility that during operation we ourself may introduce errors due to insufficient control over the gates. These types of errors are called *unitary errors*. The different types of errors are summarized below:

1. **Bit flip errors.** In analogy with the classical case we can imagine an event that flips the value of the qubit. If we consider a single qubit in a general state spanned by the basis $|0\rangle$ and $|1\rangle$ then the bit-flip errors acts as

   $$a|0\rangle + b|1\rangle \longrightarrow a|1\rangle + b|0\rangle, \tag{1.21}$$

   such that in essence the coefficients of the linear superposition swaps, $a \leftrightarrow b$. The effect of a bit-flip error is immediately clear since it destroys information just as in the classical case.

2. **Phase errors.** An error which is perhaps more subtle is if the two basis states $|0\rangle$ and $|1\rangle$ acquires a random (or at least unknown) relative phase, such that

   $$a|0\rangle + b|1\rangle \longrightarrow a|0\rangle + be^{i\theta}|1\rangle. \tag{1.22}$$

A phase error may cause operations that utilizes superpositions and interference to fail.

3. **Unitary errors.** As already noted, the qubit states are continuous and the same is true for the operations that we can do on them, since these are represensted by unitary transformations, which might not be implemented exactly. For instance we may want to apply the unitary transformation U, but in reality we apply the transformation given by
$$\tilde{U} = U(1 + \mathcal{O}(\epsilon)), \tag{1.23}$$
where $\mathcal{O}(\epsilon)$ is some other transformation of order ϵ. After many consecutive operations the small errors can accumulate and lead to a totally different result.

In the classical case we could protect the system from error by storing the information in a redundant way by simply making several physical copies of the logical bit. The same procedure is not possible for qubits since the *no cloning theorem* states that the state of a quantum system cannot be copied and reproduced in another system. For a classical bit we can just read its value and create a new bit with the same value, however, when we measure the state of a qubit we interfere with the system and project it onto one of the eigenstates of the measurement operator and the information stored in the superposition is lost. This fact was first thought to make the realization of a quantum computer practically impossible, but is has since been shown that one can in fact construct *quantum error correction codes* that allow for reverting all the possible errors [38, 34]. While this has certainly increased the optimism for the possibility of creating a working quantum computer, for the error correction codes to work, the rate of errors has to be below some finite treshhold which for typical proposed quantum computer systems seems hard to reach at the current stage.

Chapter 2

Topological quantum computation with non-abelian anyons

2.1 Abelian and non-Abelian anyons

In the quantum theory elementary particles are all treated as identical and the particle types can be classified as either Bosons or Fermions according to the behavior of their collective wavefunction under the interchange of two such particles. When interchanging two bosons their wavefunction will be exactly the same as before the interchange operation, while for fermions the wavefunction will acquire a minus or equivalently a phase of π. This results in the different statistics of the two types of particles, namely that no two fermions can exist in the same state while no such limitation exists for bosons. Mathematically this can formulated by requiring that the annihilation and creation operators for bosons, a_μ, $a_\mu^\dagger$, satisfy the canonical commutation relations

$$[a_\mu, a_\nu^\dagger] = \delta_{\mu\nu}, \quad [a_\mu, a_\nu] = 0 \tag{2.1}$$

and the annihilation and creation operators for fermions, c_μ, $c_\mu^\dagger$, satisfy the canonical *anti*-commutation relations

$$\{c_\mu, c_\nu^\dagger\} = \delta_{\mu\nu}, \quad \{c_\mu, c_\nu\} = 0. \tag{2.2}$$

This makes is easier to make sure the particle statistics is satisfied when dealing with many particles.

The reason why only two transformations of the wavefunction are possible can be seen from the fact that the operation that exchanges two particles can also be viewed as a process where one particle is taken adiabatically around the other, a so-called braid. In three dimensions the operation of taking the particle all the way around the other and coming back to its initial position is then equivalent to a situation where the particles do not move at all. To see this we can imagine tying string to the two particles as seen in Fig. 2.1 and then adiabatically move them around such that one particle is taken all the way around the other and back to its initial position. We see that the string

can always be routed such that they do not form any knots or twists and the final state can thus always be made identical to the initial state. Thus exchanging the particles do not change the physical state of the system, and after one exchange only possible transformations of the wavefunction is a multiplication of a factor of either $+1$ or -1.

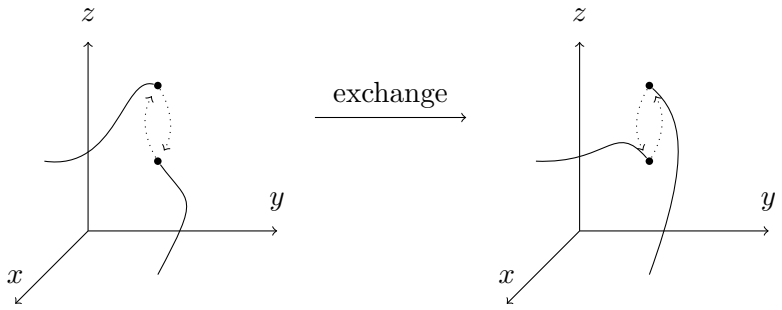

Figure 2.1: The effect of the exchange of indistinguisbale particles in three dimensions. By attaching virtual string to the particles one can keep track of the system during a physical exchange operation.

The physics of particles in a two dimensional world is however less restrictive on this point and allow for other particle statistics. To see this consider again particle with string image in Fig. 2.1 and imagine the particles to live in a two-dimensional world. When moving one particle all the way around the other it will at some point need to cross the string of the other particle and thus we cannot say that the wavefunction of the final state in general is equal to that of the inital state, since the two states may have different topology [31]. This has profound consequences for the statistics of particles in two dimensions, for instance if $\psi(\mathbf{r}_1, \mathbf{r}_2)$ is the wavefunction of two identical particles in two dimension, then if one particle is moved around the other, equivalent to two exchange operations, the wavefunction may aquire an arbitrary phase

$$\psi(\mathbf{r}_1, \mathbf{r}_2) \longrightarrow \mathrm{e}^{2\mathrm{i}\theta}\psi(\mathbf{r}_1, \mathbf{r}_2), \tag{2.3}$$

contrary to the case in three dimensions where the wavefunction has to return to itself. This also means that under a single exchange the wave function acquires a phase θ, i.e.

$$\psi(\mathbf{r}_1, \mathbf{r}_2) \longrightarrow \mathrm{e}^{\mathrm{i}\theta}\psi(\mathbf{r_1}, \mathbf{r}_2), \tag{2.4}$$

which for bosons and fermions naturally is 0 or π respectively. Particles that do not have exchange phases of 0 or π are called *anyons*, a term coined by Frack Wilczek who was one of the first to study such particles [44, 45]. In systens with more particles one can also have particles of different kinds or species and one can construct a group of so-called *braiding* operations that act on the wavefunction when two particles are interchanged. If all braiding operations commute, i.e. the order of the operation do not matter, which is the case if each brading operation satisfies the relation (2.4), the braid group is Abelian and we say that the particles are *Abelian anyons*.

As already noted, the relation (2.4) is just a certain example of the result of an exchange operation, in general the exchange may not only change the phase of the wavefunction but change the wavefunction itself, i.e. exchanging two particles takes the system to another state. Since the exchange operation should in theory be possible to carry out adiabatically this can only be possible id the states have the same energy. If there are g degenerate states with N particles we can define the orthonormal basisvector by ψ_α with $\alpha = 1, 2, \ldots, g$. The exchange of two particles, say 1 and 2, can then be expressed as

$$\psi_\alpha = [U(1 \leftrightarrow 2)]_{\alpha\beta}\psi_\beta, \tag{2.5}$$

where $U(1 \leftrightarrow 2)$ is a $g \times g$ unitary matrix corresponding to the unitary transformation of exchanging the two particles. If two such operations do not commute, ie.

$$U(1 \leftrightarrow 2)U(2 \leftrightarrow 3) \neq U(2 \leftrightarrow 3)U(1 \leftrightarrow 2), \tag{2.6}$$

the braid group consisting of all the exchange operation is non-Abelian and we say that the particles are *non-Abelian anyons*.

2.2 Anyons as topological features

Anyons are not normally seen in in nature, which is due to the fact that our world is naturally three-dimensional and so the basic particles has to obey bosonic or fermionic statistics. We may however construct a system that confines electrons or other elementary particles to move in an effectively two-dimensional space, and it turns out that such systems under certain circumstances can have localized excitations above the ground state whose corresponding *quasiparticles* obey anyonic statistics. If a system has anyonic quasiparticles it is in a *topological phase*, which is defined as a state in which all *local* correlation functions of observables vanish [31]. In essence this means that the state of the system is encoded in a nonlocal manner, namely in how the quasiparticles are located among each other, so that the state of the system is determined by its topology. Normal phases of matter can generally be described by the breaking of a symmetry and introduction of an order parameter, but a topological phase cannot be described by an order parameter, but is said to have to have topological order, characterised by the existince of robust degenerate ground state [43].

Since the underlying system consists of fermions the degenerate ground states correspond to different fermionic excitations. In the simplest case the system has two-fold degenerate groundstate, which however should still be able to realize all the different types of anyonic particles that the system support. A system with multiple degenerate ground state can be envisioned by introducing more topological defects and thus anyonic quasiparticles. When bringing defects and thus quasiparticles close together so that their wavefunctions overlap, the quasiparticles may *fuse* together to create a new quasiparticle with the combined quantum numbers.Due to the overlap of the quasiparticle wavefunctions the ground state degeneracy will split and this will allow us to determine which of the states the system is in.

There is no general scheme to find systems that can realize a topological phase, one merely discovers them experimentally or find them theoretically by some clever guesses but there are however some requirements and some distinctive features. A topological phase is in general characterized by having anyonic excitations. In order for the system to have a finite number of anyonic particles and thus a finite set of degenerate ground states, the non-anyonic quasiparticle states must be separated from the degenerate ground state by an energy gap. It doesn't matter how big the energy gap is, as long as it does not vanish even for a system of infinite size. The gap is necessary but not sufficient to guarentee the existence of anyons, because the system needs to have some features in its topology, such as a local potential, impurity or interface, where the gap locally vanishes such the anyons may form.

The fractional quantum hall effect where the conductance of special two-dimensional electron systems is found to be fractions of the standard electron conductance quantum $\frac{e^2}{h}$ was explained by the existence of abelian anyons with excange phase $\frac{\pi}{q}$, i.e. a fraction of that of normal fermions [3]. It was later showed that the fractional quantum hall system could possibly also be in a state with non-Abelian anyons [29] but even today no conclusive experimental data has proven this, and thus non-Abelian anyons are still to be observed.

2.3 Fault tolerant quantum computation using non-Abelian anyons

We have previously discussed that one of the biggest problems in constructing a usable quantum computer is its susceptibility to errors such as qubit decoherence and errors in the qubit operations. While errors can be overcome by good error correction codes these require us to increase the number of qubits and operations done making the computer bigger and slower and it is therefore desirable to minimize the rate of errors in the first place by cleverly constructing the qubit systems. In fact one can use a system with non-Abelian anyons as a quantum computer which, in theory, is completely immune to errors [18]. The scheme is to use the degenerate ground states corresponding to the locations of a fixed number of quasiparticles in the topological phase as the computational basis. Computational operations are then carried out by braiding the quasiparticles taking the system from one state to another. Since all other excitations are separated from the ground states by a finite energy gap for low temperatures the system is constrained to evolve within the space of degenerate ground states. Furthermore essentially all non-trivial unitary transformations within this space can only happen by performing a braid operation of the quasiparticles, and these depend only on the topology of the braid and not on the time or path taken [31]. This last property is a strong one, since it essentially states that no local pertubation or interaction can accidentally change the state of the system within the groundstate manifold and thereby introduce qubit errors. The reason is that the groundstates are nonlocal and a local transformation will therfore not have any non-vanishing matrix elements within these states. To show how to construct a quantum computer using non-Abelian anyons we now list the requirements and how

these can be fulfilled.

- **Qubits:** The qubit states correspond to two states among the degenerate ground-state manifold. By combining non-Abelian quasiparticles which are widely separated in space one can form a normal fermionic mode that represents the state of the qubit. The nonlocal nature of the state and means that the qubit value is well-protected against decoherence.
- **Initialization** Initialization of the qubit can be done by bringing the quasiparticles corresponding to the qubit together such that its states will acquire a finite energy splitting and one can perform a local operation that brings it into the desired state. Thereafter one can quickly move the quasiparticles away from each other and the qubit will again be topologically protected.
- **Gates** The computational gates are unitary transformations performed by braiding different quasiparticles, which will rotate the system within its ground state manifold. The transformations are uniquely determined by the topology and order of the braids and unitary errors will therefore not happen. However, far from all non-Abelian anyons have a set of braiding operations that can be used to construct a universal gate set. The missing operations may be performed by traditional unprotected gates, which together with error correction codes may still lead to a feasible quantum computer.
- **Readout** The readout of the qubit state may be done as the inverse of the initialization scheme, where the quasiparticles corresponding to the qubit are brought together to give an energy splitting between the qubit states, which may be measured by some experiment. The state my also be inferred from an interferometer-like experiment [31].

Wee see that the combination of fault tolerant qubits from non-Abelian anyons with state of the art micro- and nano-fabrication techniques could pave the way for powerful quantum computers.

2.4 Majorana Fermions

In the beginning of the development of relativistic quantum field theory the Italian physicist Ettore Majorana found that a neutral spin-$\frac{1}{2}$ in the form of a real scalar field satisfies the real part of the relativistic Dirac equation [27]. Such a particle has the property that it is its own antiparticle and it has since been proposed that the neutrinos are in fact Majorana Fermions, a claim that has yet to be verified [46]. Besides their occurance in elementary particle physics, it has been found that Majorana fermions may also emerge as non-Abelian quasiparticles in certain two-dimensional solid state systems. To see how this comes about we first note that if we let γ denote the annihilation operator corresponding to a Majorana fermion, the property that it is its own antiparticle can be stated as

$$\gamma^\dagger = \gamma. \tag{2.7}$$

Acting with this operator twice is in a sence the same as creating a Majorana fermion and destroying it leaving the system unchanged, and we therefore see that we have $\gamma^2 = 1$. Since Majorana fermions are spin-$\frac{1}{2}$ particles they obey an anticommutation relation, which due to the fact that $\gamma^2 = 1$ takes the unusual form

$$\{\gamma_i, \gamma_j\} = 2\delta_{ij}, \tag{2.8}$$

where γ_i and γ_j can correspond to different Majorana fermions. Since the underlying system consists of normal electrons, the Majorana operator may be written as an expansion of the electron creation and annihilation operators. In fact we note that with the properties above, we may use two different Majorana fermion operators γ_A and γ_B to construct an arbitrary normal fermionic operator

$$f = \frac{1}{2}(\gamma_\mathrm{A} + \mathrm{i}\gamma_\mathrm{B}), \quad f^\dagger = \frac{1}{2}(\gamma_\mathrm{A} + \mathrm{i}\gamma_\mathrm{B}), \quad \{f, f^\dagger\} = 1, \quad \{f, f\} = 0. \tag{2.9}$$

From this we see that Majorana fermions can be considered as the real and imaginary parts of a real fermion. Writing the Majorana operators in terms of the fermion opearot we have

$$\gamma_\mathrm{A} = f + f^\dagger, \quad \gamma_\mathrm{B} = f - f^\dagger, \tag{2.10}$$

from which we see that they can also be thought of as a linear combination of a particle and its antiparticle or hole, and this hints us to look for them in superconducting systems.

In conventional superconductors the excitations are separated from the superconducting groundstate by an energy gap and their quasiparticle operators take the form $\alpha = uc_\uparrow + vc_\downarrow^\dagger$, where c_σ is the annihilation operator for an electron with spin σ and u and v are in general complex coefficients. We see that this is in fact very close to be a Majorana fermion since $\alpha^\dagger$ has the same structure if $u = v$. However, the operator contains a mix of spin and can therefore not be a Majorana fermion. Instead we may consider superconductors with triplet pairing symmetry which will have quasiparticle excitations that are superpositions of electrons with the same spin. The excitations of a bulk superconductor form a continuum and are separated from the groundstate by an energy gap and are furthermore more or less delocalized over the entire superconductor so we cannot speak of a finite set of generate ground states corresponding to a number of localized quasiparticles that can be interchanged. As discussed in Sec. 2.2 we need to "puncture" the gap locally by introducing some potential or impurity in the system such that localized Majorana fermions will form at these locations and the groundstate will become degenerate, and it has actually been shown that superconductors with p and $p_x + \mathrm{i}p_y$-symmetry can have Majorana fermions in the center of vortices [36, 16, 19] and it has also been shown that an effective 2D p-wave superconductor with Majorana fermions may form at the interface between a normal bulk s-wave superconductor and a topological insulator [11].

2.4.1 Non-Abelian statistics of Majorana Fermions

The Hermitean nature of Majorana fermion operators is not enough to guarentee that they will obey non-Abelian statistics. As we saw in Eq. (2.10) we can imagine any

fermionic excitation, even one corresponding to a non-topological state, as a superposition of two Majorana fermions and these may not exhibit any non-Abelian characteristics. The non-Abelian statistics has to be calculated by considering an actual system which has Majorana fermions in its topological phase. To obtain the braiding statistics one would normally have to study the full evolution of the system and its Berry phase under the adiabatic interchange of two quasiparticles. However, in the case of $p + ip$ superconductors the braiding statistics of Majorana fermions bound to vortex cores can be obtained in a much simpler and more intuitive way [36, 16] which we are briefly going to sketch here.

It has long been known that superconductors can have vortices that encircles a single flux quantum and thus the phase of the superconducting order paramater must change by 2π when going around the vortex core, i.e. for a single vortex we may write it as $\Delta(\mathbf{r}) = |\Delta(r)|\mathrm{e}^{\mathrm{i}(\theta+\phi)}$, where r and θ are the polar coordinates and we have assumed azimuthal symmetry for simplicity. It has later been shown that $p+ip$ superconductors can have unusual vortices with only half a flux quantum. In the low energy regime the system near the vortex core can essentially be described by spinless electrons and it turns out that it has zero energy solution localized at the vortex core that happens to be a Majorana fermion. The quasiparticle operator for this solution takes the form [41]

$$\gamma = \frac{1}{\sqrt{2}} \int d\mathbf{r} \left[F(\mathbf{r})\mathrm{e}^{-\frac{\mathrm{i}}{2}\phi}\Psi(\mathbf{r}) + F^*(\mathbf{r})\mathrm{e}^{\frac{\mathrm{i}}{2}\phi}\Psi^\dagger(\mathbf{r}) \right], \tag{2.11}$$

where $F(\mathbf{r})$ is an envelope function that falls off exponentially with the distance to the vortex core, $\Psi(\mathbf{r})$ is the annihilation operator for the effectively spinless electrons and ϕ is the phase of the superconducting order parameter. We note that if the phase of the order parameter changes by 2π the quasiparticle acquires and overall π phase, $\gamma \to -\gamma$. If we consider a system of N vortices the superconducting order parameter has to rotate by 2π around each vortex and thus it cannot be single valued everywhere, but we have to introduce branch cuts. Considering two vortices at positions $\mathbf{R}_i$ and $\mathbf{R}_j$ and their corresponding Majorana fermions, γ_i and γ_j, we can write the order parameter near the i'th vortex as $\Delta(\mathbf{r}) = |\Delta(\mathbf{r})| \exp(\mathrm{i}\theta_i + \mathrm{i}\phi_i))$, where $\theta_i = \arg(\mathbf{r} - \mathbf{R}_i)$ and $\phi_i = \arg(\mathbf{R}_j - \mathbf{R}_i)$. Braiding the vortices, i.e. taking vortex j all around vortex i and back again, is the same as letting the vector $\mathbf{R}_j - \mathbf{R}_i$ rotate by 2π and we thus see that this operation takes $\gamma_i \to -\gamma_i$.

If we fix the initial positions of the vortices we can construct the braid operation of any two vortices by sequentially interchanging neighboring vortices. Thus we can construct all elements of the braid group by a product of the elementary interchange operation that exchanges γ_i with γ_{i+1}. From the discussion above we see that one of the involved Majorana fermions will always cross a branch cut in the order parameter and thereby acquire a minus. If we choose to align all branch cuts in the same direction we see that the action of an interchange can be stated as

$$T_i : \begin{cases} \gamma_i \to \gamma_{i+1} & \\ \gamma_{i+1} \to -\gamma_i & \\ \gamma_j \to \gamma_j & \text{for } j \neq i \text{ and } j \neq i+1 \end{cases} . \tag{2.12}$$

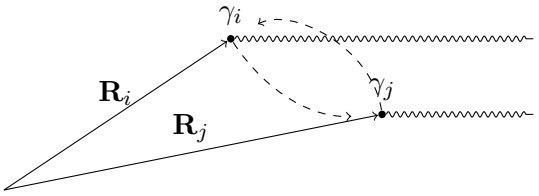

Figure 2.2: Interchange of to Majorana fermions, γ_i and γ_j, bound to vortex cores situated at $\mathbf{R}_i$ and $\mathbf{R}_j$. The phase of order parameter of the superconductor changes with 2π upon going around a vortex and order parameter will therefore have branch cutes, here shown with wiggled lines. When the two Majorana fermions are exchanged, one of them has to cross a branch point.

The interchange action (2.12) can also be written in terms of fermionic operators acting on the Hilbert space which is convenient when we want to see how the operation affects the state of the system. If we by $\tau(T_i)$ denote the fermionic operator corresponding to the interchange T_i such that

$$T(\gamma_j) = \tau(T_i)\gamma_j[\tau(T_i)]^{-1}, \tag{2.13}$$

then in terms of the Majorana operators it takes the form

$$\tau(T_i) = \exp\left(\frac{\pi}{4}\gamma_{i+1}\gamma_i\right) = \frac{1}{\sqrt{2}}(1 + \gamma_{i+1}\gamma_i), \tag{2.14}$$

which can easily be verified by insertion into Eq. (2.13). To truly reveal the non-Abelian nature of the Majorana fermions we now consider the effect of braiding in two simple systems containing two and four Majoranas, respectively.

As we noted in Eq. (2.10) we may combine two Majarana fermions into a regular fermion. In the case of a system with only two Majoranas, γ_1 and γ_2, there is only one way to do this, namely $f = \frac{1}{2}(\gamma_1 + \mathrm{i}\gamma_2)$, $f^\dagger = \frac{1}{2}(\gamma_1 - \mathrm{i}\gamma_2)$. The ground state is doubly degenerate corresponding to the occupation of the fermion level which can be measured by the operator $n = f^\dagger f = \frac{1}{2}(1 + \mathrm{i}\gamma_1\gamma_2)$. The operator corresponding to the interchange of the two Majoranas is given by

$$\tau(T) = \exp\left(\frac{\pi}{4}\gamma_2\gamma_1\right) = \exp\left(\mathrm{i}\frac{\pi}{4}[2f^\dagger f - 1]\right) = \exp\left(\mathrm{i}\frac{\pi}{4}\sigma_z\right), \tag{2.15}$$

where σ_z is a Pauli matrix acting on the basis $\{|0\rangle, |1\rangle = f^\dagger|0\rangle\}$ represented by the vectors $(1, 0)$ and $(0, 1)$ respectively. The effect of the interchange is

$$|0\rangle \to |0\rangle, \qquad |1\rangle \to -|1\rangle \tag{2.16}$$

and does therefore not change the state of the system. The reason for this is clear: the two ground states differ by a fermion and even though we consider superconducting systems where fermion number is not conserved, the fermion parity, i.e. fermion number modulus two, is conserved, and there is thus no way to remove or add a single fermion to the system.

If we consider a system with four Majorana fermions we can combine them into two regular fermions, $f_1 = \frac{1}{2}(\gamma_1 + \mathrm{i}\gamma_2)$ and $f_2 = \frac{1}{2}(\gamma_3 + \mathrm{i}\gamma_4)$. The ground state now has four degenerate states corresponding to the occupations of the two fermions. The interchange operators written in the basis $\{|0\rangle, f_1^\dagger|0\rangle, f_2^\dagger|0\rangle, f_2^\dagger f_1^\dagger|0\rangle\}$ are

$$\begin{aligned}
\tau(T_1) = \exp\left(\mathrm{i}\frac{\pi}{4}\gamma_2\gamma_1\right) &= \begin{pmatrix} \mathrm{e}^{-\mathrm{i}\pi/4} & & & \\ & \mathrm{e}^{\mathrm{i}\pi/4} & & \\ & & \mathrm{e}^{-\mathrm{i}\pi/4} & \\ & & & \mathrm{e}^{\mathrm{i}\pi/4} \end{pmatrix}, \\
\tau(T_3) = \exp\left(\mathrm{i}\frac{\pi}{4}\gamma_4\gamma_3\right) &= \begin{pmatrix} \mathrm{e}^{-\mathrm{i}\pi/4} & & & \\ & \mathrm{e}^{-\mathrm{i}\pi/4} & & \\ & & \mathrm{e}^{\mathrm{i}\pi/4} & \\ & & & \mathrm{e}^{\mathrm{i}\pi/4} \end{pmatrix}, \\
\tau(T_2) = \exp\left(\mathrm{i}\frac{\pi}{4}\gamma_2\gamma_1\right) &= \frac{1}{\sqrt{2}}\begin{pmatrix} 1 & 0 & 0 & -\mathrm{i} \\ 0 & 1 & -\mathrm{i} & 0 \\ 0 & -\mathrm{i} & 1 & 0 \\ -\mathrm{i} & 0 & 0 & 1 \end{pmatrix}
\end{aligned} \tag{2.17}$$

We see that interchanging the Majorana fermions corresponding to a single regular fermion merely add a phase to the state. On the other hand an interchange of two Majorana fermions belonging to the different fermions correspind to a rotation within the Hilbert space. For instance we have $\tau(T_2)|00\rangle = \frac{1}{\sqrt{2}}(|00\rangle - \mathrm{i}|11\rangle)$ and $\tau(T_2)|10\rangle = \frac{1}{\sqrt{2}}(|10\rangle - \mathrm{i}|01\rangle)$ from which we again observe that the fermion parity is conserved. We have thus proved that Majorana fermions in half-quantum vortex cores are non-Abelian anyons and furthermore characterised their braiding statistics.

2.5 The Kitaev chain

In last section we briefly mentioned that localized Majorana fermionic modes can appear at vortex cores of 2D p or $p_x + \mathrm{i}p_y$ superconductors or a similar effective system created by a normal superconductor and a topological insulator. However, topological insulators as well as p-wave superconductors are still quite exotic materials and if one wishes to show the anyonic feature of the Majoranas one would have to physically move the vortices around on the surface which seems like a hard task to do experimentally. In this section we are going to introduce a much simpler system first studied in this context by Kitaev in 2001 [17], which seems to avoid all the trouble of the 2D topological superconductors and in fact should be realizable with the current technology. The system of interest is that of a chain of *spinless* fermions with p-wave superconductivity, which is the only form of superconductivity realizable for spinless particles. If we let the chain consist of N spinless fermionic sites, the tight-binding Hamiltonian takes the form

$$H = \sum_{j=1}^{N}\left[-t\left(c_j^\dagger c_{j+1} + c_{j+1}^\dagger c_j\right) - \mu(c_j^\dagger c_j - \frac{1}{2}) + \Delta c_j c_{j+1} + \Delta^* c_{j+1}^\dagger c_j^\dagger\right], \tag{2.18}$$

where c_j annihilates an electron at site j, t is the hopping parameter (we will typically have $t = \frac{\hbar^2}{2ma^2}$) and μ is the chemical potential measured from the ground state energy and $\Delta = |\Delta|e^{i\theta}$ is the superconducting order parameter. We will now arbitrarily define two Majorana fermion operators for each site,

$$\gamma_{Aj} = e^{i\theta/2}c_j + e^{-i\theta/2}c_j^\dagger \tag{2.19a}$$

$$\gamma_{Bj} = -i\left(e^{i\theta/2}c_j - e^{-i\theta/2}c_j^\dagger\right) \tag{2.19b}$$

where we have included the phase of the SC order parameter in the definition, however for purely real order parameters we just have $\gamma_{Aj} = c_j + c_j^\dagger$ and $\gamma_{Bj} = i(c_j^\dagger - c_j)$. It is easy to see that these in fact do satisfy the Majorana condition $\gamma^\dagger = \gamma$ as well as the anticommutation relations $\{\gamma_{Ai}, \gamma_{Aj}\} = \{\gamma_{Bi}, \gamma_{Bj}\} = 2\delta_{ij}$ and $\{\gamma_{Ai}, \gamma_{Bj}\} = 0$. In terms of these operators the ordinary fermion operators can be expressed as

$$c_j = \frac{1}{2}e^{-i\theta/2}\left(\gamma_{Aj} + i\gamma_{Bj}\right) \tag{2.20a}$$

$$c_j^\dagger = \frac{1}{2}e^{i\theta/2}\left(\gamma_{Aj} - i\gamma_{Bj}\right), \tag{2.20b}$$

which lets us rewrite the Hamiltonian in Majorana-basis as

$$H = \frac{i}{2}\sum_{j=1}^{N}\left[-\mu\gamma_{Aj}\gamma_{Bj} + (-t+\Delta)\gamma_{Aj}\gamma_{Bj+1} + (t+\Delta)\gamma_{Bj}\gamma_{Aj+1}\right]. \tag{2.21}$$

The easiest way to see that this Hamiltonian leads to localized Majorana modes is to first consider to special cases.

(a) The first case is the trivial one with no superconductivity, $|\Delta| = 0$, and a vanishing hopping parameter $t = 0$. The Hamiltonian is then reduced to

$$H = -\mu\sum_j\left(c_j^\dagger c_j - \frac{1}{2}\right) = -i\frac{\mu}{2}\sum_j\gamma_{Aj}\gamma_{Bj}, \tag{2.22}$$

which we can interpret as a pairing (if $\mu < 0$) between Majorana A and B at the same site, see Fig. 2.3a. The ground state of the system is the normal superconducting ground state.

(b) The second case is the special situation where $t = |\Delta| > 0$ and $\mu = 0$ in which case the Hamiltonian in Majorana basis is

$$H = iw\sum_j\gamma_{Bj}\gamma_{Aj+1}. \tag{2.23}$$

This corresponds to a pairing between Majoranas at adjacent sites as illustrated in Fig 2.3b. We now define new fermionic annihilation and creations operators,

$$\tilde{c}_j = \frac{1}{2}(\gamma_{Bj} + i\gamma_{Aj+1}), \tilde{c}_j^\dagger = \frac{1}{2}(\gamma_{Bj} - i\gamma_{Aj+1}), \tag{2.24}$$

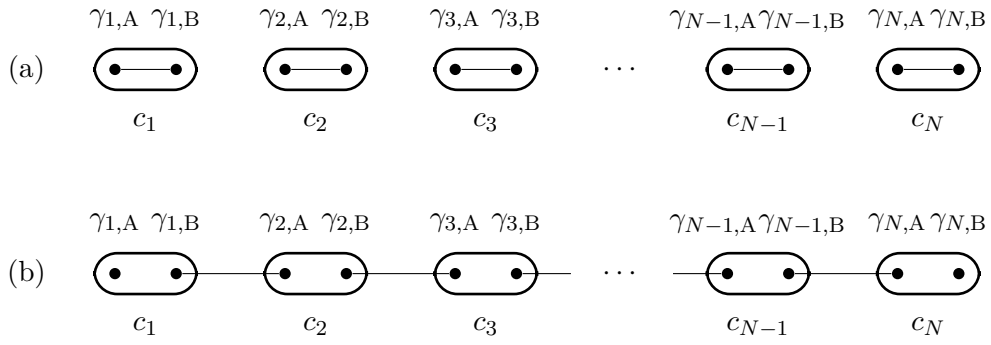

Figure 2.3: The two different types of pairing of two Majoranas into complex fermions: (a) The Majorana fermions associated with each physical fermion is paired together. (b) The Majorana fermions associated with neighboring physical fermions are paired together, which leaves two Majorana fermions at each end of the wire unpaired.

such that

$$\gamma_{Aj+1} = \mathrm{i}(\tilde{c}_j^\dagger - \tilde{c}_j), \gamma_{Bj} = \tilde{c}_j + \tilde{c}_j^\dagger, j = 1 \dots N-1. \tag{2.25}$$

In terms of the newly introduced fermionic operators the Hamiltonian becomes

$$H = 2t \sum_{j=1}^{N-1} \left(\tilde{c}_j^\dagger \tilde{c}_j - \frac{1}{2} \right), \tag{2.26}$$

which is diagonal in the basis described by the $\tilde{c}_j$ operators and thus has a ground state with none of the new fermionic states occupied. However we note that the sigle particle Hilbert space spanned by these operators is only of dimension $N-1$ and not equal the original size N. In fact the Majorana operators γ_{A1} and γ_{BN} does not enter the Hamiltonian and we can thus construct an extra fermionic operator, $\tilde{c}_0 = \frac{1}{2}(\gamma_{A1} + \mathrm{i}\gamma_{BN})$, corresponding to the missing state. One can easily check that this is also an eigenstate of the Hamiltonian and it is clear, since the $\tilde{c}_0$ operator does not appear in the Hamiltonian, that it has zero energy and thus is also a ground state.

To find out when the system has unpaired Majorana fermions for a more general paramater regime, one has in general to find the eigenfunctions to the Hamiltonian and show that these contain a zero-energy solution corresponding to unpaired Majorana fermions. It can be shown that the system actually has unpaired Majorana fermions as long as $|\Delta| \neq 0$ and $2w > |\mu|$ [17] but I will not go through the derivation here. We have now seen that a general 1d system consisting of spinless fermions with p-wave superconductivity will have unpaired Majorana fermions located at the ends of the system. Such a system is not easily found in nature but it may perhaps be able to engineer it by clever use of materials and tools that are already used in laboratories, which is what the next chapter is about.

Chapter 3

Majorana Bound States in Semiconductor Nanowires

Even though Kitaev early pointet out the possibility of having Majorana modes in one-dimensional superconducting systems it took almost 10 years before the first proposals for realistic implementations of his model appeared. The first system that was considered was suggested almost simultaneaously by Sau et Al. [37] and Oreg et Al. [32] and consists of a quasi one-dimensional semiconducting wire with strong spin-orbit interactions in proximity to a normal s-wave superconductor and with an applied magnetic field. Due to the simplicity of the system and the fact that such a system could be experimentally realizable with the current technology, sparked a big rush to study its properties and how the system could be improved.

In this chapter I will describe the system and show how Majorana fermions can appear and under which requirements. As we saw from the Kitaev model in Sec. 2.5 what we need in order to have unpaired Majoranas in a 1-dimensional wire is that of spinless electrons and superconductivity, which since the electrons are spinless must be of the p-wave type. However, this is not easily obtained in solid state systems: Electrons are natural spin-$\frac{1}{2}$ particles and in the absence of a magnetic field, the energy levels are degenerate. Trying to remove this degeneracy by e.g. applying a magnetic field or placing the superconductor in proximity to a magnetic insulator, one risks destroying the delicate supercondutivity. Instead one can follow another route which seeks to create and effective p-wave pairing by using a semiconducting wire with strong spin-orbit interaction and contacting it with a regular s-wave superconductor, such that the semicoductor will feel an effective pairing interaction through the so-called proximity effect. One then still has to split the spin-degeneracy by for example applying a magnetic field which could have the effect of destroying superconductivity, but in some semiconductors the electron can have an effective Landé g-factor which is many times bigger than that of the free electron, $g \approx 2$, so that a relative small field can be used.

In the following I will first describe how one in general can deal with superconducting systems together with some of their features and secondly I will briefly review spin-orbit interactions and how they appear in solid state systems. With this covered we are then

ready to study the specific model and show how it can realize Majorana fermions.

3.1 General properties of superconducting systems

Superconductivity is the phenomenon of exactly zero electrical resistance of a material when it is cooled to a temperature below a certain value called the critical temperature. For conventional superconductors this phase transition was first explained by Bardeen, Cooper and Schrieffer as a result of an effective attractive interaction between the otherwise mutual repulsive electrons. They showed that the attractive interaction leads to a ground state in which all electrons are paired together in so-called Cooper-pairs, that are then free to move without any apparent friction. In the BCS-theory the effective attractive interaction of the electrons was explained as a result of the electrons interaction with phononic vibrations of the positively charged atomic lattice. However for the unconventional superconductors like e.g. the cuprates the microscopic origin of attractive interaction is still an unsolved puzzle. In the following a general way of describing a superconducting system without regard to the microscopic origin will be shown, we will simply assume an attractive interaction between the electrons.

The origin of the BCS theory came from Coopers observation that if two electrons are added on top of a filled Fermi sea which they do only interact with through Pauli exclusion, then if they are subject to a net attractive interaction they pair up to form a bound state. In effect the attractive interaction renders the Fermi sea unstable and it "condenses" into a ground state in which all electrons are paired. In the case of s-wave superconductivity, each electron is paired with its time-reversed counterpart, and in a mean-field description where the total particle number is not exactly conserved, the many-body ground state is the celebrated BCS-groundstate given by [6]

$$|\psi_{\mathrm{BCS}}\rangle = \prod_{\mathbf{k}} (u_{\mathbf{k}} + v_{\mathbf{k}} c^{\dagger}_{\mathbf{k}\uparrow} c^{\dagger}_{-\mathbf{k}\downarrow}). \tag{3.1}$$

We see that the ground state consists of a superposition of states, each always containing an equal number of pairs $c^{\dagger}_{\mathbf{k}\uparrow} c^{\dagger}_{-\mathbf{k}\downarrow}$. The coefficients $u_{\mathbf{k}}$ and $v_{\mathbf{k}}$ are determined either by substituting the state into the Schrödinger equation and minimizing the energy or by a method that will be described below.

Conventional superconductors are metals for which the Couloumb interactions are effectively screened so a model that can be used to describe both the ground state and the excitations does in the simplest case only need to take the attractive interaction responsible for the pairing into account. A general Hamiltonian for such a simple model with s-wave pairing is

$$H = \sum_{\mathbf{k}\sigma} \xi_{\mathbf{k}} c^{\dagger}_{\mathbf{k}\sigma} c_{\mathbf{k}\sigma} - \sum_{\mathbf{k}\mathbf{k}'} V_{\mathbf{k}\mathbf{k}'} c^{\dagger}_{\mathbf{k}\uparrow} c^{\dagger}_{-\mathbf{k}\downarrow} c_{-\mathbf{k}'\downarrow} c_{\mathbf{k}'\uparrow}, \tag{3.2}$$

where $\xi_{\mathbf{k}} = \varepsilon_{\mathbf{k}} - \mu$ is the single electron energy measured from the chemical potential. We expect the ground state of the model to be the BCS groundstate which consist of a superposition of occupied or unoccupied pair states. This leads us to the observation

that the expectation value of the pair annihilation and creation operators, $\langle c_{\mathbf{k}\downarrow} c_{\mathbf{k}\uparrow}\rangle$ and $\langle c^\dagger_{\mathbf{k}\uparrow} c^\dagger_{\mathbf{k}\downarrow}\rangle$, is nonzero, contrary to the normal metallic case. The Hamiltonian is then typically simplified by a mean-field approximation in which the pair-creation operator is written as its expectation value plus fluctuations

$$c^\dagger_{\mathbf{k}\uparrow} c^\dagger_{-\mathbf{k}\downarrow} = \langle c^\dagger_{\mathbf{k}\uparrow} c^\dagger_{-\mathbf{k}\downarrow}\rangle + \delta_{\mathbf{k}}. \tag{3.3}$$

Assuming the fluctuations to be small we can then insert this expression in the Hamiltonian (3.2) and neglect terms bilinear in $\delta_{\mathbf{k}}$ to get

$$\begin{aligned} H = \sum_{\mathbf{k}\sigma} \varepsilon_{\mathbf{k}} c^\dagger_{\mathbf{k}\sigma} c_{\mathbf{k}\sigma} + \sum_{\mathbf{k}\mathbf{k}'} V_{\mathbf{k}\mathbf{k}'} \Big(& c^\dagger_{\mathbf{k}\uparrow} c^\dagger_{-\mathbf{k}\downarrow} \langle c_{-\mathbf{k}'\downarrow} c_{\mathbf{k}'\uparrow}\rangle \\ & + \langle c^\dagger_{\mathbf{k}'\uparrow} c^\dagger_{-\mathbf{k}'\downarrow}\rangle c_{-\mathbf{k}'\downarrow} c_{\mathbf{k}'\uparrow} + \langle c^\dagger_{\mathbf{k}\uparrow} c_{-\mathbf{k}\downarrow}\rangle \langle c_{-\mathbf{k}'\downarrow} c_{\mathbf{k}'\uparrow}\rangle \Big). \end{aligned} \tag{3.4}$$

The last term in this expression is constant and can effectively be included in the chemical potential, which has to be calculated self-consistently anyway. Now introducing the superconducting order parameter

$$\Delta_{\mathbf{k}} = -\sum_{\mathbf{k}'} V_{\mathbf{k}\mathbf{k}'} \langle c_{-\mathbf{k}\downarrow} c_{\mathbf{k}\uparrow}\rangle \tag{3.5}$$

we finally reach the BCS mean-field Hamiltonian given by

$$H_{\mathrm{BCS,MF}} = \sum_{\mathbf{k}\sigma} \xi_{\mathbf{k}} c^\dagger_{\mathbf{k}\sigma} c_{\mathbf{k}\sigma} - \sum_{\mathbf{k}} \left(\Delta_{\mathbf{k}} c^\dagger_{\mathbf{k}\uparrow} c^\dagger_{-\mathbf{k}\downarrow} + \Delta^*_{\mathbf{k}} c_{-\mathbf{k}\downarrow} c_{\mathbf{k}\uparrow} \right). \tag{3.6}$$

This Hamiltonian is quadratic in the electron annihilation and creation operators and it is therefore exactly solvable. The downside is that it no longer conserves the particle number due to the existence of terms that add or remove particle pairs like the operator $c^\dagger_{\mathbf{k}\uparrow} c^\dagger_{-\mathbf{k}\downarrow}$. This however, means that the particle *parity*, i.e. the whether the particle number is even or odd, is a still a conserved quantity. Also the mean field parameter now included in the superconducting order parameter $\Delta_{\mathbf{k}}$ has to be determined self-consistently so that is actually satisfies Eq. (3.5). The Hamiltonian (3.6) can be diagonalized by a linear transformation, the so-called Bogoliubov transformation, given by

$$\begin{aligned} c_{\mathbf{k}\uparrow} &= u^*_{\mathbf{k}} \alpha_{\mathbf{k}1} + v_{\mathbf{k}} \alpha_{\mathbf{k}2} \\ c_{-\mathbf{k}\downarrow} &= -v^*_{\mathbf{k}} \alpha_{\mathbf{k}1} + u_{\mathbf{k}} \alpha_{\mathbf{k}2}, \end{aligned} \tag{3.7}$$

where the coefficients $u_{\mathbf{k}}$ and $v_{\mathbf{k}}$ are the same coefficients as those that appear in the BCS groundstate in Eq. (3.1). The coefficients satisfy $|u_{\mathbf{k}}|^2 + |v_{\mathbf{k}}|^2 = 1$ and the newly introduced operators $\alpha_{\mathbf{k}\lambda}$ thus preserve the canonical anticommutation relations for fermions, $\{\alpha_{\mathbf{k}\lambda}, \alpha^\dagger_{\mathbf{k}'\lambda'}\} = \delta_{\mathbf{k}\mathbf{k}'}\delta_{\lambda\lambda'}$ and $\{\alpha_{\mathbf{k}\lambda}, \alpha_{\mathbf{k}'\lambda'}\} = 0$. Rewritten in terms of the quasi-particles the Hamiltonian (3.6) then takes the canonical form

$$H = \sum_{\mathbf{k}\lambda} E_{\mathbf{k}} \alpha^\dagger_{\mathbf{k}\lambda} \alpha_{\mathbf{k}\lambda} + E_0 \tag{3.8}$$

where E_0 is the BCS groundstate energy, which is lower than the ground state energy of the normal state, $E_{0,\mathrm{n}} = \mu N$. The quasi-particles described by the $\alpha_{\mathbf{k}\lambda}$ in (3.8) correspond to the excitations of the superconductor and their energies are

$$E_{\mathbf{k}} = \sqrt{\xi_{\mathbf{k}}^2 + |\Delta_{\mathbf{k}}|^2}, \tag{3.9}$$

where we see that they are separated from the groundstate by an energy gap given by $\Delta_{\mathbf{k}}$.

3.1.1 Bogoliubov method for non-homogeneous superconductors

In general one would like to study superconductors with localized impurities, spacially varying potentials or interfaces between a superconductor and another material. In such cases the homogeneous BCS Hamiltonian in Eq. (3.6) will not suffice. Instead we can introduce a real-space equivalent given by

$$H = \sum_{\sigma\sigma'} \int d\mathbf{r}\, \Psi_\sigma^\dagger(\mathbf{r}) \mathcal{H}_{0,\sigma\sigma'}(\mathbf{r}) \Psi_{\sigma'}(\mathbf{r}) - \int d\mathbf{r} \left(\Delta(\mathbf{r}) \Psi_\uparrow^\dagger(\mathbf{r}) \Psi_\downarrow^\dagger(\mathbf{r}) + \Delta^*(\mathbf{r}) \Psi_\downarrow(\mathbf{r}) \Psi_\uparrow(\mathbf{r}) \right), \tag{3.10}$$

where $\mathcal{H}_0(\mathrm{r})$ is the usual single-particle Hamiltonian for the system including potentials which can be magnetic of nature and therefore it carries spin-indices. The superconducting order parameter, $\Delta(\mathbf{r})$, is here a spatially varying scalar function, but for other pairing types than s-wave it will in general be an operator. The Hamiltonian (3.10) can be treated by introducing a generalization of the Bogoliubov transformation (3.7) given by

$$\Psi_\sigma(\mathbf{r}) = \sum_{n\lambda} \left(u_{n\lambda,\sigma}(\mathbf{r}) \alpha_{n\lambda} + v_{n\lambda,\sigma}^*(\mathbf{r}) \alpha_{n\lambda}^\dagger \right), \tag{3.11}$$

where the quasi-particle annihilation and creation operators should satisfy the canonical anti-commutation relations for fermions and λ can be thought of as a *pseodo-spin* index. The eigenfunctions $u_{n\lambda}(\mathbf{r})$ and $v_{n\lambda}(\mathbf{r})$ are determined such that the Hamiltonian (3.10) becomes diagonal in the quasi-particle operators. When doing so it turns out that the eigenfunctions has to satisfy the coupled Bogoliubov-de Gennes equations [42]

$$\begin{aligned} \sum_{\sigma'} \left[\mathcal{H}_{0,\sigma\sigma'}(\mathbf{r}) u_{\sigma'}(\mathbf{r}) + \Delta(\mathbf{r}) (\sigma_z)_{\sigma\sigma'} v_{\sigma'}(\mathbf{r}) \right] &= E u_\sigma(\mathbf{r}) \\ \sum_{\sigma'} \left[-\mathcal{H}_{0,\sigma'\sigma}^*(\mathbf{r}) v_{\sigma'}(\mathbf{r}) + \Delta^*(\mathbf{r}) (\sigma_z)_{\sigma\sigma'} u_{\sigma'}(\mathbf{r}) \right] &= E v_\sigma(\mathbf{r}). \end{aligned} \tag{3.12}$$

One can consider these as the superconducting equivalents of the single particle Schrödinger equation of the normal state. If we let $\Delta(\mathbf{r}) = 0$ then we see that these equations reduces to

$$\sum_{\sigma'} \mathcal{H}_{0,\sigma\sigma'}(\mathbf{r}) u_{\sigma'}(\mathbf{r}) = E u_\sigma(\mathbf{r}) \tag{3.13}$$

$$\sum_{\sigma'} \mathcal{H}_{0,\sigma'\sigma}^*(\mathbf{r}) v_{\sigma'}(\mathbf{r}) = -E v_\sigma(\mathbf{r}), \tag{3.14}$$

from which we observe that $u(\mathbf{r})$ is a single electron wavefunction satisfying the normal state Schrödinger equation. $v(\mathbf{r})$ on the other hand appears to be the eigenfunction for a hole, which are characterised by being the time-reversed counterparts of electrons having negative energy. One can see this from the fact that the Hamiltonian depend on time through the momentum operator $\mathbf{p} = -i\hbar\boldsymbol{\nabla}$. Thus one can represent time-reversal by complex conjugation if one at the same time flips the spin indices since angular momentum changes sign under time reversal. The Hamiltonian for holes is therefore seen to be that on the left hand side of Eq. (3.14).

It often convenient to deal with both the electron and hole eigenfunctions by introducing so-called Nambu spinors given by

$$\Psi(\mathbf{r}) = \begin{pmatrix} u_\uparrow(\mathbf{r}) \\ u_\downarrow(\mathbf{r}) \\ v_\downarrow(\mathbf{r}) \\ -v_\uparrow(\mathbf{r}) \end{pmatrix}. \tag{3.15}$$

The minus on the last component is chosen by so that the Hamiltonian may be written in a special form and has therefore no physical significance and others may use a different convention. In terms of $\Psi(\mathbf{r})$ the Bogoliubov-de Gennes equations (3.12) can be written compactly as

$$H_{\mathrm{BdG}}(\mathbf{r})\Psi(\mathbf{r}) = E\Psi(\mathbf{r}) \tag{3.16}$$

where the so-called Bogoliubov-de Gennes Hamiltonian is given by

$$H_{\mathrm{BdG}}(\mathbf{r}) = \begin{pmatrix} \mathcal{H}_0(\mathbf{r}) & \Delta(\mathbf{r})\mathbb{1} \\ \Delta^*(\mathbf{r})\mathbb{1} & -\sigma_y\mathcal{H}_0^*(\mathbf{r})\sigma_y \end{pmatrix}, \tag{3.17}$$

where $\mathbb{1}$ is the unit matrix in spin space. Here $-\sigma_y H_0^*(\mathbf{r})\sigma_y$ corresponds to the negative energy time-reversed Hamiltonian for holes. By introducing 4×4 Nambu Pauli matrices acting in particle-hole space $\tau_i = \tilde{\sigma}_i \otimes \mathbb{1}$ and in spin space $\sigma_i = \mathbb{1} \otimes \tilde{\sigma}_i$, where $\tilde{\sigma}_i$ are the usual 2×2 Pauli matrices, we can typically write the BdG Hamiltonian very compactly. Since the BdG Hamiltonian is 4×4 and a normal state Hamiltonian is only 2×2, it is clear that the Bogoliubov-de Gennes equations Eq. (3.16) will lead to twice as many eigenstates. However, the real number of independent solutions is in fact not changed, since half of the eigenstates are related to the other half by particle-hole symmetry. The particle-hole transformation can be performed by the operator

$$\mathcal{P} = \tau_y\sigma_y\mathcal{K} = \begin{pmatrix} 0 & 0 & 0 & -1 \\ 0 & 0 & 1 & 0 \\ 0 & 1 & 0 & 0 \\ -1 & 0 & 0 & 0 \end{pmatrix}\mathcal{K}, \tag{3.18}$$

where $\mathcal{K}$ is the complex conjugation operator. When particle-hole transforming the BdG Hamiltonian we see that

$$\mathcal{P}H_{\mathrm{BdG}}(\mathbf{r})\mathcal{P}^\dagger = -H_{\mathrm{BdG}}. \tag{3.19}$$

Thus when acting on the BdG equations Eq. (3.12) we see that

$$\mathcal{P}H_{\text{BdG}}\mathbf{\Psi}(\mathbf{r}) = \mathcal{P}H_{\text{BdG}}(\mathbf{r})\mathcal{P}^\dagger\mathcal{P}\mathbf{\Psi} = -H_{\text{BdG}}\mathcal{P}\mathbf{\Psi}(\mathbf{r}) = E\mathcal{P}\mathbf{\Psi}(\mathbf{r}), \tag{3.20}$$

which states that if $\Psi(\mathbf{r})$ is a solution to the BdG equations with energy E, then another solution is given by $\mathcal{P}\Psi(\mathbf{r})$ with energy $-E$.

3.2 Spin-orbit interaction in solid state systems

One of the typical ingredients necessary for Majorana modes is that the system has some sort of spin-polarizing mechanism. This can be achieved in two ways, either through the use of some ferromagnetic properties of the medium or by a spin-orbit interaction which couples the spin of the electrons in the medium to its momentum $\mathbf{p}$. Here I will give a brief explanation of how this last phenomenon comes about.

Spin-orbit interaction is a relativistic effect that is due to the fact that if the particle is moving in an electric field, in its own inertial frame it will effectively see both an electric field and a magnetic field and if the particle has spin it will interact with this field.

To see this lets consider an electron moving with velocity $\mathbf{p}$ in a constant electric field $\mathbf{E}$ and magnetic field $\mathbf{B}$. If we make a Lorentz-transformation to the reference frame that moves with the electron we will have to transform the electric and magnetic fields accordingly. For small velocities $v \ll c$ one can show [14] that the fields transforms as

$$\begin{aligned}\mathbf{E} &\to \mathbf{E}' = \mathbf{E} + \mathbf{v}\times\mathbf{B}\\ \mathbf{B} &\to \mathbf{B}' = \mathbf{B} - \frac{1}{c^2}\mathbf{v}\times\mathbf{E}.\end{aligned} \tag{3.21}$$

If no magnetic field is applied we thus see that the electron will still see a local magnetic field, $\Delta\mathbf{B} = \frac{1}{c^2}\mathbf{v}\times\mathbf{E}$, perpendicular to its motion and the electric field. This magnetic field will interact with the magnetic moment of the electron giving rise to a splitting in energy. For a free electron moving in an electric field we can include this energy in the Hamiltonian by a term

$$\Delta H_{\text{SO}} = -\boldsymbol{\mu}\cdot\Delta\mathbf{B} = \frac{g_{\text{s}}\mu_{\text{B}}}{c^2}\mathbf{S}\cdot(\mathbf{v}\times\mathbf{E}), \tag{3.22}$$

where $\mathbf{S}$ is the spin operator. For normal two-component spinors we have $\mathbf{S} = \frac{\hbar}{2}\boldsymbol{\sigma}$ with $\boldsymbol{\sigma} = (\sigma_x, \sigma_y, \sigma_z)$ being the vector of Pauli matrices. Using that the velocity is $\mathbf{v} = \frac{1}{m}\mathbf{p}$ we may thus write

$$\Delta H_{\text{SO}} = \frac{g_{\text{s}}\hbar}{2mc^2}\boldsymbol{\sigma}\cdot(\mathbf{p}\times\mathbf{E}) \tag{3.23}$$

from which we see that the energy is proportional to both the momentum of the electrons and the electric field. From just looking at the prefactors we see that the size of the splitting is extremely small if not the electron velocity is high and strength of the applied

electric field is huge. As an example we can take the velocity for an electron to the Fermi velocity of a metal, which typically is in the order of $10 \times 10^6\,\mathrm{m/s}$ and assume that the electric field is $\sim 10 \times 10^6\,\mathrm{V/m}$ which is close to the electric break down of air and with these values the spin-orbit splitting is $\Delta E_{\mathrm{so}} \sim 10 \times 10^{-9}\,\mathrm{eV}$, which is hardly measurable by any method.

In semiconductors the electron velocities are usually not considered in the range where relativistic effects needs to be taken into account, sizeable spin-orbit effects can still occur even without any applied electric fields. The reason for this is first that the g-factor for electrons is replaced by the effective Landé g-factor for the material, which can be many times larger than g_{s} and secondly because the electrons move in the strong potentials from the atomic lattice. However the electrons will only feel a net electric field if the potential does not have inversion symmetry along all axes. Systems with spin orbit interaction can generally be classified in the two ways the effect originates from: Bulk Inversion Asymmetry (BIA) or Structural Inversion Asymmetry (SIA). As the name implies, the crystal lattice for materials having bulk inversion asymmetry does not have a center of inversion. In Fig. 3.1 are shown the unit cells of the zinc-blende lattice structure (eg. GaAs, InAs and InSb) and the wurtzite lattice structure (eg. GaN) which both have bulk inversion asymmetry. As seen the lattice structure is quite

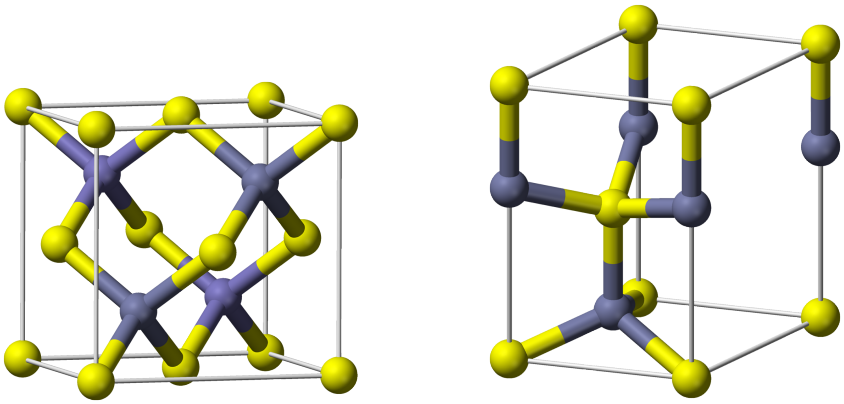

(a) The unit cell of the zinc-blende lattice structure.

(b) The unit cell of the wurtzite lattice structure.

Figure 3.1: Unit cells of lattice structures with Bulk Inversion Asymmetry.

complex and the effective electric field that the electrons experience is not constant as in the simple picture given above. To calculate the spin-orbit interaction contribution to the Hamiltonian one has to take the full lattice and its band structure into account, which was first done for the zinc-blende structure by Dresselhaus [8]. While in three dimensions the spin-orbit coupling is quite complicated, then if a material with BIA is strogly confined in two dimensions the the most dominant contribution to the spin-orbit

coupling is given by the Dresselhaus term [47]

$$H_{\text{Dresselhaus,2D}} = \beta\langle k_z\rangle(\sigma_y k_y - \sigma_x k_x), \tag{3.24}$$

where we have chosen the z-axis perpendicular to the plane and β is a material dependent parameter.

Besides materials with intrinsic spin-orbit interactions due to bulk properties one can also engineer systems that will exhibit spin-orbit interaction by some means constructing an asymmetric confining potential, which is why we call this Structural Inversion Asymmetry. This can be done by actually applying an electric field, though the required strength of this field for obtaining any measurable changes need to be huge as shown above, or by making heterostructures of different materials. When two semiconductors with different conduction band and valence band edges contact, the bands will bend near the interface resulting in a potential gradient which can be quite strong. The effect is however restricted to the electrons close to the interface but in two dimensional electron gases like those realized in quantum wells the effect is well studied.

In these cases the potential gradient will always be in the direction of the asymmetry, i.e. perpendicular to the plane or interface, and thus the spin-orbit interaction can be included in the Hamiltonian by the so-called Rashba term

$$H_{\text{Rashba}} = \alpha\boldsymbol{\sigma}\cdot(\mathbf{p}\times\hat{\mathbf{n}}), \tag{3.25}$$

where α is a parameter of the material or structure called the Rashba parameter and $\hat{\mathbf{n}}$ is the unit vector in the direction of the inversion asymmetry. It is clear that the effect of Rashba spin-orbit coupling is a momentum dependent splitting of the spin-levels. In a simple model of a free two-dimensional electron gas with Rashba spin orbit coupling the total Hamiltonian is

$$H = \varepsilon_k - \alpha(p_x\sigma_y - p_y\sigma_x), \tag{3.26}$$

where $\varepsilon_k = \frac{k_x^2+k_y^2}{2m}$ is the normal dispersion for free electrons. The Schrödinger equation for the Hamiltonian (3.26) can easily be solved and yields the energies

$$E_\pm = \varepsilon_k \pm \alpha k, \tag{3.27}$$

where we have written the momentum vector in polar coordinates, $k_x = k\cos\theta$ and $k_y = k\sin\theta$. The corresponding eigenstates are

$$|\mathbf{k},+\rangle = |\uparrow\rangle + ie^{i\theta}|\downarrow\rangle, \quad |\mathbf{k},-\rangle = ie^{-i\theta}|\uparrow\rangle + |\downarrow\rangle, \tag{3.28}$$

where $|\uparrow\rangle$ and $|\downarrow\rangle$ are the two spin eigenstates in the z-direction. It is informative to calculate the expectation value of the in-plane spin direction of the two states

$$\langle\mathbf{S}\rangle_+ = \langle\mathbf{k},+|(\sigma_x,\sigma_y)|\mathbf{k},+\rangle = (\sin\theta,\cos\theta) \tag{3.29}$$

$$\langle\mathbf{S}\rangle_- = \langle\mathbf{k},-|(\sigma_x,\sigma_y)|\mathbf{k},-\rangle = -(\sin\theta,\cos\theta), \tag{3.30}$$

and we see that the spin of electrons in the two states are always parallel and point perpendicular to the momentum, as illustrated in Fig. 3.2. If one then applies a magnetic field perpendicular to the effective spin-orbit field one will further split the bands, and if only the lowest band i occupied, the electrons are effectively spin-polarized.

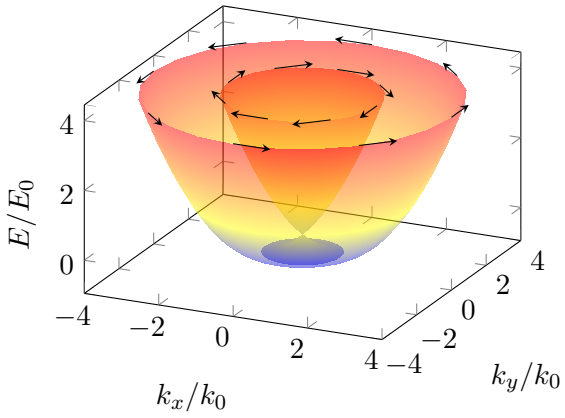

Figure 3.2: Spectrum for free electron with spin-orbit coupling moving in the plane. The arrows point in the expectation value of the spin direction. The spectrum is shown in dimensionless units in terms of the characteristic wave number $k_0 = 2m\alpha/\hbar^2$ and energy $E_0 = 2m\alpha^2/\hbar^2$.

3.3 Model of the system

The system that we are going to investigate is that of a semiconducting nanowire placed in contact with a superconductor. The wire and the superconductor are separated by an insulating barrier, eg. a thin oxide layer, but allow for electron tunnelling between the two materials which we hope will induce an effective superconducting gap in the wire, called the proximity effect. The size of the nanowire (they are typically rods width a diameter of 50 nm and a length of a few microns) will typically allow us to treat it as a quasi-1D system. We also assume that the interface between the nanowire and the substrate it is placed on will cause a sizeable Rashba spin-orbit coupling in the wire which we furthermore take as constant troughout the wire due to its small extend perpendicular to the surface. Lastly we will also need to consider the application of an external magnetic field.

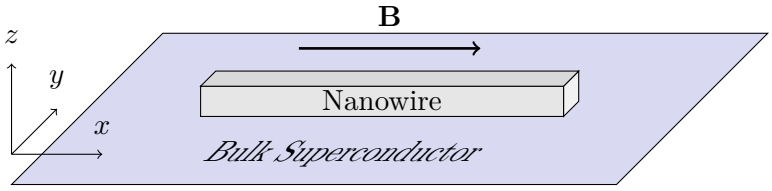

Figure 3.3: Sketch of the system considered. A semiconductor nanowire is placed on top of a conventional s-wave superconductor and a magnetic field is applied along the wire

The system so described can be modelled by the Hamiltonian

$$H = H_{\mathrm{w}} + H_{\mathrm{sc}} + H_{\mathrm{w-sc}}, \tag{3.31}$$

where H_{w} is the Hamiltonian of the wire, H_{sc} is the Hamiltonian of the superconductor and $H_{\mathrm{w-sc}}$ is the Hamiltonian decribing the tunnelling of electrons between the wire and

the superconductor. If we take the wire to lie along the x-direction and the effective spin-orbit electric field to point in the z-direction and disregard interactions the Hamiltonian of the wire can be written

$$\begin{aligned} H_{\mathrm{w}} = \sum_{\sigma\sigma'} \int d^3\mathbf{r}\, \Psi^\dagger_{w,\sigma}(\mathbf{r}) \Bigg[\left(\frac{\mathbf{p}^2}{2m^*_{\mathrm{w}}} - \mu_{\mathrm{w}} - U(\mathbf{r}) \right) \delta_{\sigma\sigma'} \\ + \alpha \boldsymbol{\sigma}_{\sigma\sigma'} \cdot (\mathbf{p} \times \hat{\mathbf{z}}) + \boldsymbol{\sigma}_{\sigma\sigma'} \cdot \mathbf{V}_{\mathrm{zm}} \Bigg] \Psi_{w,\sigma'}(\mathbf{r}), \end{aligned} \tag{3.32}$$

where m^* is the effective mass of the nano-wire, μ_{w} is the chemical potential, α is the Rasba parameter and $U(\mathbf{r})$ is an electric potential either applied or due to deformations or charged impurities. The last term is the Zeeman potential due to the applied magnetic field and takes the value

$$\mathbf{V}_{\mathrm{zm}} = -\frac{g\mu_{\mathrm{B}}}{2}\mathbf{B}, \tag{3.33}$$

where g is the effective Landé g-factor. We take the superconductor to be a conventional s-wave superconductor, eg. a slab of metal cooled below its critical temperature, which can be described within the effective BCS mean-field approximation, as considered in Sect. 3.1. We can thus decribe the superconductor by the Hamiltonian

$$\begin{aligned} H_{\mathrm{sc}} = \sum_{\sigma} \int d^3\mathbf{r}\, \Psi^\dagger_{\mathrm{sc},\sigma}(\mathbf{r}) \left(\frac{\mathbf{p}^2}{2m^*_{\mathrm{sc}}} - \mu_{\mathrm{sc}} \right) \Psi_{\mathrm{sc},\sigma}(\mathbf{r}) \\ - \int d^3\mathbf{r} \left(\Delta(\mathbf{r}) \Psi^\dagger_{\mathrm{sc},\uparrow}(\mathbf{r}) \Psi^\dagger_{\mathrm{sc},\downarrow}(\mathbf{r}) + \Delta^*(\mathbf{r}) \Psi_{\mathrm{sc},\downarrow}(\mathbf{r}) \Psi_{\mathrm{sc},\uparrow}(\mathbf{r}) \right), \end{aligned} \tag{3.34}$$

where μ_{sc} is the chemical potential and $\Delta(\mathbf{r})$ is the superconducting order parameter. The tunnel Hamiltonian may be written

$$H_{\mathrm{w-sc}} = \sum_{\sigma} \int d^3\mathbf{r} \left(t(\mathbf{r}) \Psi^\dagger_{\mathrm{w},\sigma}(\mathbf{r}) \Psi_{\mathrm{sc},\sigma}(\mathbf{r}) + t^*(\mathbf{r}) \Psi^\dagger_{\mathrm{sc},\sigma}(\mathbf{r}) \Psi_{\mathrm{w},\sigma}(\mathbf{r}) \right), \tag{3.35}$$

where the tunnel couplings are formally given by $t(\mathbf{r}) = \psi_{(w)}(\mathbf{r}) H(\mathbf{r}) \psi_{\mathrm{sc}}(\mathbf{r})$, with H being the single particle Hamiltonian of the combined system including the barrier and $\psi_{\mathrm{w}}(\mathbf{r})$ and $\psi_{\mathrm{w}}(\mathbf{r})$ being the single particle wavefunctions of the two uncoupled systems. We will not calculate the tunnel couplings from first principles but instead use reasonable estimates.

3.4 Effective low-energy 1d model

The model Hamiltonian in (3.31) is quite hard to work with due to the fact that it describes two different and coupled systems. However in the case of an homogenous superconductor $\Delta(\mathbf{r}) = \Delta_0$ it is possible to "integrate out" the superconductor degrees of freedom and create a low energy effective Hamiltonian for the wire, which does not include the superconductor but where the wire is by itself superconducting [40]. We

say that the superconductor induces superconductivity in the wire - this mechanism is called the superconducting proximity effect. In the case where the wire is effectively one-dimensional the effective Hamiltonian takes an especially simple form [39]

$$H_{\text{eff}} = ZH_{\text{w}} + H_{\text{ind.sc}}, \tag{3.36}$$

where Z is a renormalization factor that rescales the energy and $H_{\text{ind.sc}}$ is the Hamiltonian decribing the induced superconductivity. The renormalization factor is given by

$$Z = \frac{\gamma}{1+\gamma/\Delta_0}, \tag{3.37}$$

where γ is the effective coupling between the wire and superconductor and is proportional to t^2 and has the unit of energy. The term for the induced superconductivity is

$$H_{\text{ind.sc}} = -\int dx \left(\bar{\Delta}\Psi_\uparrow^\dagger(x)\Psi_\downarrow^\dagger(x) + \bar{\Delta}^*\Psi_\downarrow(x)\Psi_\uparrow(x)\right) \tag{3.38}$$

Here $\bar{\Delta}$ is the effective superconducting order parameter, which is related to the order parameter of the bulk superconductor, Δ_0 by

$$\bar{\Delta} = \frac{\gamma\Delta_0}{\gamma+\Delta_0} \tag{3.39}$$

and we see that for $\gamma \to \infty$ the induced gap approaches Δ_0. The Hamiltonian (3.36) is quite accurate in reproducing the spectrum of the full model Eq. (3.31) for energies lower than gap of the superconductor [39] which is sufficient for our purpose, namely showing that the system has Majorana bound states.

We now consider the case of a clean wire where the coupling to the superconductor is considered weak so that the renormalization constant is $Z \approx 1$. If we take the Zeeman field to be in the x-direction (along the wire) and for simplicity chose Δ to be real, the Hamiltonian can be written

$$\begin{aligned}\mathcal{H} = \int dx \Bigg\{ &\sum_{\sigma\sigma'} \Psi_\sigma^\dagger(x) \left[\frac{\hbar^2}{2m^*}\partial_x^2 - \mu + i\alpha_{\text{r}}(\sigma_y)_{\sigma\sigma'}\partial_x + V(\sigma_z)_{\sigma\sigma'}\right]\Psi_{\sigma'}(x) \\ &+ \Delta\Psi_\uparrow^\dagger(x)\Psi_\downarrow^\dagger(x) + \Delta\Psi_\downarrow(x)\Psi_\uparrow(x)\Bigg\},\end{aligned}$$

where $\alpha_{\text{r}} = \hbar\alpha$. The corresponding single particle Bogoliubov-de Gennes Hamiltonian in the Nambu basis $\mathbf{\Psi}(x) = (u_\uparrow(x), u_\downarrow(x), v_\downarrow(x), -v_\downarrow(x))$ as introduced in Sect. 3.1.1 can be written

$$H_{\text{BdG}} = \begin{pmatrix} \frac{\hbar^2}{2m^*}\partial_x^2 - \mu & \alpha\partial_x + V & \Delta & 0 \\ -\alpha\partial_x + V & \frac{\hbar^2}{2m^*}\partial_x^2 - \mu & 0 & \Delta \\ \Delta & 0 & -\frac{\hbar^2}{2m^*}\partial_x^2 + \mu & -\alpha\partial_x + V \\ 0 & \Delta & \alpha\partial_x + V & -\frac{\hbar^2}{2m^*}\partial_x^2 + \mu \end{pmatrix} \tag{3.40}$$

or written in terms of Pauli matrices in spin space, $\sigma_{x,y,z}$ and in particle/hole-space, $\tau_{x,y,z}$,

$$H_{\mathrm{BdG}} = \left[\left(\frac{\hbar^2}{2m^*}\partial_x^2 - \mu + i\alpha_\hbar\sigma_y\partial_x\right)\tau_z + V\sigma_x + \Delta\tau_x\right]. \tag{3.41}$$

The Hamiltonian (3.41) can be put in a convenient dimensionless form

$$\tilde{H}_{\mathrm{BdG}} = \left[\left(\frac{1}{2}\partial_{\tilde{x}}^2 - \tilde{\mu} + i\sigma_y\partial_{\tilde{x}}\right)\tau_z + \tilde{V}\sigma_x + \tilde{\Delta}\tau_x\right], \tag{3.42}$$

where parameters with a tilde have been rescaled by the characteristic energy $E_\alpha = \frac{m^*\alpha_\hbar^2}{\hbar^2}$ and lengths are measured in units of the characteristic length $l_\alpha = \frac{\hbar^2}{m^*\alpha_\hbar}$. Following the procedure introduced in Sect. 3.1.1 the Hamiltonian (3.40) can be put in a diagonal form by introducing Bogoliubov quasiparticle operators

$$\alpha_n = \int dx[u_{n,\uparrow}(x)\psi_\uparrow(x) + u_{n,\downarrow}(x)\psi_\downarrow(x) + v_{n,\downarrow}\psi_\downarrow^\dagger(x) + v_{n,\uparrow}(x)\psi_\uparrow(x)], \tag{3.43}$$

where $u_{n,\sigma}(x)$, $v_{n,\sigma}(x)$ are solutions to the BdG equations $H_{\mathrm{BdG}}\mathbf{\Psi}(x) = E\mathbf{\Psi}(x)$ that satisfies the boundary conditions of the problem. The BdG equations are a set of four coupled linear second order differential equations which in theory should allow for exact solutions. The form of the general solutions is however not very enlightening because it depends very much on the involved parameters. Instead we will consider the system in some special cases or solve it numerically.

First we are going to study the spectrum of the bulk states, which we can approximate by that of a similar but translationally invariant system. In this case we can take the solutions to the BdG equation to have the form $\mathbf{\Psi}(x) = e^{ikx}(u_\uparrow, u_\downarrow, v_\downarrow, -v_\downarrow)$ and the BdG Hamiltonian reduces to

$$H_{\mathrm{BdG}} = (\xi_k - \alpha_\hbar k\sigma_y)\,\tau_z + V\sigma_x + \Delta\tau_x, \tag{3.44}$$

where $\xi_k = \frac{\hbar^2k^2}{2m^*} - \mu$. The solutions to the BdG equations $H_{\mathrm{BdG}}\Psi(x) = E\Psi(x)$ have energies $\pm E$, where the solutions with $-E$ are related to the solutions with $+E$ by particle-hole symmetry, as discussed in Sect. 3.1.1. The energy spectrum can be found exactly and is given by

$$E_\pm^2 = \varepsilon_k^2 + \alpha_\hbar^2k^2 + V^2 + \Delta^2 \pm 2\sqrt{\Delta^2V^2 + \alpha^2k^2\varepsilon_k^2 + V^2\varepsilon_k^2}, \tag{3.45}$$

where $\varepsilon_k = \frac{\hbar^2k^2}{2m^*}$ and the two branches + and − are due to spin-splitting. In Fig. 3.4 several examples of the spectrum for various values of the parameters are shown. As we expect, the spectrum is non-gapped when $\Delta = 0$. Even though the Zeeman field can open up a gap at $k = 0$, the spectrum goes to zero for other momenta. When turning on superconductivity $\Delta \neq 0$ we see that the spectrum acquires an overall non-zero gap, which is however not given by the same value as the induced SC order parameter. From the lower branch of (3.45) we see that the gap at $k = 0$ is

$$E_0 = E(k=0) = \sqrt{\mu^2 + V^2 + \Delta^2 - 2\sqrt{V^2\Delta^2 + V^2\mu^2}} = |V - \sqrt{\Delta^2 + \mu^2}| \tag{3.46}$$

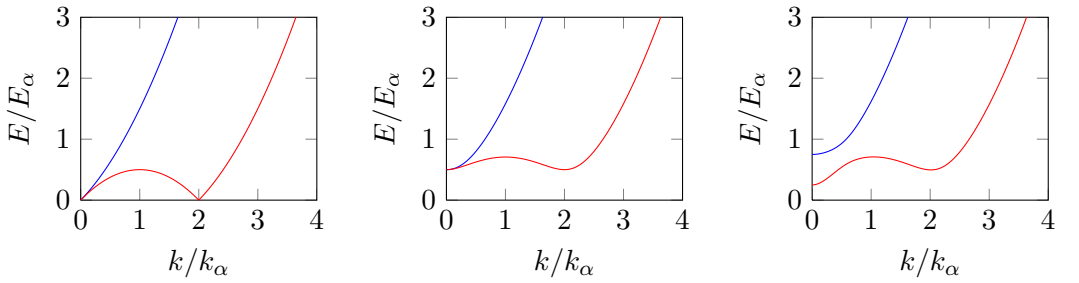

(a) $\tilde{\mu} = 0, \tilde{V} = 0, \tilde{\Delta} = 0$ (b) $\tilde{\mu} = 0, \tilde{\Delta} = 0,\ \tilde{V} = 1/4$ (c) $\tilde{\mu} = 0, \tilde{Delta} = 1/10, \tilde{V} = 1/4$

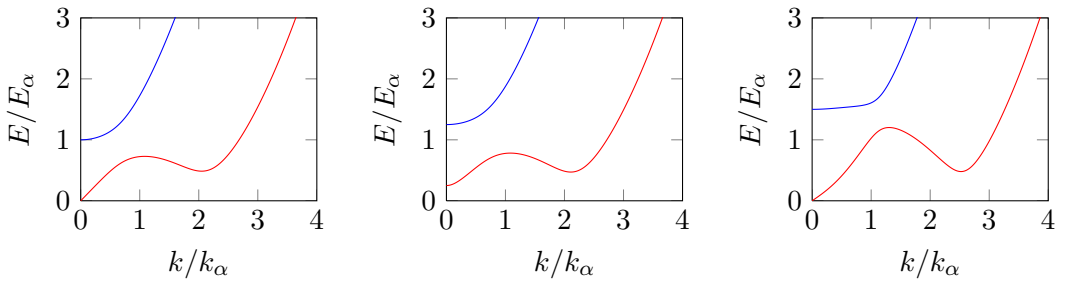

(d) $\tilde{\mu} = 0, \tilde{\Delta} = 1/4, \tilde{V} = 1/4$ (e) $\tilde{\mu} = 0, \tilde{\Delta} = 0.4, \tilde{V} = 1/4$ (f) $\tilde{\mu} = \sqrt{21}/20, \tilde{\Delta} = 1/10, \tilde{V} = 1/4$

Figure 3.4: Energy spectrum for the bulk Bogoliubov quasiparticle *excitations* in the 1d nanowire as given by Eq. (3.45). The blue lines are E_+ and the red lines are E_-. The energy and all parameters are given in units of $E_\alpha = \frac{2m\alpha_\hbar}{\hbar^2}$ and the momentum is given in units of $k_\alpha = \frac{m\alpha}{\hbar^2}$. (a) Excitation energy for an electron in the non-supercondting wire without Zeeman field. (b) Without Zeeman field, superconductivity open an overall gap of size Δ. With superconductivity, the excitations are a combination of electrons and holes. (c) An applied Zeeman field leads to a splitting at $k = 0$ and the gap diminishes here. (d) At a certain value of the Zeeman field the gap closes completely. The closing of the gap signalizes a topological phase transition. (e) Increasing the Zeemand field above the critical value reopens the gap. In this regime the wire is in a topological phase. (f) A finite chemical potential may close the gap and eventually destroy the topological phase.

which closes for $V = \sqrt{\Delta^2 - \mu^2}$. We see that if $C = V^2 - \Delta^2 + \mu^2 > 0$ the gap is dominated by the value of V and for $C < 0$ it is dominated by Δ. We will show later that for $C < 0$ the system is in a topological trivial phase, while for $C > 0$ the wire is in a topological phase characterized by a zero-energy Majorana bound state. Another interesting thing worth noticing is that the second gap for finite k in the topological phase, $C < 0$, is lower than the $k = 0$ gap for large Zeeman fields and increasing Zeeman field value decreases the gap, see Fig. 3.5. This fact restricts the parameter regime in which Majorana bound states in nanowires are feasible for quantum computation purposes, since the coherence time of a Majorana qubit depends on the gap between the Majorana states and the bulk states. Increasing the Zeemand field increases the gap at $k = 0$ but descreases the gap at finite k, so to ensure the greatest topological protection of the Majorana fermions, one have to adjust the parameters to a "sweet spot" [26]. In order to find the parameter regime that best protects the Majorana qubit, we have calculated the minimum gap as a function of the Zeeman field for various realistic parameters and the results are shown in 3.6. In the calculation we have included the effective coupling to the superconductor, γ, as it determines the induced gap. From Fig. 3.6 we however see that the minimum gap in the topological phase, i.e. for $V > V_{\text{critical}}$, is not proportional to the induced gap. The SC coupling and thus the induced gap does have some influence on the gap in the topological phase, but the most important controlling parameter seems to be the Rashba spin-orbit coupling - a strong spin-orbit coupling is essential for the protection of the Majorna qubit.

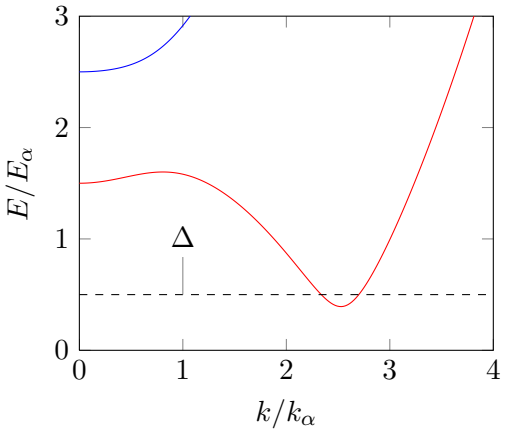

Figure 3.5: Quasiparticle excitation spectrum for $\tilde{\Delta} = \frac{1}{2}$, $\tilde{V} = \frac{3}{2}$ and $\tilde{\mu} = 0$. The wire is in the topological phase but the size of the Zeeman field has caused the gap in the "wing" to be smaller than both the gap at $k = 0$ and the induced superconducting gap Δ.

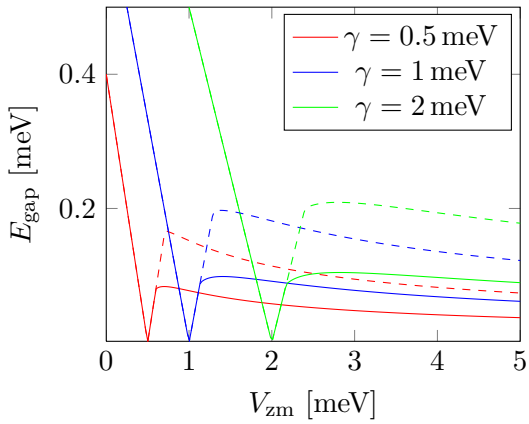

Figure 3.6: The minimum gap as a function of Zeeman field plottet for different SC couplings γ. The solid lines is for a Rashba parameter of $\alpha_{\text{r}} = 0.1\,\text{eV Å}$ and the dashed lines are for $\alpha_{\text{r}} = 0.2\,\text{eV Å}$. The curves have been calculated for a wire with electron mass $m = 0.015 m_{\text{e}}$ and a superconductor with $\Delta = 2\,\text{meV}$.

3.4.1 Reduction of model to Kitaev chain

In previous section we studied the spectrum of the bulk quasiparticle excitations for the Hamiltonian of the effective 1d wire model and saw how the Zeeman field at a certain critical value causes the energy gap to exactly close and we argued that this signifies a topological phase transition. So far our arguments have been completely without proof, we have not yet shown that in the two regions $V < V_{\text{crit}}$ and $V > V_{\text{crit}}$ the wire is in two different phases with different topology characterised by the existince or non-existence of a Majorana bound state. We will now make that up by showing that in the low-energy regime, the model described by the Hamiltonian (3.40) can be mapped to the Kitaev model. We now consider the Hamiltonian (3.41) without superconductivity, which in terms of the momentum operator $p = -i\hbar\partial_x$ reads

$$H_{\text{BdG}} = \left(\frac{p^2}{2m^*} - \mu - \alpha p \sigma_y \right) \tau_z + \Delta \tau_x. \tag{3.47}$$

Since we take the wire to be homogenous, we can consider p as a c-number and proceed to diagonalize the Hamiltonian in the usual way. The positive energy solutions are given by

$$E_\pm = \frac{p^2}{2m^*} - \mu \pm \sqrt{\alpha^2 p^2 + V^2}, \tag{3.48}$$

with the corresponding Nambu eigenspinors

$$\Psi_+ = \frac{1}{\sqrt{2}}(e^{i\theta}, 1, 0, 0), \quad \Psi_- = \frac{1}{\sqrt{2}}(-e^{i\theta}, 1, 0, 0), \tag{3.49}$$

where the angle θ is given by the relations $\sqrt{\alpha^2 p^2 + V^2}\cos\theta = V$ and $\sqrt{\alpha^2 p^2 + V^2}\sin\theta = \alpha p$. The negative energy solutions are determined from electron-hole symmetry, ie. $\bar{\Psi} = -\tau_x \sigma_y \Psi^*$ and are thus

$$\bar{\Psi}_+ = \frac{1}{\sqrt{2}}(0, 0, -\mathrm{e}^{-\mathrm{i}\theta}, 1), \quad \bar{\Psi}_- = \frac{1}{\sqrt{2}}(0, 0, \mathrm{e}^{-\mathrm{i}\theta}, 1). \tag{3.50}$$

The unitary transformation that diagonalizes the Hamiltonian is given by

$$U = \frac{1}{\sqrt{2}} \begin{pmatrix} \mathrm{e}^{\mathrm{i}\theta/2} & -\mathrm{e}^{\mathrm{i}\theta/2} & 0 & 0 \\ \mathrm{e}^{-\mathrm{i}\theta/2} & \mathrm{e}^{-\mathrm{i}\theta/2} & 0 & 0 \\ 0 & 0 & \mathrm{e}^{-\mathrm{i}\theta/2} & -\mathrm{e}^{-\mathrm{i}\theta/2} \\ 0 & 0 & \mathrm{e}^{\mathrm{i}\theta/2} & \mathrm{e}^{\mathrm{i}\theta/2} \end{pmatrix} \tag{3.51}$$

so that $H_0 = U\Lambda U^\dagger$, where $\Lambda = \text{diag}(E_+, E_-, -E_-, -E_+)$. Transforming the total Hamiltonian including the superconducting pairing term to the eigenbasis of H_0 we have

$$\tilde{H} = U^\dagger H U = \begin{pmatrix} E_+ & 0 & \Delta\cos\theta & \mathrm{i}\Delta\sin\theta \\ 0 & E_- & \mathrm{i}\Delta\sin\theta & \Delta\cos\theta \\ \Delta\cos\theta & -\mathrm{i}\Delta\sin\theta & -E_- & 0 \\ -\mathrm{i}\Delta\sin\theta & \Delta\cos\theta & 0 & -E_+ \end{pmatrix}. \tag{3.52}$$

If we assume the Zeeman field to be strong we may ignore the E_+ branch and only study the low-energy physics by projecting the Hamiltonian on the E_- branch, which yields

$$\tilde{H} \approx \begin{pmatrix} E_- & \mathrm{i}\sin\theta \\ -\mathrm{i}\sin\theta & -E_- \end{pmatrix} = \left(\frac{p^2}{2m^*} - \mu - \sqrt{\alpha^2 p^2 + V^2} \right) \tau_z - \Delta \frac{\alpha p}{\sqrt{\alpha^2 p^2 + V^2}} \tau_y. \quad (3.53)$$

If we furthermore make a low momentum expansion taking $\frac{\alpha p}{V} \ll 1$ we end up with

$$H \approx \left(\frac{p^2}{2m^*} - \mu - V \right) \tau_z - \Delta \frac{\alpha p}{V} \tau_y, \quad (3.54)$$

which has the corresponding many-body Hamiltonian

$$\mathcal{H} = \int dx\, \Psi^\dagger(x) \left(\frac{p^2}{2m^*} - \tilde{\mu} \right) \Psi(x) + \int dx \left[\frac{\alpha\Delta}{V} \Psi^\dagger(x) p \Psi^\dagger(x) + \frac{\alpha\Delta}{V} \Psi(x) p \Psi(x) \right], \quad (3.55)$$

where V has been included in the chemical potential. We see that this Hamiltonian exactly maps to the Hamiltonian of the Kitaev model, Eq. (2.18), and we do therefore expect it to lead to a Majorana bound state.

3.5 Analytical Majorana Bound States

We have in the previous sections investigated the bulk spectrum of the SM-SC wire and shown that the model in the small momentum approximation reduces to the Kitaev model. However while we have gotten hints that this system can host a topological phase with a pair of Majorana fermions, we still lack to show that this is actually true for a general region in parameter space. We are now going to fill out this gap by explicitly solving the single particle Hamiltonian given by Eq. (3.36) in the case of a semi-infinite wire.

The BdG equations corresponding to the Hamiltonian (3.41) is a system of four coupled second order linear differential equations which in theory can be solved analytically by decoupling the equations. This can be done by writing the equations in matrix form

$$\partial_x \mathbf{v} = \mathbf{M}\mathbf{v}, \quad (3.56)$$

where $\mathbf{v} = (\Psi(x), \partial_x \Psi(x))^{\mathrm{T}}$ is a vector containing the Nambu spinor and its first derivative and $\mathbf{M}$ is an 8×8 matrix consisting of the coefficients in the differential equations. If we let $\mathbf{\Lambda}$ be the matrix of eigenvalues of $\mathbf{M}$ and $\mathbf{U}$ the corresponding matrix of eigenvectors so that $\mathbf{M} = \mathbf{U}\mathbf{\Lambda}\mathbf{U}^{-1}$ we can rewrite the differential equations (3.56) in a decoupled way by introducing $\mathbf{u} = \mathbf{U}\mathbf{v}$ as

$$\partial_x \mathbf{u} = \mathbf{\Lambda}\mathbf{u}. \quad (3.57)$$

The solutions to this equation are of the form $\mathbf{u} = (c_1 \mathrm{e}^{\lambda_1(E)x}, c_2 \mathrm{e}^{\lambda_2(E)x}, \ldots, c_8 \mathrm{e}^{\lambda_8(E)x})$, where $\lambda_i(E), i = 1, 2, \ldots, 8$ are the eigenvalues of $\mathbf{M}$ which in general depend on the energy E. The solutions to the original BdG equation, Eq. (3.56) is then found from

the relation $\mathbf{v} = \mathbf{U}^{-1}\mathbf{u}$ and we thus see that in general the Nambu spinor components of a solution takes the form

$$u_\sigma(x) = \sum_{i=1}^{8} c_i (U^{-1})_{i\sigma} \mathrm{e}^{\lambda_i(E)x}, \tag{3.58}$$

where the 8 coefficients and the energy has to be determined from the boundary conditions and normalization. So it is indeed possible to solve the system analytically and find all the eigenstates and their energies. Unfortunately, in the general case the algebraic equations for the eigenvalues and -vectors are so big and complicated that they cannot be used for investigating if and when the system has Majorana solutions an how these solutions then might look. Due to the form and symmetries of the BdG Hamiltonian (3.41) we can rewrite the equations in a way (following Refs. 37 and 25) that allow us to see that the system can have Majorana bound states localized at the wire ends.

In the following we will consider an infinitely long wire, and if it supports a Majorana bound state, we expect it to have exactly zero energy $E = 0$ and that its wavefunctions are localized at the ends of the wire. From the general argument of particle-hole symmetry we know that if Ψ_+ is a solution with energy $E_+ = 0$, then $\Psi_- = \tau_y\sigma_y\Psi_+^*$ is also a solution with zero energy, $E_- = 0$. Furthermore we note that the Hamiltonian (3.41) is real[1] and therefore Ψ_+^* and Ψ_-^* are also solutions. But we only expect $E = 0$ to be once degenerate, so these two solutions cannot be linearly independent from the other two. In general we may therefore write

$$\Psi_+^* = a\Psi_+ + b\Psi_- \tag{3.59}$$

$$\Psi_-^* = (\tau_y\sigma_y\Psi_+^*)^* = \tau_y\sigma_y\Psi_+ = c\Psi_+ + d\Psi_-. \tag{3.60}$$

Inserting the above expression for Ψ_+^* in the the expression for Ψ_- we find

$$\Psi_- = \tau_y\sigma_y\Psi_+^* = \tau_y\sigma_y(a\Psi_+ + b\Psi_-) \qquad \Leftrightarrow \tag{3.61}$$

$$\Psi_- = (1 - b\tau_y\sigma_y)^{-1} a\tau_y\sigma_y\Psi_+ = \frac{a}{1-b^2}(\tau_y\sigma_y - b)\Psi_+. \tag{3.62}$$

Inserting (3.62) in the expression for Ψ_-^* in (3.60) we get

$$\tau_y\sigma_y\Psi_+ = c\Psi_+ + \frac{ad}{1-b^2}(\tau_y\sigma_y - b)\Psi_+, \tag{3.63}$$

which by rearranging gives the relation

$$\tau_y\sigma_y\Psi_+ = \frac{c(1-b^2) - abd}{1 - b^2 - ad}\Psi_+ = \lambda\Psi_+, \tag{3.64}$$

where λ is a scalar constant. Acting from the left with $\tau_x\sigma_y$ we have

$$(\tau_y\sigma_y)^2\Psi_+ = \lambda(\tau_y\sigma_y)\Psi_+ = \lambda^2\Psi_+, \tag{3.65}$$

[1] As long as the Zeeman field and the effective Rashba spin-orbit field are orthogonal we can always rotate the coordinate system to make the Hamiltonian real.

which, since $(\tau_y\sigma_y)^2 = 1$, constrains λ to take the values ± 1. This means that instead of solving the system for the original Nambu spinor, we can solve for the two Nambu spinors satifying the relation Eq. (3.64) with $\lambda = \pm 1$, ie. where $v_\sigma(x) = \lambda u_\sigma(x)$. In essence, the solution for each λ value correpond to the Majorana wavefunctions of the full fermion solution. To see this we note that the general Nambu spinor solution takes the form

$$\Psi(x) = \begin{pmatrix} u_{\uparrow,+}(x) + u_{\uparrow,-}(x) \\ u_{\downarrow,+}(x) + u_{\downarrow,-}(x) \\ u_{\downarrow,+}(x) - u_{\downarrow,-}(x) \\ -u_{\uparrow,+}(x) + u_{\uparrow,-}(x) \end{pmatrix}, \tag{3.66}$$

where the index $\pm$ denotes the solution for $\lambda = \pm$ respectively. The corresponding quasiparticle operator is then

$$\begin{aligned} \hat{\alpha} = \int dx \Big\{ &[u_{\uparrow,+}(x) + u_{\uparrow,-}]\hat{\Psi}_\uparrow(x) + [u_{\downarrow,+}(x) + u_{\downarrow,-}]\hat{\Psi}_\downarrow(x) \\ &+[u_{\downarrow,+}(x) - u_{\downarrow,-}]\hat{\Psi}^\dagger_\downarrow(x) + [u_{\uparrow,+}(x) - u_{\uparrow,-}]\hat{\Psi}^\dagger_\uparrow(x) \Big\}. \end{aligned} \tag{3.67}$$

This can be written as $\hat{\alpha} = \hat{\gamma}_+ + \mathrm{i}\hat{\gamma}_-$, where the Majorana operators are given by

$$\begin{aligned} \hat{\gamma}_+ &= \frac{1}{2}(\hat{\alpha} + \hat{\alpha}^\dagger) \\ &= \int dx \left(u_{\uparrow,+}(x)\hat{\Psi}_\uparrow(x) + u_{\downarrow,+}(x)\hat{\Psi}_\downarrow(x) + u_{\downarrow,+}(x)\hat{\Psi}^\dagger_\downarrow(x) + u_{\uparrow,+}(x)\hat{\Psi}^\dagger_\uparrow(x) \right), \end{aligned} \tag{3.68}$$

$$\begin{aligned} \hat{\gamma}_- &= -\frac{\mathrm{i}}{2}(\hat{\alpha} - \hat{\alpha}^\dagger) \\ &= -\mathrm{i}\int dx \left(u_{\uparrow,-}(x)\hat{\Psi}_\uparrow(x) + u_{\downarrow,-}(x)\hat{\Psi}_\downarrow(x) - u_{\downarrow,-}(x)\hat{\Psi}^\dagger_\downarrow(x) - u_{\uparrow,-}(x)\hat{\Psi}^\dagger_\uparrow(x) \right), \end{aligned} \tag{3.69}$$

where it can easily be verified that $\hat{\gamma}^\dagger_\pm = \hat{\gamma}_\pm$. Thus if the system has a Majorana bound state we expect to find zero energy solutions for which $u_{\sigma,\pm}$ is located at each end of the wire.

Instead of solving the BdG equations for the full system we may now instead solve for the $\lambda = \pm$ parts separately. In the dimensionless form the BdG equations for one of the Nambu spinors then take the form

$$\begin{aligned} H\Psi(x) &= \begin{pmatrix} -\frac{1}{2}\partial_{\tilde{x}} - \tilde{\mu} & \partial_{\tilde{x}} + \tilde{V} & \tilde{\Delta} & 0 \\ -\partial_{\tilde{x}} + \tilde{V} & -\frac{1}{2}\partial^2_{\tilde{x}} - \tilde{\mu} & 0 & \tilde{\Delta} \\ \tilde{\Delta} & 0 & \frac{1}{2}\partial^2_{\tilde{x}} + \tilde{\mu} & -\partial_{\tilde{x}} + \tilde{V} \\ 0 & \tilde{\Delta} & \partial_{\tilde{x}} + \tilde{V} & \frac{1}{2}\partial^2_{\tilde{x}} + \tilde{\mu} \end{pmatrix} \begin{pmatrix} u_\uparrow(\tilde{x}) \\ u_\downarrow(\tilde{x}) \\ \lambda u_\downarrow(\tilde{x}) \\ -\lambda u_\uparrow(\tilde{x}) \end{pmatrix} \\ &= \begin{pmatrix} \left(-\frac{1}{2}\partial^2_{\tilde{x}} - \tilde{\mu}\right) u_\uparrow(\tilde{x}) + (\partial_{\tilde{x}} + \tilde{V}_x)u_\downarrow(\tilde{x}) + \lambda\tilde{\Delta}u_\uparrow(\tilde{x}) \\ \left(-\frac{1}{2}\partial^2_{\tilde{x}} - \tilde{\mu}\right) u_\downarrow(\tilde{x}) + (-\partial_{\tilde{x}} + \tilde{V}_x)u_\uparrow(\tilde{x}) - \lambda\tilde{\Delta}u_\downarrow(\tilde{x}) \\ \lambda\left(\frac{1}{2}\partial^2_{\tilde{x}} + \tilde{\mu}\right) u_\downarrow(\tilde{x}) - \lambda(-\partial_{\tilde{x}} + \tilde{V}_x)u_\uparrow(\tilde{x}) + \tilde{\Delta}u_\uparrow(\tilde{x}) \\ -\lambda\left(\frac{1}{2}\partial^2_{\tilde{x}} + \tilde{\mu}\right) u_\uparrow(\tilde{x}) + \lambda(\partial_{\tilde{x}} + \tilde{V}_x)u_\downarrow(\tilde{x}) + \tilde{\Delta}u_\downarrow(\tilde{x}) \end{pmatrix} = 0 \end{aligned} \tag{3.70}$$

From this we see that we may reduce the equation involving the 4×4 BdG Hamiltonian to an equivalent equation, involving only a 2×2 matrix, given by

$$\begin{pmatrix} -\frac{1}{2}\partial_{\tilde{x}}^2 - \tilde{\mu} & \partial_{\tilde{x}} + \tilde{V}_x + \lambda\tilde{\Delta} \\ -\partial_{\tilde{x}} + \tilde{V}_x - \lambda\tilde{\Delta} & -\frac{1}{2}\partial_{\tilde{x}}^2 - \tilde{\mu} \end{pmatrix} \begin{pmatrix} u_\uparrow(\tilde{x}) \\ u_\downarrow(\tilde{x}) \end{pmatrix} = 0, \tag{3.71}$$

We note that we may write Eq. (3.71) as two coupled 2nd order differential equations given by

$$u_\uparrow'' + 2\tilde{\mu}u_\uparrow - 2u_\downarrow' - 2(\tilde{V} + \lambda\tilde{\Delta})u_\downarrow = 0 \tag{3.72}$$

$$u_\downarrow'' + 2\tilde{\mu}u_\downarrow + 2u_\uparrow' - 2(\tilde{V} - \lambda\tilde{\Delta})u_\uparrow = 0. \tag{3.73}$$

To decouple the equations we now differentiate Eq. (3.72) twice to find

$$u_\uparrow'''' + 2\tilde{\mu}u_\uparrow'' - 2u_\downarrow''' - (\tilde{V} + \lambda\tilde{\Delta})u_\downarrow'' = 0, \tag{3.74}$$

which now depends on the second and third derivative of $u_\downarrow(\tilde{x})$. An expression for the second derivative is found from Eq. (3.73), which implies

$$u_\downarrow'' = 2(\tilde{V} - \lambda\tilde{\Delta})u_\uparrow - 2u_\uparrow' - 2\tilde{\mu}u_\downarrow, \tag{3.75}$$

and by differentiating we also have

$$u_\downarrow''' = 2(\tilde{V} - \lambda\tilde{\Delta})u_\uparrow' - 2u_\uparrow'' - 2\tilde{\mu}u_\downarrow'. \tag{3.76}$$

Inserting these expressions in Eq. (3.74) we have

$$\begin{aligned} 0 &= u_\uparrow'''' + 2\tilde{\mu}u_\uparrow'' - 2\left[2(\tilde{V} - \lambda\tilde{\Delta})u_\uparrow' - 2u_\uparrow'' - 2\tilde{\mu}u_\downarrow')\right] \\ &\quad - 2(\tilde{V}_x + \lambda\tilde{\Delta})\left[2(\tilde{V}_x - \lambda\tilde{\Delta})u_\uparrow - 2u_\uparrow' - 2\tilde{\mu}u_\downarrow(\tilde{x})\right] \\ &= u_\uparrow'''' + 2(\tilde{\mu}+2)u_\uparrow'' - 8\lambda\tilde{\Delta}u_\uparrow' - 4(\tilde{V}^2 - \tilde{\Delta}^2)u_\uparrow + 4\tilde{\mu}[u_\downarrow' + (\tilde{V}_x + \lambda\tilde{\Delta})u_\downarrow]. \end{aligned} \tag{3.77}$$

From Eq. (3.72) we have $u_\downarrow' + (\tilde{V} + \lambda\tilde{\Delta})u_\downarrow = \frac{1}{2}u_\uparrow'' + \tilde{\mu}u_\uparrow$ which when inserted in Eq. (3.77) totally decouples the differential equations, yielding a homogeneous 4th order linear differential equation for $u_\uparrow(\tilde{x})$ given by

$$0 = u_\uparrow'''' + 4(\tilde{\mu}+1)u_\uparrow'' + 8\lambda\tilde{\Delta}u_\uparrow' + 4[\tilde{\mu}^2 + \tilde{\Delta}^2 - \tilde{V}^2]u_\uparrow. \tag{3.78}$$

A equation of the exact same form is valid for $u_\downarrow(\tilde{x})$. In general this has solutions of the form $u(\tilde{x}) = Ae^{z\tilde{x}}$ and the corresponding characteristic equation for z is

$$z^4 + 4(E + \tilde{\mu} + 1)z^2 + 8\lambda\tilde{\Delta}z + 4C_0 = 0, \tag{3.79}$$

where $C_0 = \tilde{\mu}^2 + \tilde{\Delta}^2 - \tilde{V}^2$. A general full solution to Eq. (3.78) takes the form

$$u_\uparrow(\tilde{x}) = c_1e^{z_1\tilde{x}} + c_2e^{z_2\tilde{x}} + c_3e^{z_3\tilde{x}} + c_4e^{z_4\tilde{x}}, \tag{3.80}$$

where z_n, $n = 1, 2, 3, 4$ are the roots of the characteristic polynomial and c_n are coefficients to be found by matching boundary conditions and by requiring the solutions to be normalized. We note that by writing the characteristic polynomial as an expansion in its roots,

$$\begin{aligned} P(z) &= z^4 + 4(\tilde{\mu}+1)z^2 + 8\lambda\tilde{\Delta}z + 4C_0 \\ &= (z-z_1)(z-z_2)(z-z_3)(z-z_4) \\ &= z^4 - (z_1+z_2+z_3+z_4)z^3 + (z_1z_2+z_1z_3+z_1z_4+z_2z_3+z_2z_4+z_3z_4)z^2 \\ &\quad - (z_1z_2z_3+z_2z_3z_4+z_1z_3z_4)z + z_1z_2z_3z_4, \end{aligned} \tag{3.81}$$

the roots are seen to satisfy the relations given by

$$\prod_{n=1}^{4} z_n = 4C_0 \qquad \text{and} \qquad \sum_{n=1}^{4} z_n = 0. \tag{3.82}$$

These relations allow us to make some general remarks on the existence of Majorana modes. In the case $C_0 > 0$ and all z_n are real the relations (3.82) implies that two of the roots will be < 0 while the other two must be > 0. If one of the roots is complex, $z_1 = a + ib$, then another solution is its complex conjugate, $z_2 = a - ib$ and then from the relations (3.82) we have

$$(a+ib)(a-ib)z_3z_4 = (a^2+b^2)z_3z_4 = 4C_0, \qquad (a+ib)+(a-ib)+z_3+z_4 = 0, \tag{3.83}$$

which combined gives a second order equation for the two remaining roots,

$$z^2 - 2az + \frac{4C_0}{a^2+b^2}, \tag{3.84}$$

having the solutions $z_{3,4} = -a \pm \sqrt{a - 4C_0/(a^2+b^2)}$. In the case where $C_0 > 0$ it is guaranteed that $|a| > |\mathrm{Re}\sqrt{a - 4C_0/(a^2+b^2)}|$, so in general for the C_0 case there are always two solutions with $\mathrm{Re}(z) < 0$ and two with $\mathrm{Re}(z) > 0$, as shown in Fig. 3.7a. From the form of the characteristic polynomium it is clear that the term with λ determines the position of the lowest point of the polynomium, so in the above analysis we see that the value of λ determines the sign of a, and the analysis thus holds for both values of λ. Therefore in the $C_0 > 0$ case there are two decaying and two growing solutions for each value of λ. The solution for each λ value corresponds to the Majorana wavefunctions which should be localised at each end of the wire, and they should satisfy the local boundary condition and are furthermore required to vanish inside the wire and be normalized[2]. The vanishing into the wire forces two of the coefficients to be zero and we are left with two coefficients to determine from boundary conditions and normalization. However, Eq. (3.58) states that the solutions for different spin are connected, and this gives us two boundary conditions and only two coefficients to match, which cannot be fulfilled if the solutions at the same time should be normalized. Thus for $C_0 > 0$ no zero-energy Majorana solutions exists.

[2]Since the left and right solutions do not overlap they can each be normalized separately.

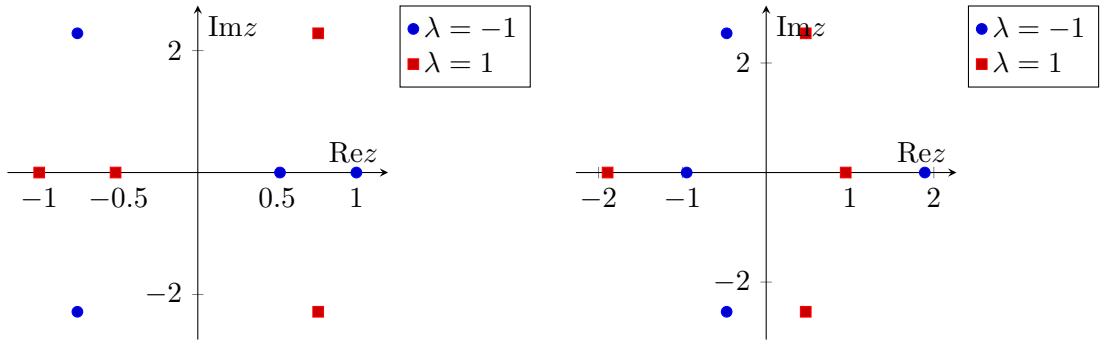

(a) Roots for $C_0 > 0$ with $\mu = 0$, $\Delta = 1$, $V = \frac{1}{2}$.

(b) Roots for $C_0 < 0$ with $\mu = 0$, $\Delta = 1$, $V = 2$.

Figure 3.7: Roots of the characteristic polynomium (3.79) for (a) $C_0 = \frac{3}{4} > 0$ with $\tilde{V} = \frac{1}{2}$ and (b) $C_0 = -3 < 0$ with $\tilde{V} = 2$. In both cases we have used $\tilde{\mu} = 0$ and $\tilde{\Delta} = 1$.

Repeating the analysis for the $C_0 < 0$ case, we see that in this case we always have three solutions with the same sign of Re(z), as seen in Fig. 3.7b. We therefore have three coefficients to find and two constraints from boundary conditions and one from normalization, which can always be satisfied. Zero-energy solutions which are localised at the wire ends does therefore exist for $C_0 < 0$. In Fig. 3.8 one of the spinor components of the wavefunction of the left Majorana for specific set of parameters is shown. It is seen that it is an oscillating function that decays ito the wire, with the frequency and decay length set by the specific parameters. When considering a wire of finite length we will have to relax the requirement of extact zero energy and in general the energy has to be found from satisfying boundary conditions and requiring solutions to be normalized.

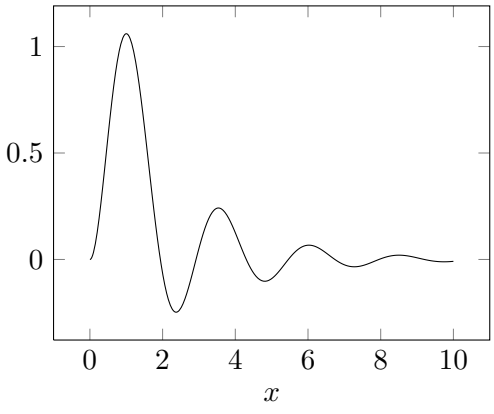

Figure 3.8: Plot of the Majorana wavefunction

3.6 Numerical solutions

In previous section we outlined a method by which the spectrum and eigenfunctions of the Bogoliubov-de Gennes equations for the wire in theory could be solved analytically, but also noted that algebraic equations involved were practically useless. Solving the system for a set of given parameters may be more duable, but it stills involves matching boundary conditions and finding the energy from some probably very complicated relation for each eigenmode. While the acquired accuracy of the eigenfunctions and energies are to the precision of the calculator one uses, this method is still quite tedious, and the precision is rarely needed. To solve the BdG equations for its spctrum and eigenfunctions we are instead going to put the system on a lattice by discretizing the Hamiltonian thereby transforming the BdG equations to a set of linear equations that can be solved effeciently on a computer. This method further has the advantage that we can leave the simple picture of a strictly one-dimensional homogeneous wire and instead consider more realistic systems with several subbands and inhomogenous potentials from e.g. disorder and impurities.

To make the model suitable for numerical solution we discretize the quantum field operators by a lattice constant a such that $\psi(\mathbf{r}) \to c_{\mathbf{i}}$ with $\mathbf{i} = (i_x, i_y, i_z)$ where $1 \leq i_{x,y,z} \leq N_{x,y,z}$. The dimensions of the wire are then given by $L_{x,y,z} = a(N_{x,y,z} + 1)$. By this procedure we have for e.g. the x-direction

$$\begin{aligned}\frac{\partial}{\partial x}\psi(\mathbf{r}) &\to \frac{1}{2a}[c_{\mathbf{i}+\boldsymbol{\delta}_x} - c_{\mathbf{i}-\boldsymbol{\delta}_x}] \\ \frac{\partial^2}{\partial x^2}\psi(\mathbf{r}) &\to \frac{1}{a^2}[c_{\mathbf{i}+\boldsymbol{\delta}_x} + c_{\mathbf{i}-\boldsymbol{\delta}_x} - 2c_{\mathbf{n}}],\end{aligned}$$

with $\boldsymbol{\delta}_x = (1, 0, 0)$. The Hamiltonian thus takes the tight-binding form

$$H = H_0 + H_{\text{so}} + H_{\text{zm}} + H_{\text{sc}} \tag{3.85}$$

with

$$\begin{aligned}H_0 &= \sum_{\mathbf{i},\mathbf{j},\sigma} t_{\mathbf{ij}} c^\dagger_{\mathbf{i}\sigma} c_{\mathbf{j}\sigma} - \mu \sum_{\mathbf{i}\sigma} c^\dagger_{\mathbf{i}\sigma} c_{\mathbf{i}\sigma} \\ H_{\text{so}} &= i\frac{\alpha}{2a} \sum_{\mathbf{i},\boldsymbol{\delta}} \left[c_{\mathbf{i}+\boldsymbol{\delta}_x,\sigma} (\sigma_y)_{\sigma\sigma'} c_{\mathbf{i},\sigma} - c_{\mathbf{i}+\boldsymbol{\delta}_y,\sigma} (\sigma_x)_{\sigma\sigma'} c_{\mathbf{i},\sigma'} + h.c. \right] \\ H_{\text{zm}} &= \sum_{\mathbf{i},\sigma\sigma'} c^\dagger_{\mathbf{i},\sigma} (\mathbf{V} \cdot \boldsymbol{\sigma})_{\sigma\sigma'} c_{\mathbf{i},\sigma} \\ H_{\text{sc}} &= \sum_{\mathbf{i}} \left[\Delta_{\mathbf{i}} c^\dagger_{\mathbf{i},\uparrow} c_{\mathbf{i},\downarrow} + h.c. \right]\end{aligned}$$

We only consider nearest neighbor hopping, $t_{\mathbf{ii}} = 2t_0$ and an on-site contribution $t_{\mathbf{ii}+\boldsymbol{\delta}} = -t_0$, where $t_0 = \frac{\hbar^2}{2m^* a^2}$. This model can easily be implemented numerically by projecting the corresponding Bogoliubov-de Gennes Hamiltonian on the single-particle position states. However with $N_x \sim 10^3$, $N_y \sim 10^2$ and $N_z \sim 10$ the Hilbert space will be of

size $\sim 4 \times 10^6$ making a direct diagonalization computationally intensive. Instead we will treat the spin-orbit interaction, Zeeman-field and superconductivity as pertubations to the free Hamiltonian and project the full Hamiltonian on the low energy states of H_0, which will contain the most relevant physics, thereby reducing the Hilbert space drastically. Solving the eigenproblem of H_0 is lucklily easily done and the eigenfunctions are

$$\psi_{\mathbf{n}\sigma}(\mathbf{i}) = \prod_{\mu=x,y,z} \sqrt{\frac{2}{N_\mu + 1}} \sin \frac{\pi n_\mu i_\mu}{N_\mu + 1} \chi_\sigma \tag{3.86}$$

where $\mathbf{n} = (n_x, n_y, n_z)$, with $1 \leq n_\mu \leq N_\mu$, and χ_σ is an eigenvector of a Pauli matrix. The corresponding eigenenergies are

$$\epsilon_{\mathbf{n}} = -2t_0 \sum_{\mu=x,y,z} \left(\cos \frac{\pi n_\mu}{N_\mu + 1} - 1 \right) - \mu. \tag{3.87}$$

To include all the other parts of the Hamiltonian, they have to be rewritten in this basis. By some math the matrix elements of the spin-orbit part is given by

$$\begin{aligned} \langle \psi_{\mathbf{n}\sigma} | H_{\text{sc}} | \psi_{\mathbf{n}'\sigma'} \rangle = \alpha \delta_{n_z n_z'} \Bigg\{ & \frac{1 - (-1)^{n_x + n_x'}}{N_x + 1} (i\sigma)_{\sigma\sigma'} \frac{\sin \frac{\pi n_x}{N_x+1} \sin \frac{\pi n_x'}{N_x+1}}{\cos \frac{\pi n_x}{N_x+1} - \cos \frac{\pi n_x'}{N_x+1}} \delta_{n_y n_y'} \\ & - (x \leftrightarrow y) \Bigg\}, \end{aligned} \tag{3.88}$$

where the $(x \leftrightarrow y)$ term corresponds to the first term with x and y interchanged. The electric and magnetic potential terms are

$$\langle \psi_{\mathbf{n}\sigma} | H_{\text{el}} | \psi_{\mathbf{n}'\sigma'} \rangle = \sum_{\mathbf{i}} U_{\mathbf{i}} \psi^*_{\mathbf{n}\sigma}(\mathbf{i}) \psi_{\mathbf{n}'\sigma'}(\mathbf{i}) \tag{3.89}$$

$$\langle \psi_{\mathbf{n}\sigma} | H_{\text{zm}} | \psi_{\mathbf{n}'\sigma'} \rangle = \sum_{\mathbf{i}} \psi_{\mathbf{n}\sigma}(\mathbf{i}) \{ \mathbf{V}(\mathbf{i}) \cdot \boldsymbol{\sigma} \}_{\sigma\sigma'} \psi^*_{\mathbf{n}\sigma}(\mathbf{i}) \tag{3.90}$$

The numerical implementation has been carried out in MATLAB which was chosen due to its accessible and effecient matrix tools. I will here sketch how the implementation has been performed. We want to numerically investigate a one- or two-dimensional model of the wire and thus the wave-functions are multidimensional scalar fields. In MATLAB a scalar field can simply be represented as a vector with the index corresponding to position. However for multidimensional fields we need to combine the dimensions so that the position can be represented by a single index. The wavefunctions, Eq. (3.86), are a product of wavefunctions in each dimension so a single index wavefunction vector

is constructed by taking the Kronecker product of the wavefunctions in each dimension

$$\Psi = \psi_z \otimes \psi_y \otimes \psi_x = \begin{bmatrix} \psi_z(1)\psi_y(1)\psi_x(1) \\ \psi_z(1)\psi_y(1)\psi_x(2) \\ \vdots \\ \psi_z(1)\psi_y(1)\psi_x(N_x) \\ \psi_z(1)\psi_y(2)\psi_x(1) \\ \vdots \\ \psi_z(N_z)\psi_y(N_y)\psi_x(N_x) \end{bmatrix} \tag{3.91}$$

The eigenbasis Hamiltonian matrix $\mathbf{H}_0$ is constructed as a matrix consisting of the energies given by Eq. (3.87) in the diagonal up to a certain cutoff energy $E_{\max}$ thereby approximating the system to only involve a certain number of states $N_{\mathrm{m}} \ll N_x N_y N_z$. The corresponding wavefunctions are given as the columns of the wavefunction matrix $\mathbf{M}$ of size $N_x N_y N_z \times N_{\mathrm{m}}$. When the electric and magnetic potentials have been rewritten as single index vectors their representation in the eigenbasis of $\mathbf{H}_0$ are then easily calculated as

$$\tilde{\mathbf{U}} = \mathbf{M}^\dagger \mathbf{U} \mathbf{M}, \qquad \tilde{\mathbf{V}}_{x,y,z} = \mathbf{U}^\dagger \mathbf{V}_{x,y,z} \mathbf{U}, \qquad \tilde{\mathbf{\Delta}} = \mathbf{U}^\dagger \mathbf{\Delta} \mathbf{U}. \tag{3.92}$$

We then construct the BdG Hamiltonian as given by Eq. (3.41) and solve the corresponding eigenvalue problem to obtain the the spectrum and wavefunctions.

To carry out the numerical calculations we take as parameters values which are the same or close to those reported in recent experiments with InSb nanowires in contact with a NbTiN superconductor [30]. In InSb the effective electron mass is $m = 0.015\,\mathrm{m_e}$ and in nanowires a spin-orbit length of $l_{\mathrm{so}} = 200\,\mathrm{nm}$ has been reported, leading to a Rashba parameter $\alpha = 0.2\,\mathrm{eV\,Å}$. This sets the energy scale of the spectrum to $E_0 = \frac{m\alpha^2}{2} = 79\,\mu\mathrm{eV}$ and the corresponding length scale is $l_0 = \frac{m\alpha}{\hbar} = 254\,\mathrm{nm}$. NbTiN has a superconducting gap of $\sim 2\,\mathrm{meV}$ and Mourik et al. reported a supposedly induced superconducting gap of $\sim 250\,\mu\mathrm{eV}$ so we have used values of that same order. In the effective model of section 3.4 this means that the effectice superconductor coupling is of order $\sim 0.3\,\mathrm{meV}$. InSb has an effective g-factor of ~ 50 which implies that we only need to apply a moderate magnetic field, small enough to not destroy the superconductivity. In the numerical calculations we have used a lattice constant of 5 Å which means that a wire of length $5\,\mu\mathrm{m}$ will be discretized in 10^4 sites. Moreover we assume that the wire is very flat so that only one subband in the z-direction is occupied and thus we can neglect this dimension all together by simply taking the number of sites in the z-direction as $N_z = 1$.

We first consider a $5\,\mu\mathrm{m}$ long strictly one-dimensional wire with $N_x = 1 \times 10^4$ and $N_y = 1$ with Rashba parameter $\alpha_{\mathrm{r}} = 0.2\,\mathrm{eV\,Å}$ and induced gap of $200\,\mu\mathrm{eV}$. The BDG spectrum of the first modes is shown in Fig. 3.9. In Fig. 3.9a showing the spectrum of the first 100 modes and their hole equivalents the general features of the bulk spectrum can be seen and one can somewhat read off the induced superconducting gap which however has been suppressed by the magnetic field for the lowest energy modes. In Fig. 3.9b the lowest energy modes are shown and here we clearly see the existence of a

zero-energy mode. As such the fact that this mode has zero energy does not neccessarily

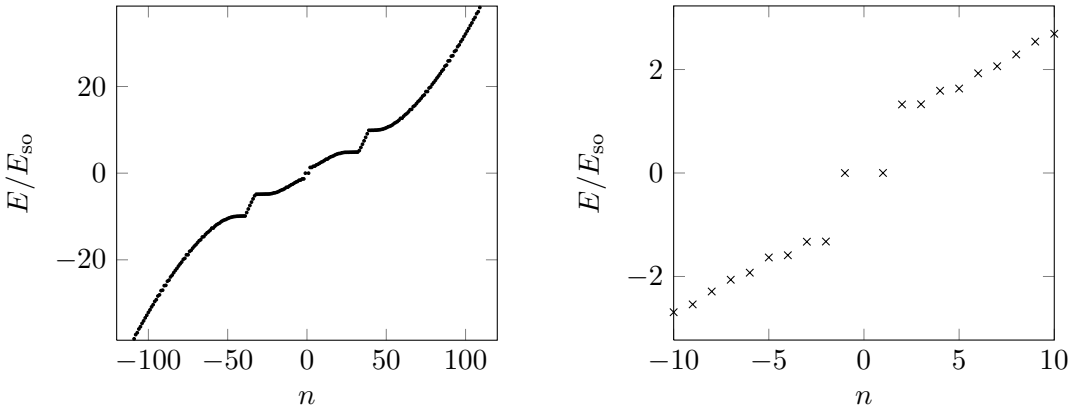

(a) Lowest 100 states.

(b) Lowest 10 states.

Figure 3.9: Excitation energies. The energies have been calculated using parameters corresponding to a spin-orbit energy $E_{\mathrm{so}} = 79\,\mu\mathrm{eV}$ a length scale of $l_0 = 254\,\mathrm{nm}$ and a length of the wire of $L = 5.3\,\mu\mathrm{m}$.

imply that it is a Majorana bound state. One could change the system parameters and check if the state stayed at zero energy, but still this only verifies that it is a bound state and does not show that it corresponds to localized majorana modes. Instead we consider the wavefunction as shown in Fig. 3.10 and see that the mode is in fact localized at the ends of the wire whereas the $n = 2$ (and higher) modes extends over the full width of the wire. To fully verify that this is due to localized Majoranas we explicitly calculate

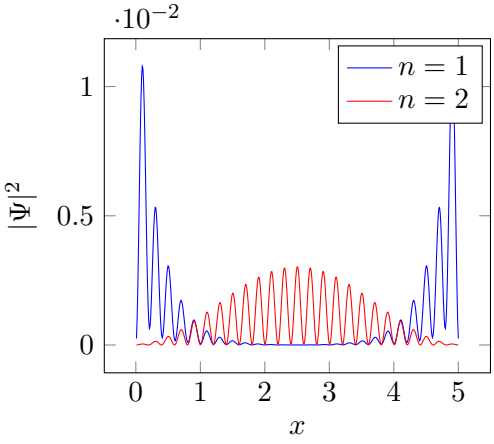

Figure 3.10: Squared amplitude of the particle part of the wavefunctions of the lowest modes.

the wavefunctions corresponding to the left/right Majorana operators $\gamma_{\mathrm{L},n} = c_n + c_n^\dagger$ and $\gamma_{\mathrm{R},n} = -i(c_n - c_n^\dagger)$. The particle components of the wavefunctions are thus given by $u_{\mathrm{R}n\sigma}(x) = u_{n\sigma}(x) + v_{n\sigma}^*(x)$ and $u_{\mathrm{L}n\sigma}(x) = u_{n\sigma}(x) - v_{n\sigma}^*(x)$. In Fig. 3.11 we see that

the wavefunctions of the left and right Majoranas for the zero-energy mode are located at each end of the wire confirming that this is a Majorana bound state. In constrast we see that the Majorana wavefunctions for the higher energy state overlaps over the entire length of the wire and are thus clearly not localized. We also note that even though we consider a wire of finite length, the wavefunction of the Majorana modes does not change qualitatively from them obtained in the case of an infinite wire shown in Fig. 3.8.

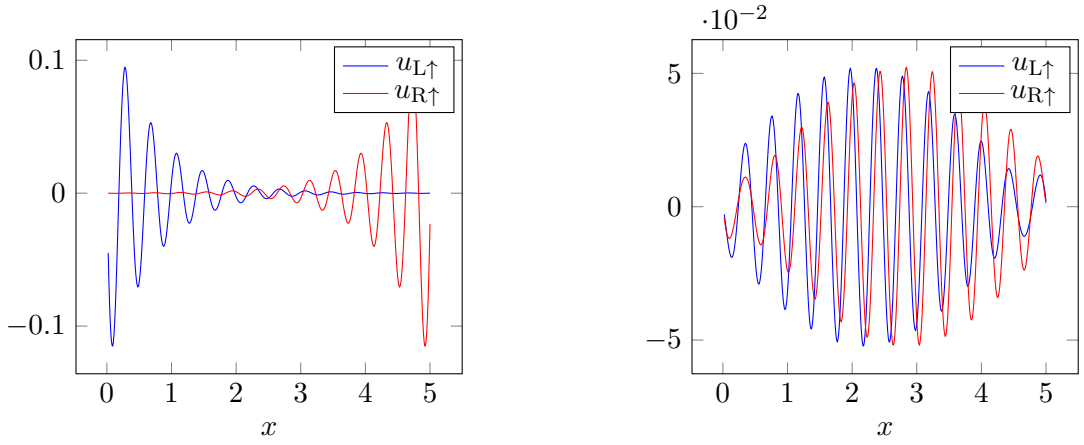

(a) Mode n=1

(b) Mode n=2

Figure 3.11: Particle spin up components of the left and right Majorana wavefunctions of the two lowest energy modes. (a) For the first mode the majorana wavefunctions do barely overlap and the state has localized Majoranas. (b) The Majorana wavefunctions corresponding to the state with $n = 2$ overlaps over the whole length of the wire and the Majoranas can therefore not be considered localized.

Though not clear from the spectrum, Fig. 3.9b, the Majorana modes are not situated at exactly zero energy, but do have a small energy do to the finite overlap of their wavefunctions. When increasing the Zeeman field we expect the decay length of the wavefunctions to increase leading to a bigger overlap and thus higher energy. Furthermore we expect the bulk gap to decrease for increasing Zeeman field as we saw in Fig. 3.6, so in Fig. 3.12 we show how these features carries over in the finite length wire. From the figure it is clear that the bulk gap follows pretty well the behavior found for the infinite wire for small Zeeman fields, but for larger Zeeman fields an oscillating behavior is seen. The same is true for the energy of the Majorana mode, which after the wire has entered the topological phase at the critical Zeeman field is effectively zero until the Zeeman field causes it to oscillate with an increasing amplitude. The oscillating behavior is due to the finite size and can be understood as the result of interference between the left and right parts of the wavefunctions. Again we note that the size of the spin-orbit coupling sets the scale of the bulk gap, as we also found earlier. The spin-orbit coupling also sets the decay length of the Majorana wavefunctions and thus we see that for a big spin-orbit coupling the energy of the Majorana mode generally stays at approximately

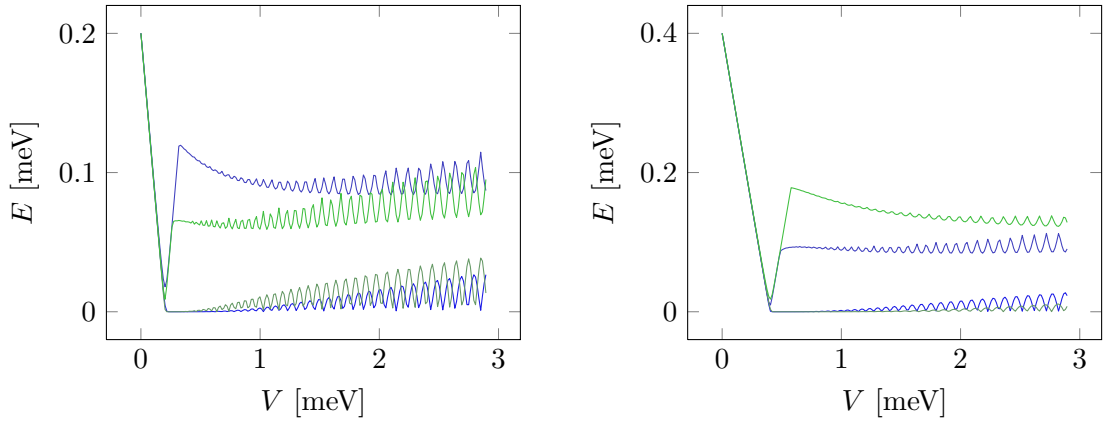

(a) (b)

Figure 3.12: Energy of the two lowest modes as a function of Zeeman field.

zero energy for larger Zeeman fields.

3.7 Quantum Computation with Majorana bound states in nanowires

While two separated Majorana fermions may be combined into a nonlocal fermion to define a topologically protected qubit system, in order to use this system to perform any calculations one will have to physically braid Majorana fermions from two distict qubit systems. This could initially be thought to be a mayor problem for this 1d system, since first of all we need to move the Majoranas along the wire and secondly we need to braid two Majoranas, a process which is ill-defined in one dimension since there seems to be no way the particles can move around each other. The first problem can be overcome by placing gates along the wire such that the local chemical potential can be controlled. In this way one can move the domain walls of the topological phase an thereby the Majorana fermions by gradually switching gates on and off. The second problem can in fact also "easily" be overcome by constructing networks of nanowires perpendicular to each other such that they form intersections. It is then, in theory, possible to move one Majorana fermion from one wire into another and temporarily park it here while another Majorana from a connecting takes its initial position, see Fig. 3.13. If this process of a Majorana three point turn is repeated, one actually ends up braiding the two Majorana fermions. It has been shown [1, 7] that this process actually has the same braiding statistics as the vortices on the surface on p-wave superconductor.

However, there are other problems with using Majorana fermions as qubits systems. First of all the two degenerate groundstates corresponding to a Majorana pair differ by one fermion. This fermion is essentially an electron which is in the wire or superconductor somewhere. This means that if an electron can tunnel into the system from the

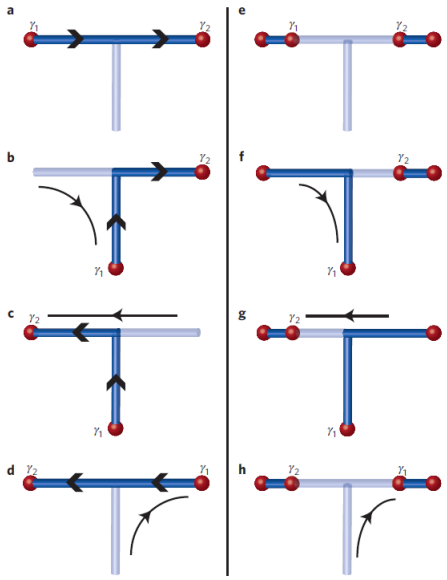

Figure 3.13: Networks of nanowires can be used to braid Majorana fermions. Figure a to d shows how two Majorana fermions belonging to the same fermion can be braided by use of an auxilary wire. Figure e to h shows how two Majoranas belonging to different fermions can be braided using an auxilary wire. Figure from Ref. 1.

environment this will change the state of the fermion level, a process called *quasiparticle poisoning*. One can avoid this by electrically isolating the wire and superconductor from the surrounding system and making sure that the electronic states of the neighboring materials are separated by a gap to the Majorana levels. But then there is the problem that the Majorana is now sitting on an isolated "island" and the two states, which differ by a fermion, will then be capacitatively coupled to other islands implicitly coupling the different fermion systems. The solution to this problem is to store each qubit in two pairs of Majorana fermions, i.e. by placing two wires on the same superconductor. The combined system will always have the same fermion number and the qubit states then correspond to whether one of the wires is in the even or odd parity state. This however means that one has to measure the state of both wires to determine the qubit state.

Chapter 4

Tunnelling Spectroscopy

Perhaps the simplest way to experimentally detect the presence of a Majorana bound state in a superconductor-nanowire system is by measuring its transport characteristics like tunnelling differential conductance. This can be done by connecting leads with a thin insulating layer to the ends of the wire so than when a bias voltage is applied the current-voltage characteristics can be measured, see Fig. 4.1. Since the Majorana bound state is ensured to have zero energy electrons are free to tunnel in and out of the wire with no energy cost and in the presence of a MBS we therefore expect the differential conductance to have a peak at zero bias voltage. In real systems zero bias peaks may also arise due to other artifacts or competeting phenomena, however a quite clear signature of the Majorana is if the zero bias peak sustains while changing the system parameters. Still transport experiments like those described above can only detect the presence of a mode with zero energy and as we will see, to some extend be used to map the amplitude of its wavefunction and thus these types of experiments only exploit whether the *necessary* conditions for Majorana states are satisfied. Another necessary signature of a Majorana bound state is the 4π periodic Josephson current [17, 12], which is also called the fractional Josephson effect, since it is stems from the fact that the Josephson current is not carried by Cooper pairs but instead by a single electron which is half of a Cooper pair. While these two signatures will probably convince the most people of the existence of a Majorana bound state, the unambigiously proof this one has to verify the braiding statistics via some interference experiment.

In this section we will focus on the determination of the tunnelling characteristics of a nanowire with Majorana bound states. There are traditionally two ways of calculating the current from one system to another: a) the method of using scattering matrix theory where one calculates the transmission and reflection coefficients of a wave incoming on the interface between the two systems or b) og using the tunnelling Hamiltonian approach where the two systems are initially treated indenpendently and the contact between the systems are provided by a tunnelling term in the total Hamiltonian that couples the two systems. In this method an expression for the current can typically be found by use of the formalism of non-equilibrium Green's functions also called the Keldysh formalism. However, since we consider a superconducting system which has terms in

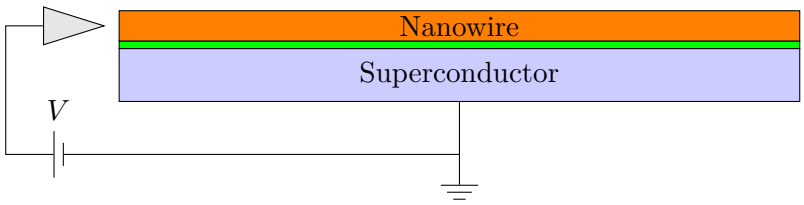

Figure 4.1: A schematic showing the setup. The superconductor does not conserve the electron number and can thus be considered connected to ground.

the Hamiltonian that does not conserve the particle number, the usual usual methods have to by altered slightly. In the normal transport picture when an electron with momentum k and energy E in the lead impinges on the interface between the lead and considered system it will get reflected if there are no available states in the system with energy less than E and transmitted otherwise. If the energy levels in the system are well enough separated, i.e. if the system is small enough, this leads to the experimental observation of quantized conductance. In superconductors we would therefore naively expect that the conductance is strictly zero (at zero temperature) for bias voltages below the superconducting gap, which is the minimum excitation energy. This is however not true, because if two electrons with the same energy tunnelled into the system at the same time they could form a Cooperpair which will be added to the superconducting groundstate, a process which can happen for any energy above the groundstate energy. In the formalism of Blonder, Tinkham and Klapwijk [5] one can also view this process as a single particle process where an electron with energy E impinging on the interface is reflected as a hole with energy $-E$, which is called an Andreev reflection [2]. If $t(E)$ is the transmission amplitude for a single electron with energy E then the transmission amplitude for an Andreev reflection is of the order $t(E)^2$ since it is a two electron process, and we therefore expect the conductance due to Andreev reflection to be suppressed in the weak tunnelling limit and dominated by Andreev reflections in the opposite regime.

The scattering matrix and BTK-method are easy ways to calculate the tunnelling current and conductance of a superconducting system when one is only interested in a few modes or when a continuous variable such as momentum is a good quantum number and they have already been used to predict the zero bias conductance peak of a system with Majorana bound states [21, 23, 33]. On the other hand if the system is complicated in the sense that it may be of finite size, special geometry, be inhomogeneous, have disorder or impurities or have interaction effects, it may be easier to treat it using the tunnelling Hamiltonian approach, where current can be expressed in terms of non-equilibrium Green's functions. Since the nanowire system we are investigating is already a complicated system, we adobt the non-equilibrium Green's function method, which as we will see also has the advantage that it is very easily implemented numerically using the methods of Sec. 3.6.

4.1 General expression for the current into a superconducting system

In this section we will develop an expression for the current through a superconducting system in a setup similar to that shown in Fig. 4.1. We will use the tunnelling Hamiltonian approach and the calculations will in general follow the lines of Ref. 28 where a non-superconcucting system is treated.

We will denote the superconducting system as the central system and for the sake of generality consider the case where the central region can be connected to multiple leads. The system can then be modelled by the following effective Hamiltonian

$$H = H_{\mathrm{c}} + \sum_{\alpha} H_{\alpha} + \sum_{\alpha} H_{\mathrm{t},\alpha}, \tag{4.1}$$

where H_α is the Hamiltonian of the the lead denoted by α, H_{c} is the Hamiltonian of the central superconducting system and $H_{\mathrm{t},\alpha}$ is the tunnelling Hamiltonian, describing the coupling of each lead and the central region. Initially at time $t = -\infty$ we assume that the systems are uncoupled and in equilibrium, i.e. $H_{\mathrm{T}} = 0$. The systems are then brought into contact, and since the chemical potentials of the subsystems may not be equal, the system will in general not be in equilibrium and a current will flow between the systems. If the leads are connected to big electron resevoirs such as a battery or a powersupply the chemical potentials of the leads will be constant and after some time, say at $t = 0$, a steady state current through the central region has been reached.

While we want to study a nanowire with induced superconductivity, we will for the time being simply consider the central region as being an arbitrary superconducting system, which can be modelled by

$$H_{\mathrm{c}} = \sum_{ij} \psi^{\dagger}_{\mathrm{c}i} \mathcal{H}_{ij} \psi_{\mathrm{c}j} + \sum_{ij} \left(\psi^{\dagger}_{\mathrm{c}i} \Delta_{ij} \psi^{\dagger}_{\mathrm{c}j} + \psi_{\mathrm{c}i} \Delta^{*}_{ij} \psi_{\mathrm{c}j} \right) + V_{\mathrm{int}}(\{\psi^{\dagger}_{\mathrm{c}i}\}, \{\psi_{\mathrm{c}j}\}), \tag{4.2}$$

where the summation indices represents the the quantum numbers, typically spacial position and spin, i.e. $i = (\mathbf{r}, \sigma)$. The corresponding free Hamiltonian, i.e. with $V_{\mathrm{int}}(\{\psi^{\dagger}_{\mathrm{c}i}\}, \{\psi_{\mathrm{c}j}\}) = 0$ can be diagonalized by a Bogoliubov transformation

$$\begin{pmatrix} \psi_{\mathrm{c}i} \\ \psi^{\dagger}_{\mathrm{c}i} \end{pmatrix} = \sum_{\mu} \mathbf{U}_{i\mu} \begin{pmatrix} d_{\mu} \\ d^{\dagger}_{\mu} \end{pmatrix} \quad \Leftrightarrow \quad \begin{pmatrix} d_{\mu} \\ d^{\dagger}_{\mu} \end{pmatrix} = \sum_{i} \mathbf{U}^{\dagger}_{i\mu} \begin{pmatrix} \psi_{\mathrm{c}i} \\ \psi^{\dagger}_{\mathrm{c}i} \end{pmatrix}, \quad \mathbf{U}_{i\mu} = \begin{pmatrix} u_{i\mu} & v_{i\mu} \\ v^{*}_{i\mu} & u^{*}_{i\mu} \end{pmatrix}, \tag{4.3}$$

where the coefficients $u_{i\mu}$, $v_{i\mu}$ are found from solving the corresponding Bogoliubov-de-Gennes equations. In the eigenbasis the Hamiltonian simply takes the form

$$H_{\mathrm{c}} = \sum_{\mu} \epsilon_{\mu} d^{\dagger}_{\mu} d_{\mu} + V_{\mathrm{int}}(\{d^{\dagger}_{\mu}\}, \{d_{\mu}\}), \tag{4.4}$$

where ϵ_μ are the positive energy solutions to the BdG equations and $V_{\mathrm{int}}(\{d^{\dagger}_{\mu}\}, \{d_{\mu}\})$ is the interaction part rewritten in the eigenbasis. The leads will typically be metallic and describing them as a free electron gas is thus a good approximation and this will in

fact be required for this method to work. However, in theory we can also include the case where the leads are superconducting as long as this can be described in the BCS framework. Though we will actually not consider that case we here just briefly show how this general case treated. The BCS Hamiltonians for the leads are

$$H_\alpha = \sum_{ij} \psi^\dagger_{\alpha i} \mathcal{H}_{\alpha ij} \psi_{\alpha j} + \sum_{ij} \left(\psi_{\alpha i} \Delta_{\alpha ij} \psi_{\alpha j} + \psi^\dagger_{\alpha i} \Delta^*_{\alpha ij} \psi^\dagger_{\alpha j} \right). \tag{4.5}$$

As in the case of the central region the eigenbasis is found by solving the BdG-equations and the corresponding eigenstate annihilation operator is $c_{\alpha k} = \sum_i (u^*_{i\alpha k} \psi_{\alpha i} + v_{i\alpha k} \psi^\dagger_{\alpha i})$ where k labels the eigenstate. The Hamiltonian can then be written

$$H_\alpha = \sum_k \varepsilon_{\alpha k} c^\dagger_{\alpha k} c_{\alpha k}. \tag{4.6}$$

As usual we can define a matrix in Nambu space, $\mathbf{U}_{i\alpha k}$ defining the Bogoliubov transformation diagonalization of the lead Hamiltonian. We also ote that in the case of normal metallic leads the hole part of the eigenstates vanish, $v_{i\alpha k} = 0$. The tunnelling Hamiltonian describes the tunnelling of electron between the lead and the central region and is

$$H_{\mathrm{t},\alpha} = \sum_{ij} \left(t_{\alpha ij} \psi^\dagger_{\alpha i} \psi_{\mathrm{c}j} + t^*_{\alpha ij} \psi^\dagger_{\mathrm{c}i} \psi_{\alpha j} \right) \tag{4.7}$$

$$= \begin{pmatrix} \psi^\dagger_{\alpha i} & \psi_{\alpha i} \end{pmatrix} \begin{pmatrix} t_{\alpha ij} & 0 \\ 0 & -t^*_{\alpha ij} \end{pmatrix} \begin{pmatrix} \psi_{\mathrm{c}j} \\ \psi^\dagger_{\mathrm{c}j} \end{pmatrix} \tag{4.8}$$

$$= \begin{pmatrix} \psi^\dagger_{\alpha i} & \psi_{\alpha i} \end{pmatrix} \mathbf{T}_{\alpha ij} \begin{pmatrix} \psi_{\mathrm{c}j} \\ \psi^\dagger_{\mathrm{c}j} \end{pmatrix}. \tag{4.9}$$

In the eigenbasis this becomes

$$H_{\mathrm{t}\alpha} = \sum_{ij,k\mu} \begin{pmatrix} c^\dagger_{\alpha k} & c_{\alpha k} \end{pmatrix} \mathbf{U}^\dagger_{i\alpha k} \mathbf{T}_{\alpha ij} \mathbf{U}_{j\mu} \begin{pmatrix} d_\mu \\ d^\dagger_\mu \end{pmatrix} \tag{4.10}$$

$$= \sum_{k\mu} \begin{pmatrix} c^\dagger_{\alpha k} & c_{\alpha k} \end{pmatrix} \mathbf{T}_{\alpha k\mu} \begin{pmatrix} d_\mu \\ d^\dagger_\mu \end{pmatrix} \tag{4.11}$$

$$= \sum_{k\mu} \left(t_{\alpha k\mu} c^\dagger_{\alpha k} d_\mu + w_{\alpha k\mu} c^\dagger_{\alpha k} d^\dagger_\mu + t^*_{\alpha k\mu} d^\dagger_\mu c_{\alpha k} + w^*_{\alpha k\mu} d_\mu c_{\alpha k} \right), \tag{4.12}$$

where we have defined

$$\mathbf{T}_{\alpha k\mu} = \begin{pmatrix} t_{\alpha k\mu} & w_{\alpha k\mu} \\ -w^*_{\alpha k\mu} & -t^*_{\alpha k\mu} \end{pmatrix} = \sum_{ij} \mathbf{U}^\dagger_{i\alpha k} \mathbf{T}_{\alpha ij} \mathbf{U}_{j\mu}. \tag{4.13}$$

Having rewritten the problem in the eigenbasis of the lead and wire we are now able to write an expression for the current from lead α and into the central region. The electrical

current is the current of positive charge from the lead into the central region which is equal to the number of electrons leaving the wire and getting into the lead per unit time times the elementary charge, therefore when a steady state situation has been obtained at $t = 0$ the current is given by

$$I_\alpha = e\langle \dot{N}_\alpha(0)\rangle = \frac{ie}{\hbar}\langle [H, N_\alpha](0)\rangle \tag{4.14}$$

The number operator N_α commutes with the both lead Hamiltonian and the central region Hamiltonian so we only need to calculate the commutator of the number operator and the tunneling Hamiltonian, which is

$$[H_{t\alpha}, N_\alpha] = \left[\sum_{k\mu}\left\{t_{\alpha k\mu}c^\dagger_{\alpha k}d_\mu + w_{\alpha k\mu}c^\dagger_{\alpha k}d^\dagger_\mu + t^*_{\alpha k\mu}d^\dagger_\mu c_{\alpha k} + w_{\alpha k\mu}d_\mu c_{\alpha k}\right\}, \sum_{k'} c^\dagger_{\alpha k'}c_{\alpha k'}\right] \tag{4.15}$$

$$\begin{aligned} &= \sum_{kk',\mu}\Big\{t_{\alpha k\mu}[c^\dagger_{\alpha k}d_\mu, c^\dagger_{\alpha k'}c_{\alpha k'}] + w_{\alpha k\mu}[c^\dagger_{\alpha k\sigma}d^\dagger_\mu, c^\dagger_{\alpha k'}c_{\alpha k'}] \\ &\quad + t^*_{\alpha k\mu}[d^\dagger_\mu c_{\alpha k}, c^\dagger_{\alpha k'}c_{\alpha k'}] + w^*_{\alpha k\mu}[d_\mu c_{\alpha k}, c^\dagger_{\alpha k'}c_{\alpha k'}]\Big\}. \end{aligned} \tag{4.16}$$

Using that

$$\begin{aligned} [c^\dagger_{\alpha k}d^{(\dagger)}_\mu, n_{\alpha k'}] &= -c_{\alpha k}d^{(\dagger)}_\mu\delta_{kk'} \\ [d^{(\dagger)}_\mu c_{\alpha k}, n_{\alpha k'}] &= d^{(\dagger)}_\mu c_{\alpha k}\delta_{kk'} \end{aligned} \tag{4.17}$$

we end up with

$$[H_{t\alpha}, N_\alpha] = \sum_{k\mu}\left\{-t_{\alpha k\mu}c^\dagger_{\alpha k}d_\mu - w_{\alpha k\mu}c^\dagger_{\alpha k}d^\dagger_\mu + t^*_{\alpha k\mu}d^\dagger_\mu c_{\alpha k} + w_{\alpha k\mu}d_\mu c_{\alpha k}\right\}. \tag{4.18}$$

Thus the current may be written

$$I_\alpha = \frac{ie}{\hbar}\sum_{k\mu}\left\{-t_{\alpha k\mu}\langle c^\dagger_{\alpha k}d_\mu\rangle - w_{\alpha k\mu}\langle c^\dagger_{\alpha k}d^\dagger_\mu\rangle + t^*_{\alpha k\mu}\langle d^\dagger_\mu c_{\alpha k}\rangle + w_{\alpha k\mu}\langle d_\mu c_{\alpha k}\rangle\right\} \tag{4.19}$$

and we see that in general it contains terms corresponding to anormalous tunnelling, where a conduction electron from the lead tunnels into the superconductor as a hole. It will later prove useful to have the expression standing in both a particle-hole, which we obtain by anti-commuting half of all the terms,

$$I_\alpha = \frac{ie}{2\hbar}\sum_{k\mu}\Big\{-t_{\alpha k\mu}\langle c^\dagger_{\alpha k}d_\mu\rangle - w_{\alpha k\mu}\langle c^\dagger_{\alpha k}d^\dagger_\mu\rangle - w^*_{\alpha k\mu}\langle c_{\alpha k}d_\mu\rangle - t^*_{\alpha k\mu}\langle c_{\alpha k}d^\dagger_\mu\rangle \tag{4.20}$$

$$+t^*_{\alpha k\mu}\langle d^\dagger_\mu c_{\alpha k}\rangle + w_{\alpha k\mu}\langle d^\dagger_\mu c^\dagger_{\alpha k}\rangle + w^*_{\alpha k\mu}\langle d_\mu c_{\alpha k}\rangle + t_{\alpha k\mu}\langle d_\mu c^\dagger_{\alpha k}\rangle\Big\} \tag{4.21}$$

$$= -\frac{e}{2\hbar}\sum_{k\mu}\Big\{t_{\alpha k\mu}G^<_{\mu\alpha k}(0) + w_{\alpha k\mu}F^<_{\mu\alpha k}(0) + w^*_{\alpha k\mu}\bar{F}^<_{\mu\alpha k}(0) + t^*_{\alpha k\mu}\bar{G}^<_{\mu\alpha k}(0) \tag{4.22}$$

$$-t^*_{\alpha k\mu}G^<_{\alpha k\mu}(0) - w_{\alpha k\mu}F^<_{\alpha k\mu}(0) - w^*_{\alpha k\mu}\bar{F}^<_{\alpha k\mu}(0) - t_{\alpha k\mu}\bar{G}^<_{\alpha k\mu}(0)\Big\} \tag{4.23}$$

where we have introduced the non-equilibrium Green's "lesser" function $G^<_{\mu\alpha k}(t,t') = i\langle c^\dagger_{\alpha k}(t')d_\mu(t)\rangle$ and the anomalous Green's function $F^<_{\mu\alpha k}(t,t') = i\langle c^\dagger_{\alpha k}(t')d^\dagger_\mu(t)\rangle$ and their equivalent hole versions $\bar{G}^<_{\mu\alpha k}(t,t') = i\langle c_{\alpha k}(t')d^\dagger_\mu(t)\rangle$ and $\bar{F}^<_{\mu\alpha k}(t,t') = i\langle c_{\alpha k}(t')d_\mu(t)\rangle$. With these introduced we see that the current can be written very compactly as

$$\begin{aligned} I_\alpha &= -\frac{e}{2\hbar}\sum_{k\mu}\mathrm{Tr}\left[\begin{pmatrix} G^<_{\mu\alpha k}(0) & \bar{F}^<_{\mu\alpha k}(0)\\ F^<_{\mu\alpha k}(0) & \bar{G}^<_{\mu\alpha k}(0)\end{pmatrix}\begin{pmatrix} t_{\alpha k\mu} & w_{\alpha k\mu}\\ w^*_{\alpha k\mu} & t^*_{\alpha k\mu}\end{pmatrix}\right.\\ &\quad\left.-\begin{pmatrix} t^*_{\alpha k\mu} & w_{\alpha k\mu}\\ w^*_{\alpha k\mu} & t_{\alpha k\mu}\end{pmatrix}\begin{pmatrix} G^<_{\alpha k\mu}(0) & \bar{F}^<_{\alpha k\mu}(0)\\ F^<_{\alpha k\mu}(0) & \bar{G}^<_{\alpha k\mu}(0)\end{pmatrix}\right]\\ &= \frac{e}{2\hbar}\sum_{k\mu}\mathrm{Tr}\left[\mathbf{G}^<_{\mu\alpha k}(0,0)\boldsymbol{\sigma}_z\mathbf{T}_{\alpha k\mu} - \mathbf{T}^\dagger_{\alpha k\mu}\boldsymbol{\sigma}_z\mathbf{G}^<_{\alpha k\mu}(0,0)\right], \end{aligned} \tag{4.24}$$

where we have defined the Nambu Green's functions as

$$\mathbf{G}^<_{\mu\alpha k}(t,t') = \begin{pmatrix} G^<_{\mu\alpha k}(t,t') & \bar{F}^<_{\mu\alpha k}(t,t')\\ F^<_{\mu\alpha k}(t,t') & \bar{G}^<_{\mu\alpha k}(t,t')\end{pmatrix} \tag{4.25}$$

and

$$\mathbf{G}^<_{\alpha k\mu}(t,t') = \begin{pmatrix} G^<_{\alpha k\mu}(t,t') & \bar{F}^<_{\alpha k\mu}(t,t')\\ F^<_{\alpha k\mu}(t,t') & \bar{G}^<_{\alpha k\mu}(t,t')\end{pmatrix}. \tag{4.26}$$

To find expressions for the lesser Green's functions we start with considering their general time-ordered equivalents given by

$$\mathbf{G}^{\mathrm{t}}_{\mu\alpha k}(t,t') = -i\langle \mathrm{T}\begin{Bmatrix} d_\mu(t)c^\dagger_{\alpha k}(t') & d_\mu(t)c_{\alpha k}(t')\\ d^\dagger_\mu(t)c^\dagger_{\alpha k}(t') & d^\dagger_\mu(t)c_{\alpha k}(t')\end{Bmatrix}\rangle \tag{4.27}$$

We now apply the equation of motion technique to obtain closed expressions for the Green's function. For a general time-ordered fermionic Green's function of the form

$$G^{\mathrm{t}}_{A,B}(t,t') = -i\langle \mathrm{T}\{A(t)B(t')\}\rangle = -i\theta(t-t')\langle A(t)B(t')\}\rangle - (-i)\theta(t'-t)\langle B(t')A(t)\rangle \tag{4.28}$$

we have

$$\begin{aligned} i\partial_t G^{\mathrm{t}}_{A,B}(t,t') &= \delta(t-t')\langle A(t)B(t')\rangle + \theta(t-t')\langle \partial_t A(t)B(t')\rangle\\ &\quad + \delta(t'-t)\langle B(t')A(t)\rangle + \theta(t'-t)\langle B(t')\partial_t A(t)\rangle\\ &= \delta(t-t')\langle\{A,B\}(t)\rangle + \langle \mathrm{T}\{\partial_t A(t)B(t')\}\rangle\\ &= \delta(t-t')\langle\{A,B\}(t)\rangle + i\langle \mathrm{T}\{[H,A](t)B(t')\}\rangle \end{aligned} \tag{4.29}$$

Similarly, if we differentiate with respect to t' we have

$$i\partial_{t'} G^{\mathrm{t}}_{A,B}(t,t') = -\delta(t-t')\langle\{A,B\}(t)\rangle + i\langle \mathrm{T}\{A(t)[H,B](t')\}\rangle \tag{4.30}$$

The EOM for the Green's function ((4.27)) is

$$-i\hbar\partial_{t'}\mathbf{G}_{\mu\alpha k}(t,t') = -i\left\langle \mathrm{T}\begin{Bmatrix} d_\mu(t)[H,c^\dagger_{\alpha k}](t') & d_\mu(t)[H,c_{\alpha k}](t')\\ d^\dagger_\mu(t)[H,c^\dagger_{\alpha k}](t') & d^\dagger_\mu(t)[H,c_{\alpha k}](t')\end{Bmatrix}\right\rangle \tag{4.31}$$

We have

$$[H, c_{\alpha k}] = [H_{\mathrm{l}}, c_{\alpha k}] + [H_{\mathrm{T}}, c_{\alpha k}], \quad [H, c^\dagger_{\alpha k}] = [H_{\mathrm{l}}, c^\dagger_{\alpha k}] + [H_{\mathrm{T}}, c^\dagger_{\alpha k}], \tag{4.32}$$

where

$$[H_\alpha, c_{\alpha k}] = \sum_{k'} \varepsilon_{k'} [n_{\alpha k'}, c_{\alpha k}] = -\varepsilon_{\alpha k} c_{\alpha k} \tag{4.33}$$

$$[H_\alpha, c^\dagger_{\alpha k}] = \sum_{k'} \varepsilon_{\alpha k'} [n_{\alpha k'}, c^\dagger_{\alpha k}] = \varepsilon_{\alpha k} c^\dagger_{\alpha k} \tag{4.34}$$

$$\begin{aligned}[H_{\mathrm{t}\alpha}, c_{\alpha k}] = \sum_{kk'\mu} \Big(& t_{\alpha k'\mu} [c^\dagger_{\alpha k'} d_\mu, c_{\alpha k}] + w_{\alpha k'\mu} [c^\dagger_{\alpha k'} d^\dagger_\mu, c_{\alpha k}] \\ & + t^*_{\alpha k'\mu} [c_{\alpha k'} d_\mu, c_{\alpha k}] + w_{\alpha k'\mu} [c_{\alpha k'} d^\dagger_\mu, c_{\alpha k}] \Big)\end{aligned} \tag{4.35}$$

$$= \sum_\mu \left(-t_{\alpha k \mu} d_\mu - w_{\alpha k \mu} d^\dagger_\mu \right) \tag{4.36}$$

$$\begin{aligned}[H_{\mathrm{t},\alpha}, c^\dagger_{\alpha k}] = \sum_{kk'\mu} \Big(& t_{\alpha k'\mu} [c^\dagger_{\alpha k'} d_\mu, c^\dagger_{\alpha k}] + w_{\alpha k'\mu} [c^\dagger_{\alpha k'} d^\dagger_\mu, c^\dagger_{\alpha k}] \\ & + t^*_{\alpha k'\mu} [c_{\alpha k'} d_\mu, c^\dagger_{\alpha k}] + w_{\alpha k'\mu} [c_{\alpha k'} d^\dagger_\mu, c^\dagger_{\alpha k}] \Big)\end{aligned} \tag{4.37}$$

$$= \sum_\mu \left(t^*_{\alpha k \mu} d^\dagger_\mu + w^*_{k\mu} d_\mu \right). \tag{4.38}$$

We then see that the EOM for the Green's function is

$$\begin{aligned}
-i\hbar\partial_{t'} \mathbf{G}_{\mu\alpha k}(t,t') &= -i \left\langle \mathrm{T} \begin{Bmatrix} \varepsilon_{\alpha k} d_\mu(t) c_{\alpha k}(t')^\dagger & -\varepsilon_{\alpha k} d_\mu(t) c_{\alpha k}(t') \\ \varepsilon_{\alpha k} d^\dagger_\mu(t) c^\dagger_{\alpha k}(t') & -\varepsilon_{\alpha k} d^\dagger_\mu(t) c_{\alpha k}(t') \end{Bmatrix} \right\rangle \\
- i \sum_{\mu'} \Bigg\langle T \begin{Bmatrix} t^*_{\alpha k \mu'} d_\mu(t) d^\dagger_{\mu'}(t') + t^*_{\alpha k \mu'} d_\mu(t) d_{\mu'}(t') & -t_{\alpha k \mu'} d_\mu(t) d_{\mu'}(t') - t_{\alpha k \mu'} d_\mu(t) d^\dagger_{\mu'}(t') \\ t^*_{\alpha k \mu'} d^\dagger_\mu(t) d^\dagger_{\mu'}(t') + t^*_{\alpha k \mu'} d^\dagger_\mu(t) d_{\mu'}(t') & -t_{\alpha k \mu'} d^\dagger_\mu(t) d_{\mu'}(t') - t_{\alpha k \mu'} d^\dagger_\mu(t) d^\dagger_{\mu'}(t') \end{Bmatrix} \Bigg\rangle \\
&= \begin{pmatrix} G_{\mu\alpha k}(t,t') & \bar{F}_{\mu\alpha k}(t,t') \\ F_{\mu\alpha k}(t,t') & \bar{G}_{\mu\alpha k}(t,t') \end{pmatrix} \begin{pmatrix} \varepsilon_{\alpha k} & 0 \\ 0 & -\varepsilon_{\alpha k} \end{pmatrix} \\
&\quad + \sum_{\mu'} \begin{pmatrix} G_{\mu\mu'}(t,t') & \bar{F}_{\mu\mu'}(t,t') \\ F_{\mu\mu'}(t,t') & \bar{G}_{\mu\mu'}(t,t') \end{pmatrix} \begin{pmatrix} t^*_{\alpha k \mu'} & -t_{\alpha k \mu'} \\ t^*_{\alpha k \mu'} & -t_{\alpha k \mu'} \end{pmatrix} \\
&= \varepsilon_{\alpha k} \mathbf{G}_{\mu\alpha k}(t,t') \boldsymbol{\sigma}_z + \sum_{\mu'} \mathbf{G}_{\mu\mu'}(t,t') \mathbf{T}^\dagger_{\alpha k, \mu'}
\end{aligned} \tag{4.39}$$

If we consider the time arguments as matrix indices we note that we may write

$$\mathbf{G}_{\mu\alpha k, tt'} (-i\hbar\partial_{t'} - \varepsilon_{\alpha k} \boldsymbol{\sigma}_z) = \mathbf{G}_{\mu\alpha k, tt'} \mathbf{g}^{-1}_{\alpha k, t't'} = \mathbf{G}_{\mu\mu', tt'} \mathbf{T}^\dagger_{\alpha k \mu'}, \tag{4.40}$$

where $\mathbf{g}^{-1}_{\alpha k, tt'} = -i\hbar\partial_{t'} - \varepsilon_{\alpha k}\boldsymbol{\sigma}_z$ is the inverse of the lead free Green's function satisfying the equation of motion $\mathbf{g}^{-1}_{\alpha k, tt''} \mathbf{g}_{\alpha k, t''t'} = \delta_{tt'}$. We can therefore cancel this factor by

multiplication from the right with the lead free Green's function and we get

$$\begin{aligned}\mathbf{G}_{\mu\alpha k}(t,t') &= \mathbf{G}_{\mu\alpha k,tt''}\mathbf{g}^{-1}_{\alpha k,t''t''}\mathbf{g}_{\alpha k,t''t'} = \mathbf{G}_{\mu\mu',tt''}\mathbf{T}^{\dagger}_{\alpha k\mu'}\mathbf{g}_{\alpha k,t''t'} \\ &= \int dt''\, \mathbf{G}_{\mu\alpha k}(t,t'')\mathbf{T}^{\dagger}_{\mu\alpha k}\mathbf{g}_{\alpha k}(t'',t') \end{aligned} \tag{4.41}$$

Since we consider a time-independent problem, the Green's functions only depend on the time difference $t-t'$ and it may thus prove useful to consider the frequency space function which are obtained by Fourier transformation,

$$\mathbf{G}_{\mu\alpha k}(\omega) = \mathbf{G}_{\mu\mu'}(\omega)\mathbf{T}^{\dagger}_{\alpha k\mu'}\mathbf{g}_{\alpha k}(\omega). \tag{4.42}$$

Similarly one finds the equation for the other Green's function

$$i\hbar\partial_t \mathbf{G}_{\alpha k\mu}(t,t') = \varepsilon_{\alpha k}\boldsymbol{\sigma}_z\mathbf{G}_{\alpha k\mu}(t,t') + \sum_{\mu'}\mathbf{T}_{\alpha k\mu'}\mathbf{G}_{\mu'\mu}(t,t'), \tag{4.43}$$

from which we get

$$\mathbf{G}_{\alpha k\mu}(t,t') = \int dt'' \sum_{\mu'}\mathbf{g}_{\alpha k}(t,t'')\mathbf{T}_{\alpha k\mu'}\mathbf{G}_{\mu'\mu}(t'',t'), \tag{4.44}$$

which has the Fourier transform

$$\mathbf{G}_{\alpha k\mu}(\omega) = \sum_{\mu'}\mathbf{g}_{\alpha k}(\omega)\mathbf{T}_{\alpha k\mu'}\mathbf{G}_{\mu'\mu}(\omega). \tag{4.45}$$

Inserting these expressions in the current we have

$$\begin{aligned} I_\alpha &= -\frac{e}{2\hbar}\int\frac{d\omega}{2\pi}\sum_{k\mu\mu'}\mathrm{Tr}\left[\mathbf{G}_{\mu\mu'}(\omega)\mathbf{T}^{\dagger}_{\alpha k\mu'}\mathbf{g}_{\alpha k}(\omega)\boldsymbol{\sigma}_z\mathbf{T}_{\alpha k\mu} - \mathbf{T}^{\dagger}_{\alpha k\mu}\boldsymbol{\sigma}_z\mathbf{g}_{\alpha k}(\omega)\mathbf{T}_{\alpha k\mu'}\mathbf{G}_{\mu'\mu}(\omega)\right]^{<} \\ &= -\frac{e}{2\hbar}\int\frac{d\omega}{2\pi}\sum_{\mu\mu'}\mathrm{Tr}\left[\mathbf{G}_{\mu\mu'}(\omega)(\boldsymbol{\Sigma}^{\mathrm{e}}_{\alpha\mu'\mu}(\omega) - \boldsymbol{\Sigma}^{\mathrm{h}}_{\alpha\mu'\mu}(\omega)) - (\boldsymbol{\Sigma}^{\mathrm{e}}_{\alpha\mu\mu'}(\omega) - \boldsymbol{\Sigma}^{\mathrm{h}}_{\alpha\mu\mu'})\mathbf{G}_{\mu'\mu}(\omega)\right]^{<} \end{aligned} \tag{4.46}$$

where the "lesser" part should be taken of each of the terms before taking the trace. We have also used that

$$\sum_k \mathbf{T}_{\alpha k\mu}\boldsymbol{\sigma}_z\mathbf{g}_{\alpha k}(\omega)\mathbf{T}_{\alpha k\mu'} = \boldsymbol{\Sigma}^{\mathrm{e}}_{\alpha\mu\mu'}(\omega) - \boldsymbol{\Sigma}^{\mathrm{h}}_{\alpha\mu\mu'}(\omega) \tag{4.47}$$

with

$$\begin{aligned}\boldsymbol{\Sigma}^{\mathrm{e}}_{\alpha\mu\mu'}(\omega) &= \sum_k \mathbf{T}^{\dagger}_{\alpha k\mu}\begin{pmatrix} g_{\alpha k}(\omega) & 0 \\ 0 & 0\end{pmatrix}\mathbf{T}_{\alpha k\mu'} = \sum_k \boldsymbol{\Omega}^{\mathrm{e}}_{\alpha k,\mu\mu'}g_{\alpha k}(\omega) \\ \boldsymbol{\Sigma}^{\mathrm{h}}_{\mu\mu'}(\omega) &= \sum_k \mathbf{T}^{\dagger}_{\alpha k\mu}\begin{pmatrix} 0 & 0 \\ 0 & \bar{g}_{\alpha k}(\omega)\end{pmatrix}\mathbf{T}_{\alpha k\mu'} = \sum_k \boldsymbol{\Omega}^{\mathrm{h}}_{\alpha k,\mu\mu'}\bar{g}_{\alpha k}(\omega).\end{aligned}$$

Using the Keldysh contour continuation rule $(AB)^< = A^{\mathrm{R}}B^< + A^<B^{\mathrm{A}}$ the current becomes

$$\begin{aligned} I_\alpha =& -\frac{e}{2\hbar}\int\frac{d\omega}{2\pi}\sum_{\mu\mu'}\mathrm{Tr}\Big[\mathbf{G}^{\mathrm{R}}_{\mu\mu'}\left(\mathbf{\Sigma}^{\mathrm{e}<}_{\alpha\mu'\mu}-\mathbf{\Sigma}^{\mathrm{h}<}_{\alpha\mu'\mu}\right)+\mathbf{G}^<_{\mu\mu'}\left(\mathbf{\Sigma}^{\mathrm{eA}}_{\alpha\mu'\mu}-\mathbf{\Sigma}^{\mathrm{hA}}_{\alpha\mu'\mu}\right)\\ &-\left(\mathbf{\Sigma}^{\mathrm{eR}}_{\alpha\mu\mu'}-\mathbf{\Sigma}^{\mathrm{hR}}_{\alpha\mu\mu'}\right)\mathbf{G}^<_{\mu\mu'}-\left(\mathbf{\Sigma}^{\mathrm{e}<}_{\alpha\mu\mu'}-\mathbf{\Sigma}^{\mathrm{h}<}_{\alpha\mu\mu'}\right)\mathbf{G}^{\mathrm{A}}_{\mu'\mu}\Big]\\ =& -\frac{e}{2\hbar}\int\frac{d\omega}{2\pi}\sum_{\mu\mu'}\mathrm{Tr}\Big[\left(\mathbf{G}^{\mathrm{R}}_{\mu\mu'}-\mathbf{G}^{\mathrm{A}}_{\mu\mu'}\right)\left(\mathbf{\Sigma}^{\mathrm{e}<}_{\alpha\mu'\mu}-\mathbf{\Sigma}^{\mathrm{h}<}_{\alpha\mu'\mu}\right)\\ &-\mathbf{G}^<_{\mu\mu'}\left([\mathbf{\Sigma}^{\mathrm{eR}}_{\alpha\mu\mu'}-\mathbf{\Sigma}^{\mathrm{hR}}_{\alpha\mu\mu'}]-[\mathbf{\Sigma}^{\mathrm{eA}}_{\alpha\mu\mu'}-\mathbf{\Sigma}^{\mathrm{eA}}_{\alpha\mu\mu'}]\right)\Big] \end{aligned} \tag{4.48}$$

The retarded and advanced lead free Green's functions are

$$\begin{aligned} g^{\mathrm{R/A}}_{\alpha k}(\omega) &= \frac{1}{\omega-\varepsilon_{\alpha k}\pm i\eta}\\ \bar{g}^{\mathrm{R/A}}_{\alpha k}(\omega) &= \frac{1}{\omega+\varepsilon_{\alpha k}\pm i\eta} \end{aligned} \tag{4.49}$$

such that we have by use of the usual rules of complex analysis

$$\begin{aligned} \mathbf{\Sigma}^{\mathrm{e,R/A}}_{\alpha\mu\mu'}(\omega) &= \sum_k \mathbf{\Omega}^{\mathrm{e}}_{\alpha k,\mu\mu'}\frac{1}{\omega-\varepsilon_{\alpha k}\pm i\eta} = \mathbf{\Lambda}^{\mathrm{e}}_{\alpha\mu\mu'}(\omega)\mp\frac{i}{2}\mathbf{\Gamma}^{\mathrm{e}}_{\alpha\mu\mu'}(\omega)\\ \mathbf{\Sigma}^{\mathrm{h,R/A}}_{\alpha\mu\mu'}(\omega) &= \sum_k \mathbf{\Omega}^{\mathrm{h}}_{\alpha k,\mu\mu'}\frac{1}{\omega+\varepsilon_{\alpha k}\pm i\eta} = \mathbf{\Lambda}^{\mathrm{h}}_{\alpha\mu\mu'}(\omega)\mp\frac{i}{2}\mathbf{\Gamma}^{\mathrm{h}}_{\alpha\mu\mu'}(\omega), \end{aligned} \tag{4.50}$$

where the linewidths are given by

$$\begin{aligned} \mathbf{\Gamma}^{\mathrm{e}}_{\alpha\mu\mu'}(\omega) &= 2\pi\sum_k \mathbf{\Omega}^{\mathrm{e}}_{\alpha k\mu\mu'}\delta(\omega-\varepsilon_{\alpha k}) = 2\pi\int d\varepsilon_{\alpha k}\,\rho_\alpha(\varepsilon_{\alpha k})\mathbf{\Omega}^{\mathrm{e}}_{\alpha\mu\mu'}(\varepsilon_{\alpha k})\delta(\omega-\varepsilon_{\alpha k})\\ &= 2\pi\rho(\omega)\mathbf{\Omega}^{\mathrm{e}}_{\mu\mu'}(\omega) \end{aligned} \tag{4.51}$$

$$\begin{aligned} \mathbf{\Gamma}^{\mathrm{h}}_{\alpha\mu\mu'}(\omega) &= 2\pi\sum_k \mathbf{\Omega}^{\mathrm{h}}_{\alpha k\mu\mu'}\delta(\omega+\varepsilon_{\alpha k}) = 2\pi\int d\varepsilon_{\alpha k}\,\rho_\alpha(\varepsilon_{\alpha k})\mathbf{\Omega}^{\mathrm{h}}_{\alpha\mu\mu'}(\varepsilon_{\alpha k})\delta(\omega+\varepsilon_{\alpha k})\\ &= 2\pi\rho(-\omega)\mathbf{\Omega}^{\mathrm{h}}_{\mu\mu'}(-\omega), \end{aligned} \tag{4.52}$$

where $\rho_\alpha(\varepsilon)$ is the density of states in the lead. The $\mathbf{\Lambda}$ matrices are given by

$$\mathbf{\Lambda}^{\mathrm{e}}_{\alpha\mu\mu'}(\omega) = \mathcal{P}\int\frac{d\omega'}{2\pi}\frac{\mathbf{\Gamma}^{\mathrm{e}}_{\alpha\mu\mu'}(\omega')}{\omega-\omega'},\quad \mathbf{\Lambda}^{\mathrm{h}}_{\alpha\mu\mu'}(\omega) = \mathcal{P}\int\frac{d\omega'}{2\pi}\frac{\mathbf{\Gamma}^{\mathrm{h}}_{\alpha\mu\mu'}(\omega')}{\omega-\omega'}, \tag{4.53}$$

where $\mathcal{P}$ denotes Cauchy's principal value of the integral. The "lesser" lead free Green's function is

$$g^<_{\alpha k}(t,t') = i\langle c^\dagger_{\alpha k}(t)c_{\alpha k}(t')\rangle_0, \tag{4.54}$$

where $\langle\cdot\rangle_0$ denotes the thermal average at before the systems are brought into contact. Thus we have

$$g^<_{\alpha k}(t,t') = i\langle c^\dagger_{\alpha k}(t)c_{\alpha k}(t')\rangle_0 = \mathrm{i}\mathrm{e}^{-\mathrm{i}\varepsilon_{\alpha k}(t-t')}\langle c^\dagger_{\alpha k}c_{\alpha k}\rangle_0 = if_\alpha(\varepsilon_{\alpha k})\mathrm{e}^{-\mathrm{i}\varepsilon_{\alpha k}(t-t')}, \tag{4.55}$$

where $f_\alpha(\varepsilon)$ is the Fermi-Dirac distribution of the electron levels in the lead. Similarly the free Green's function for holes is given by

$$\bar{g}^<_{\alpha k}(t,t') = i\langle c_{\alpha k}(t)c^\dagger_{\alpha k}(t')\rangle_0 = \mathrm{i}e^{\mathrm{i}\varepsilon_{\alpha k}(t-t')}\langle c^\dagger_{\alpha k}c_{\alpha k}\rangle_0 = i\bar{f}_\alpha(\varepsilon_{\alpha k})e^{\mathrm{i}\varepsilon_{\alpha k}(t-t')}, \tag{4.56}$$

where $\bar{f}_\alpha(\varepsilon) = 1 - f_\alpha(\varepsilon)$ is the distribution function for holes in the lead. Their Fourier transforms are given by

$$\begin{aligned} g^<_{\alpha k}(\omega) &= \mathrm{i}\int d\tau\, e^{\mathrm{i}\tau\omega} f_\alpha(\varepsilon_{\alpha k})e^{-\mathrm{i}\varepsilon_{\alpha k}\tau} = 2\pi\mathrm{i} f_\alpha(\varepsilon_{\alpha k})\delta(\omega-\varepsilon_{\alpha k}) \\ \bar{g}^<_{\alpha k}(\omega) &= \mathrm{i}\int d\tau\, e^{\mathrm{i}\tau\omega} \bar{f}_\alpha(\varepsilon_{\alpha k})e^{\mathrm{i}\varepsilon_{\alpha k}\tau} = 2\pi\mathrm{i} \bar{f}_\alpha(\varepsilon_{\alpha k})\delta(\omega+\varepsilon_{\alpha k}). \end{aligned} \tag{4.57}$$

We then see that the lesser self-energies are

$$\begin{aligned} \mathbf{\Sigma}^{\mathrm{e}<}_{\alpha\mu\mu'}(\omega) &= 2\pi i\sum_k \mathbf{\Omega}^{\mathrm{e}}_{\alpha k,\mu\mu'} f_\alpha(\varepsilon_{\alpha k})\delta(\omega-\varepsilon_{\alpha k}) \\ &= 2\pi i\int d\varepsilon_{\alpha k}\, \rho_\alpha(\varepsilon_{\alpha k})\mathbf{\Omega}^{\mathrm{e}}_{\alpha\mu\mu'}(\varepsilon_{\alpha k}) f_\alpha(\varepsilon_{\alpha k})\delta(\omega-\varepsilon_{\alpha k}) \\ &= 2\pi i\rho_\alpha(\omega)\mathbf{\Omega}^{\mathrm{e}}_{\alpha\mu\mu'}(\omega) f_\alpha(\omega) \\ &= i\mathbf{\Gamma}^{\mathrm{e}}_{\alpha\mu\mu'}(\omega) f_\alpha(\omega) \end{aligned} \tag{4.58}$$

$$\begin{aligned} \mathbf{\Sigma}^{\mathrm{h}<}_{\alpha\mu\mu'}(\omega) &= 2\pi i\sum_k \mathbf{\Omega}^{\mathrm{h}}_{\alpha k,\mu\mu'} \bar{f}_\alpha(\varepsilon_{\alpha k})\delta(\omega+\varepsilon_{\alpha k}) \\ &= 2\pi i\int d\varepsilon_{\alpha k}\, \rho_\alpha(\varepsilon_{\alpha k})\mathbf{\Omega}^{\mathrm{h}}_{\alpha\mu\mu'}(\varepsilon_{\alpha k}) \bar{f}_\alpha(\varepsilon_{\alpha k})\delta(\omega+\varepsilon_{\alpha k}) \\ &= 2\pi i\rho_\alpha(-\omega)\mathbf{\Omega}^{\mathrm{h}}_{\alpha\mu\mu'}(-\omega) \bar{f}_\alpha(-\omega) \\ &= i\mathbf{\Gamma}^{\mathrm{h}}_{\alpha\mu\mu'}(\omega) \bar{f}_\alpha(-\omega) \end{aligned} \tag{4.59}$$

Inserting the expressions for the self-energies in (4.48) the expression for the current takes the form

$$I_\alpha = -\frac{ie}{2\hbar}\int \frac{d\omega}{2\pi}\,\mathrm{tr}\left\{[\mathbf{G}^{\mathrm{R}}_\omega - \mathbf{G}^{\mathrm{A}}_\omega][f_{\alpha,\omega}\mathbf{\Gamma}^{\mathrm{e}}_{\alpha,\omega} - \bar{f}_{\alpha,-\omega}\mathbf{\Gamma}^{\mathrm{h}}_{\alpha,\omega}] + \mathbf{G}^<_\omega[\mathbf{\Gamma}^{\mathrm{e}}_{\alpha,\omega} - \mathbf{\Gamma}^{\mathrm{h}}_{\alpha,\omega}]\right\}. \tag{4.60}$$

This is the final result when we do not have any other knowledge of the system or make any further assumptions or approximations. However in the simple case when we take the electrons in the central system to be non-interacting we can find a closed expression for the central region Green's function. The time-ordered wire Green's function is

$$\mathbf{G}_{\mu\mu'}(t,t') = -i\left\langle \mathrm{T}\begin{Bmatrix} d_\mu(t)d^\dagger_{\mu'}(t') & d_\mu(t)d_{\mu'}(t') \\ d^\dagger_\mu(t)d^\dagger_{\mu'}(t') & d^\dagger_\mu(t)d_{\mu'}(t') \end{Bmatrix}\right\rangle \tag{4.61}$$

and its equation of motion is thus

$$i\hbar\partial_t\mathbf{G}_{\mu\mu'}(t,t') = \delta(t-t')\delta_{\mu\mu'} + i\left\langle \mathrm{T}\begin{Bmatrix} [H,d_\mu](t)d^\dagger_{\mu'}(t') & [H,d_\mu](t)d_{\mu'}(t') \\ [H,d^\dagger_\mu](t)d^\dagger_{\mu'}(t')](t') & [H,d^\dagger_\mu](t)d_{\mu'}(t') \end{Bmatrix}\right\rangle \tag{4.62}$$

The wire operators commute with the lead Hamiltonians so we have

$$[H, d_\mu] = [H_\mathrm{c}, d_\mu] + \sum_\alpha [H_{\mathrm{t},\alpha}, d_\mu] \tag{4.63}$$

$$[H, d_\mu^\dagger] = [H_\mathrm{c}, d_\mu^\dagger] + \sum_\alpha [H_{\mathrm{t},\alpha}, d_\mu^\dagger], \tag{4.64}$$

where

$$[H_\mathrm{c}, d_\mu] = -\varepsilon_\mu d_\mu \tag{4.65}$$

$$[H_\mathrm{c}, d_\mu^\dagger] = \varepsilon_\mu d_\mu^\dagger \tag{4.66}$$

$$[H_{\mathrm{t},\alpha}, d_\mu] = \sum_k (w_{\alpha k\mu} c_{\alpha k}^\dagger - t_{\alpha k\mu}^* c_{\alpha k}) \tag{4.67}$$

$$[H_{\mathrm{t},\alpha}, d_\mu^\dagger] = \sum_k (t_{\alpha k\mu} c_{\alpha k}^\dagger - w_{\alpha k\mu}^* c_{\alpha k}). \tag{4.68}$$

We then have

$$\begin{aligned}
i\hbar\partial_t \mathbf{G}_{\mu\mu'}(t,t') &= \delta(t-t')\delta_{\mu\mu'} - i\left\langle \mathrm{T}\begin{Bmatrix} \varepsilon_\mu d_\mu(t) d_{\mu'}(t') & \varepsilon_\mu d_\mu(t) d_{\mu'}(t') \\ -\varepsilon_\mu d_\mu^\dagger(t) d_{\mu'}^\dagger(t') & -\varepsilon_\mu d_\mu^\dagger(t) d_{\mu'}(t') \end{Bmatrix} \right\rangle \\
&- i\sum_{\alpha k}\left\langle \mathrm{T}\begin{Bmatrix} t_{\alpha k\mu}^* c_{\alpha k}(t) d_{\mu'}^\dagger(t') - w_{\alpha k\mu} c_{\alpha k}^\dagger(t) d_{\mu'}^\dagger(t') & t_{\alpha k\mu}^* c_{\alpha k}(t) d_{\mu'}(t') - w_{\alpha k\mu} c_{\alpha k}^\dagger(t) d_{\mu'}(t') \\ w_{\alpha k\mu}^* c_{\alpha k}(t) d_{\mu'}^\dagger(t') - t_{\alpha k\mu} c_{\alpha k}^\dagger(t) d_{\mu'}^\dagger(t') & w_{\alpha k\mu}^* c_{\alpha k}(t) d_{\mu'}(t') - t_{\alpha k\mu} c_{\alpha k}^\dagger(t) d_{\mu'}(t') \end{Bmatrix} \right\rangle \\
&= \delta(t-t')\delta_{\mu\mu'} + \begin{pmatrix} \varepsilon_\mu & 0 \\ 0 & -\varepsilon_\mu \end{pmatrix} \begin{pmatrix} G_{\mu\mu'}(t,t') & \bar{F}_{\mu\mu'}(t,t') \\ F_{\mu\mu'}(t,t') & \bar{G}_{\mu\mu'}(t,t') \end{pmatrix} \\
&\quad + \sum_{\alpha k} \begin{pmatrix} t_{\alpha k\mu}^* & -w_{\alpha k\mu} \\ w_{\alpha k\mu}^* & -t_{\alpha k\mu} \end{pmatrix} \begin{pmatrix} G_{\alpha k\mu'}(t,t') & \bar{F}_{\alpha k\mu'}(t,t') \\ F_{\alpha k\mu'}(t,t') & \bar{G}_{\alpha k\mu'}(t,t') \end{pmatrix} \\
&= \delta(t-t')\delta_{\mu\mu'} + \varepsilon_\mu \boldsymbol{\sigma}_z \mathbf{G}_{\mu\mu'}(t,t') + \sum_{\alpha k} \mathbf{T}_{\alpha k\mu}^\dagger \mathbf{G}_{\alpha k\mu'}(t,t')
\end{aligned} \tag{4.69}$$

The equation of motion for the free Green's function for the wire is $(i\hbar\partial_t - \varepsilon_\mu \boldsymbol{\sigma}_z)\mathbf{g}_{\mu\mu'}(t,t') = \delta(t-t')\delta_{\mu\mu'}$ so by multiplication by the free Green's function from the left we get

$$\begin{aligned}
\mathbf{G}_{\mu\mu'}(t,t') &= \int dt'' \left[\mathbf{g}_{\mu\mu}(t,t'')\delta(t''-t')\delta_{\mu\mu'} + \sum_{\alpha k} \mathbf{g}_{\mu\mu}(t,t'') \mathbf{T}_{\alpha k\mu}^\dagger \mathbf{G}_{\alpha k\mu'}(t'',t') \right] \\
&= \delta_{\mu\mu'} \mathbf{g}_{\mu\mu'}(t,t') + \sum_{\alpha k} \int dt''\, \mathbf{g}_{\mu\mu}(t,t'') \mathbf{T}_{\alpha k\mu}^\dagger \mathbf{G}_{\alpha k\mu'}(t'',t')
\end{aligned} \tag{4.70}$$

The Fourier transform is

$$\mathbf{G}_{\mu\mu'}(\omega) = \delta_{\mu\mu'} \mathbf{g}_{\mu\mu'}(\omega) + \sum_{\alpha k} \mathbf{g}_{\mu\mu}(\omega) \mathbf{T}_{\alpha k\mu}^\dagger \mathbf{G}_{\alpha k\mu'}(\omega). \tag{4.71}$$

Inserting the expression for the lead-wire Green's function found in (4.45) we arrive at the Dyson equation

$$\begin{aligned}\mathbf{G}_{\mu\mu'}(\omega) &= \delta_{\mu\mu'}\mathbf{g}_{\mu\mu}(\omega) + \sum_{\alpha k,\nu} \mathbf{g}_{\mu\mu}(\omega)\mathbf{T}^{\dagger}_{\alpha k\mu}\mathbf{g}_{\alpha k}(\omega)\mathbf{T}_{k\nu}\mathbf{G}_{\nu\mu'}(\omega) \\ &= \delta_{\mu\mu'}\mathbf{g}_{\mu\mu}(\omega) + \sum_{\alpha,\nu} \mathbf{g}_{\mu\mu}(\omega)\mathbf{\Sigma}_{\alpha\mu\nu}(\omega)\mathbf{G}_{\nu\mu'}(\omega) \end{aligned} \tag{4.72}$$

where the total lead self-energy is given by

$$\mathbf{\Sigma}_{\alpha\mu\mu'}(\omega) = \sum_{k} \mathbf{T}^{\dagger}_{\alpha k\mu}\mathbf{g}_{\alpha k}(\omega)\mathbf{T}_{\alpha k\mu'} = \mathbf{\Sigma}^{\mathrm{e}}_{\alpha\mu\mu'}(\omega) + \mathbf{\Sigma}^{\mathrm{h}}_{\alpha\mu\mu'}(\omega). \tag{4.73}$$

From iterating over the Dyson equation and using that we consider a steady state situation we have [15]

$$\mathbf{G}^{</>}_{\omega} = \sum_{\alpha} \mathbf{G}^{\mathrm{R}}_{\omega}\mathbf{\Sigma}^{</>}_{\alpha,\omega}\mathbf{G}^{\mathrm{A}}_{\omega}, \tag{4.74}$$

which can be used together with the relation between the non-equilibrium Green's functions $G^{\mathrm{R}} - G^{\mathrm{A}} = G^{>} - G^{<}$ to rewrite the expression given by

$$\begin{aligned}\mathbf{G}^{\mathrm{R}}_{\omega} - \mathbf{G}^{\mathrm{A}}_{\omega} = \mathbf{G}^{>}_{\omega} - \mathbf{G}^{<}_{\omega} &= \sum_{\alpha} \mathbf{G}^{\mathrm{R}}_{\omega}(\mathbf{\Sigma}^{>}_{\alpha,\omega} - \mathbf{\Sigma}^{<}_{\alpha,\omega})\mathbf{G}^{\mathrm{A}}_{\omega} \\ &= \sum_{\alpha} \mathbf{G}^{\mathrm{R}}_{\omega}(\mathbf{\Sigma}^{\mathrm{R}}_{\alpha,\omega} - \mathbf{\Sigma}^{\mathrm{A}}_{\alpha,\omega})\mathbf{G}^{\mathrm{A}}_{\omega} = -i\sum_{\alpha} \mathbf{G}^{\mathrm{R}}_{\omega}(\mathbf{\Gamma}^{\mathrm{e}}_{\alpha,\omega} + \mathbf{\Gamma}^{\mathrm{h}}_{\alpha,\omega})\mathbf{G}^{\mathrm{A}}_{\omega} \end{aligned} \tag{4.75}$$

The expression for the current (4.60) can then be simplified to

$$\begin{aligned} I_{\alpha} = &-\frac{e}{2\hbar}\sum_{\alpha'}\int_{-\infty}^{\infty}\frac{d\omega}{2\pi}\,\mathrm{tr}\Big\{\mathbf{G}^{\mathrm{R}}_{\omega}(\mathbf{\Gamma}^{\mathrm{e}}_{\alpha',\omega} + \mathbf{\Gamma}^{\mathrm{h}}_{\alpha',\omega})\mathbf{G}^{\mathrm{A}}(\mathbf{\Gamma}^{\mathrm{e}}_{\alpha,\omega}f_{\alpha,\omega} - \mathbf{\Gamma}^{\mathrm{h}}_{\alpha,\omega}\bar{f}_{\alpha,-\omega}) \\ &-\mathbf{G}^{\mathrm{R}}_{\omega}(\mathbf{\Gamma}^{\mathrm{e}}_{\alpha',\omega}f_{\alpha',\omega} + \mathbf{\Gamma}^{\mathrm{h}}_{\alpha',\omega}\bar{f}_{\alpha',-\omega})\mathbf{G}^{\mathrm{A}}_{\omega}(\mathbf{\Gamma}^{\mathrm{e}}_{\alpha,\omega} - \mathbf{\Gamma}^{\mathrm{h}}_{\alpha,\omega})\Big\} \\ = &-\frac{e}{2\hbar}\sum_{\alpha'}\int_{-\infty}^{\infty}\frac{d\omega}{2\pi}\,\mathrm{tr}\Big\{\mathbf{G}^{\mathrm{R}}_{\omega}\mathbf{\Gamma}^{\mathrm{e}}_{\alpha',\omega}\mathbf{G}^{\mathrm{A}}_{\omega}\mathbf{\Gamma}^{\mathrm{e}}_{\alpha,\omega}(f_{\alpha,\omega} - f_{\alpha',\omega}) - \mathbf{G}^{\mathrm{R}}_{\omega}\mathbf{\Gamma}^{\mathrm{e}}_{\alpha',\omega}\mathbf{G}^{\mathrm{A}}_{\omega}\mathbf{\Gamma}^{\mathrm{h}}_{\alpha,\omega}(\bar{f}_{\alpha,-\omega} - f_{\alpha',\omega}) \\ &+\mathbf{G}^{\mathrm{R}}_{\omega}\mathbf{\Gamma}^{\mathrm{h}}_{\alpha',\omega}\mathbf{G}^{\mathrm{A}}\mathbf{\Gamma}^{\mathrm{e}}_{\alpha,\omega}(f_{\alpha,\omega} - \bar{f}_{\alpha',-\omega}) - \mathbf{G}^{\mathrm{R}}_{\omega}\mathbf{\Gamma}^{\mathrm{h}}_{\alpha',\omega}\mathbf{G}^{\mathrm{A}}_{\omega}\mathbf{\Gamma}^{\mathrm{h}}_{\alpha,\omega}(\bar{f}_{\alpha,-\omega} - \bar{f}_{\alpha',-\omega})\Big\} \\ = &-\frac{e}{2\hbar}\int_{-\infty}^{\infty}\frac{d\omega}{2\pi}\Big[M^{\mathrm{ee}}_{\alpha'\alpha}(\omega)(f_{\alpha,\omega} - f_{\alpha',\omega}) - M^{\mathrm{eh}}_{\alpha'\alpha}(\omega)(\bar{f}_{\alpha,-\omega} - f_{\alpha',\omega}) \\ &+M^{\mathrm{he}}_{\alpha\alpha'}(\omega)(f_{\alpha,\omega} - \bar{f}_{\alpha',-\omega}) - M^{\mathrm{hh}}_{\alpha'\alpha}(\omega)(\bar{f}_{\alpha,-\omega} - \bar{f}_{\alpha',-\omega})\Big], \end{aligned} \tag{4.76}$$

where we have set

$$M^{\mathrm{ee}}_{\alpha\alpha'}(\omega) = \mathrm{tr}\,\mathbf{G}^{\mathrm{R}}_{\omega}\mathbf{\Gamma}^{\mathrm{e}}_{\alpha,\omega}\mathbf{G}^{\mathrm{A}}\mathbf{\Gamma}^{\mathrm{e}}_{\alpha',\omega} \tag{4.77}$$

$$M^{\mathrm{eh}}_{\alpha\alpha'}(\omega) = \mathrm{tr}\,\mathbf{G}^{\mathrm{R}}_{\omega}\mathbf{\Gamma}^{\mathrm{e}}_{\alpha,\omega}\mathbf{G}^{\mathrm{A}}\mathbf{\Gamma}^{\mathrm{h}}_{\alpha',\omega} \tag{4.78}$$

$$M^{\mathrm{he}}_{\alpha\alpha'}(\omega) = \mathrm{tr}\,\mathbf{G}^{\mathrm{R}}_{\omega}\mathbf{\Gamma}^{\mathrm{h}}_{\alpha,\omega}\mathbf{G}^{\mathrm{A}}\mathbf{\Gamma}^{\mathrm{e}}_{\alpha',\omega} \tag{4.79}$$

$$M^{\mathrm{hh}}_{\alpha\alpha'}(\omega) = \mathrm{tr}\,\mathbf{G}^{\mathrm{R}}_{\omega}\mathbf{\Gamma}^{\mathrm{h}}_{\alpha,\omega}\mathbf{G}^{\mathrm{A}}\mathbf{\Gamma}^{\mathrm{h}}_{\alpha',\omega}. \tag{4.80}$$

A closer study (see Appendix A) finds that $M^{\mathrm{hh}}(\omega) = M^{\mathrm{ee}}(-\omega)$ and $M^{\mathrm{he}}(\omega) = M^{\mathrm{eh}}(-\omega)$. In the case where the central region is connected to a left and right lead were the left lead is held at voltage V and the right lead is held at $V = 0$, the current then takes the form

$$I = -\frac{e}{\hbar}\int \frac{d\omega}{2\pi}\left\{M^{\mathrm{ee}}_{\mathrm{LR}}\left[f(\omega+eV) - f(\omega)\right] - M^{\mathrm{eh}}_{\mathrm{LL}}(\omega)\left[f(\omega+eV) - f(\omega-eV)\right]\right\}. \quad (4.81)$$

We see that the first term is just the normal Landauer formula for the current through a non-interacting region. The second term is only non-zero if the central region is superconducting and thus allow for Andreev reflection. If we only consider a single lead coupled to a superconductor the current is simply

$$I = \frac{e}{\hbar}\int \frac{d\omega}{2\pi} M^{\mathrm{eh}}(\omega)\left[f(\omega+eV) - f(\omega-eV)\right]. \quad (4.82)$$

This is the main result of this section and it shows that a non-zero current can flow from the lead into a superconducting system, since the Hamiltonian of the superconducting system does not preserve the electron number. In principle one could modify the superconducting Hamiltonian such that it preserves the total number of Cooper pairs, but we will not consider this here and instead think of the superconductor as being connected to ground as also depicted in Fig. 4.1.

If the energy levels of the superconducting system does not depend on the bias voltage it is easy to derice the differential conductance from Eq. (4.82), which yields

$$\frac{dI}{dV} = -\frac{e^2}{\hbar}\int_{-\infty}^{\infty}\frac{d\omega}{2\pi} M^{\mathrm{ee}}(\omega)\left[\left.\frac{df}{d\epsilon}\right|_{\omega+eV} + \left.\frac{df}{d\epsilon}\right|_{\omega-eV}\right]. \quad (4.83)$$

The Fermi-Dirac distributions merely broadens the conductance spectrum due to fluctutations from finite temperature. At zero temperature the Fermi-Dirac distribution turns into a step function and the differential conductance is simply.

$$\left.\frac{dI}{dV}\right|_{T=0} = \frac{e^2}{h}\left[M^{\mathrm{eh}}(-eV) + M^{\mathrm{eh}}(eV)\right]. \quad (4.84)$$

Though this formula looks simple, to determine $M^{\mathrm{eh}}(\varepsilon)$ one has to determine the Green's functions for the system, which need not be a simple task. In the following we will investigate a few simple cases where the $M^{\mathrm{eh}}(\varepsilon)$ can easily be found analytically.

4.1.1 Wideband limit

If we further make the assumption that the tunnelling coefficients does not depend on the momentum of the lead electron, the so-called wide-band approximation, further simplification is possible. Multiplying the Dyson equation, Eq. 4.72, with the now lead indenpendent tunnelling coefficient matrix $\mathbf{T}_\mu$ we have

$$\begin{aligned}\sum_\mu \mathbf{T}_\mu \mathbf{G}_{\mu\mu'} &= \sum_\mu \mathbf{T}_\mu \mathbf{g}_{\mu\mu}\delta_{\mu\mu'} + \left(\sum_\mu \mathbf{T}_\mu \mathbf{g}_{\mu\mu}\mathbf{T}_\mu^\dagger\right)\left(\sum_k \mathbf{g}_{\alpha k}\right)\left(\sum_\nu \mathbf{T}_\nu \mathbf{G}_{\nu\mu'}\right)\\ &= \mathbf{T}_{\mu'}\mathbf{g}_{\mu'\mu'} + \mathbf{\Sigma}_0\boldsymbol{\rho}_{\mathrm{l}}\left(\nu\mathbf{T}_\nu\mathbf{G}_\nu\right), \end{aligned} \quad (4.85)$$

where we have set

$$\mathbf{\Sigma}_0 = \sum_\mu \mathbf{T}_\mu \mathbf{g}_{\mu\mu} \mathbf{T}_\mu^\dagger, \qquad \boldsymbol{\rho}_\mathrm{l} = \sum_k \mathbf{g}_{\alpha k}. \tag{4.86}$$

We see that we now have a closed equation for the summed product on the left hand site in Eq. (4.85), which can then be inverted to give

$$\sum_\mu \mathbf{T}_\mu \mathbf{G}_{\mu\mu'} = \left(1 - \mathbf{\Sigma}_0 \boldsymbol{\rho}_\mathrm{l}\right)^{-1} \mathbf{T}_{\mu'} \mathbf{g}_{\mu'\mu'}. \tag{4.87}$$

This can then be reinserted in the Dyson equation and the full Green's function is thus given by

$$\mathbf{G}_{\mu\mu'} = \delta_{\mu\mu'} \mathbf{g}_{\mu\mu} + \mathbf{g}_{\mu\mu} \mathbf{T}_\mu^\dagger \boldsymbol{\rho}_\mathrm{l} \left(1 - \mathbf{\Sigma}_0 \boldsymbol{\rho}_\mathrm{l}\right)^{-1} \mathbf{T}_{\mu'} \mathbf{g}_{\mu'\mu'}. \tag{4.88}$$

Using that the linewidth matrix can be written as $\mathbf{\Gamma}^\mathrm{e}_{\mu\mu'} = 2\pi\rho_\mathrm{l}(\omega)\mathbf{T}_\mu^\dagger \mathbf{\Pi}^\mathrm{e} \mathbf{T}_{\mu'}$ where $\mathbf{\Pi} = \left(\begin{smallmatrix} 1 & 0 \\ 0 & 0 \end{smallmatrix}\right)$ we see that the transparency function may be written

$$\begin{aligned} M(\omega) &= \mathrm{tr}\{\mathbf{G}^\mathrm{R}_\omega \mathbf{\Gamma}^\mathrm{e}_\omega \mathbf{G}^\mathbf{A}_\omega \mathbf{\Gamma}^\mathrm{e}\} \\ &= \left(2\pi\rho_\mathrm{l}(\omega)\right)^2 \mathrm{tr}\{\mathbf{T}\mathbf{G}^\mathrm{R}\mathbf{T}^\dagger \mathbf{\Pi}^\mathrm{e} \mathbf{T}\mathbf{G}^\mathrm{R}\mathbf{T}^\dagger \mathbf{\Pi}^\mathrm{e}\} \\ &= \left(2\pi\rho_\mathrm{l}(\omega)\right)^2 \mathrm{tr}\{\mathbf{C}^\mathrm{R} \mathbf{\Pi}^\mathrm{e} \mathbf{C}^\mathrm{A} \mathbf{\Pi}^\mathrm{e}\}, \end{aligned} \tag{4.89}$$

where we have defined

$$\begin{aligned} \mathbf{C} &= \mathbf{T}\mathbf{G}\mathbf{T}^\dagger \\ &= \mathbf{T}\mathbf{g}\left[1 + \mathbf{T}^\dagger \boldsymbol{\rho}_\mathrm{l} (1 - \mathbf{\Sigma}_0 \boldsymbol{\rho}_\mathrm{l})^{-1} \mathbf{T}\mathbf{g}\right] \mathbf{T}^\dagger & (4.90) \\ &= \mathbf{\Sigma}_0 \left[1 + \boldsymbol{\rho}_\mathrm{l} (1 - \mathbf{\Sigma}_0 \boldsymbol{\rho})^{-1} \mathbf{\Sigma}_0\right] & (4.91) \end{aligned}$$

4.2 Analytical investigation

4.2.1 Tunnelling current through a single level

We are now going to apply the formula for the tunnelling current found in previous section on simple system consisting of a lead connected to a system containing a single superconducting level. One can think of this level as a single sub-gap excitation like a Majorana bound state, though we will also treat the case where the level is of normal fermionic of nature.

As the Hamiltonian for the single level system we take

$$H = \epsilon_0 d^\dagger d, \tag{4.92}$$

The d is some linear combination of the underlying electronic operators of the superconductor. In this simplified picture we can take the tunnelling matrix as defined in Eq. (4.13) as

$$\mathbf{T} = t \begin{pmatrix} u & v \\ v & u \end{pmatrix}. \tag{4.93}$$

where t is the tunnelling amplitude and u, v, $u^2+v^2=1$, sets the amount of normal and anormalous tunneling. Taking the density of states in the lead to be constant, $\rho(\varepsilon)=\rho_0$, from Eq. (4.51) and Eq. (4.52) we see that the electron and hole linewidths are given by

$$\mathbf{\Gamma}^{\mathrm{e}}_{\omega} = 2\pi t^2\rho_0 \begin{pmatrix} u & v \\ v & u \end{pmatrix}\begin{pmatrix} 1 & 0 \\ 0 & 0 \end{pmatrix}\begin{pmatrix} u & v \\ v & u \end{pmatrix} = \Gamma \begin{pmatrix} u^2 & uv \\ uv & v^2 \end{pmatrix} \tag{4.94}$$

$$\mathbf{\Gamma}^{\mathrm{h}}_{\omega} = 2\pi t^2\rho_0 \begin{pmatrix} u & v \\ v & u \end{pmatrix}\begin{pmatrix} 0 & 0 \\ 0 & 1 \end{pmatrix}\begin{pmatrix} u & v \\ v & u \end{pmatrix} = \Gamma \begin{pmatrix} v^2 & uv \\ uv & u^2 \end{pmatrix}, \tag{4.95}$$

where we have defined the coupling strength $\Gamma = 2\pi\rho_0 t^2$. The retarded/advanced self-energy is then

$$\mathbf{\Sigma}^{\mathrm{R/A}}_{\omega} = \mp\frac{i}{2}(\mathbf{\Gamma}^{\mathrm{e}}_{\omega}+\mathbf{\Gamma}^{\mathrm{h}}_{\omega}) = -\mathrm{i}\frac{\Gamma}{2}\begin{pmatrix} 1 & 2uv \\ 2uv & 1 \end{pmatrix}. \tag{4.96}$$

To use the formula for the current, Eq. (4.82), we first have to find the full Green's function for the site, $\mathbf{G}(\omega)$. Since we only have a single level this is lucklily easily calculated from the Dyson equation (4.72), which in this special case reads,

$$\mathbf{G}_{\omega} = \mathbf{g}_{\omega} - \mathbf{g}_{\omega}\mathbf{\Sigma}_{\omega}\mathbf{G}_{\omega}. \tag{4.97}$$

This equation is solved for the Green's function and we see that we have

$$\mathbf{G}_{\omega} = \frac{\mathbf{g}_{\omega}}{1-\mathbf{g}_{\omega}\mathbf{\Sigma}_{\omega}} = \frac{1}{\omega - \mathbf{H} - \mathbf{\Sigma}_{\omega}}, \tag{4.98}$$

where we have used that the inverse of the free Green's function is $\mathbf{g}^{-1} = \omega - \mathbf{H}$ with the Nambu Hamiltonian simply being $\mathbf{H} = \left(\begin{smallmatrix} \epsilon_0 & 0 \\ 0 & -\epsilon_0 \end{smallmatrix}\right)$. Inserting the expression for the self energy (4.96), the retarded Green's function is

$$\begin{aligned} \mathbf{G}^{\mathrm{R}}_{\omega} &= \left[\omega - \begin{pmatrix} \epsilon_0 & 0 \\ 0 & -\epsilon_0 \end{pmatrix} + i\frac{\Gamma}{2}\begin{pmatrix} 1 & 2uv \\ 2uv & 1 \end{pmatrix}\right]^{-1} \\ &= \frac{1}{\kappa(\omega)}\begin{pmatrix} \omega-\epsilon+i\Gamma/2 & i\Gamma\rho_{\omega}uv \\ i\Gamma uv & \omega+\epsilon+i\Gamma/2 \end{pmatrix} \end{aligned} \tag{4.99}$$

where

$$\kappa(\omega) = (\omega-\epsilon+i\Gamma/2)(\omega+\epsilon+i\Gamma/2) + \Gamma^2u^2v^2. \tag{4.100}$$

The advanced Greens function is most easily found by taking the Hermitean adjoint, $\mathbf{G}^{\mathrm{A}}_{\omega} = \mathbf{G}^{\mathrm{R}\dagger}_{\omega}$. The anormalous transmission function is found to be

$$\begin{aligned} M^{\mathrm{eh}}(\omega) &= \mathrm{tr}\,\mathbf{G}^{\mathrm{R}}_{\omega}\mathbf{\Gamma}^{\mathrm{e}}\mathbf{G}^{\mathrm{A}}_{\omega}\mathbf{\Gamma}^{\mathrm{h}} \\ &= \frac{4\Gamma^2u^2v^2\omega^2}{|(\omega-\epsilon+i\Gamma/2)(\omega+\epsilon+i\Gamma/2)+\Gamma^2u^2v^2|^2} \end{aligned} \tag{4.101}$$

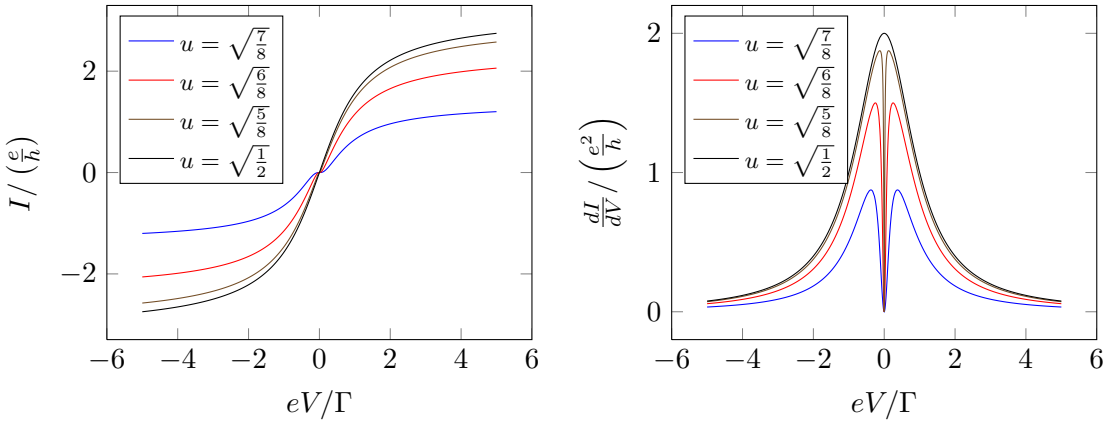

(a) Current

(b) Differential conductace

Figure 4.2: Tunnelling current and differential conductance of a single superconducting level at energy $\epsilon = 0$ for several values of the BCS parameter u.

and we can then proceed to calculate the current (4.82) and conductance (4.84). In Fig. 4.2 we show the current and differential conductance for a single level with zero energy $\epsilon = 0$ for a range of values of the BCS-parameter u. It is clear that for a normal fermionic level with $u = 1$ no anormalous current may flow so the conductance is trivially zero. When the value of u is decreased from 1 the conductance develops two peaks symmetrically around $eV = 0$ with increasing height and smaller separation. The peak height culminates when the quasiparticle level is an equal superposition of particle and hole, ie. $u = \sqrt{1/2}$, and thus is like a Majorana bound state. Here the conductance has a single zero bias peak of height $\frac{2e^2}{h}$ confirming what has been found by many others [21, 10, 23]. Introducing a finite level energy, $\epsilon \neq 0$, has the effect of splitting the conductance peaks for any value of u.

4.3 Numerical Investigations

We now employ the numerical formalism presented in section 3.6 to calculate the conductance of the full wire system in more realistic settings. One of the strengths of the non-equilibrium Green's function approach for obtaining an expression for the current and conductance as developed in section 4.1 is that it is very easily implemented numerically. When writing the BdG tight-binding Hamiltonian (3.85) in an arbitrary basis, then the wire Green's function can simply be calculated as

$$\mathbf{G}^{\mathrm{r}}(\omega) = (\omega\mathbf{1} - \mathbf{H} - \mathbf{\Sigma})^{-1}\,. \tag{4.102}$$

In the wide-band approximation and assuming constant density of states in the lead we have

$$\mathbf{\Sigma}^{\mathrm{R}} = -i\pi\rho_0\mathbf{T}^\dagger\mathbf{T}, \tag{4.103}$$

where $\mathbf{T}$ is the tunnel coupling matrix in the basis chosen. In the following we consider a strictly one-dimensional wire, ie. $N_y = 1$, and assume that the lead is connected to any point x_0 along the wire and that the tunnel coupling decays exponentially away from this point

$$t(x) = t_0 \mathrm{e}^{-\frac{|x-x_0|}{l_\mathrm{t}}}, \tag{4.104}$$

where t_0 is the coupling strength and l_t is a characteristic length. We will usually take $l_\mathrm{t} = 10a = 5\,\mathrm{nm}$ which basically ensures that the lead is only coupled to very few lattice sites. Since we do not calculate the coupling matrix from first principles but instead arbitrarily select representative values, we choose to incorporate the constant density of states of the lead into t_0 by setting $\rho_0 = 1$. This means that when not stated otherwise t_0 really means $t_0/\sqrt{\rho_0}$ and has the dimension of $\sqrt{\text{energy}}$. We may also use the linewidth constant $\Gamma_0 = 2\pi\rho t^2$, which has the dimension of energy.

We now start out study by considering a wire of length $5\,\mu\mathrm{m}$ and with a Rashba parameter of $\alpha_\mathrm{r} = 0.15\,\mathrm{eV\,\AA}$ and the usual effective mass of InSb, $m^* = 0.015 m_\mathrm{e}$, which yields a characteristic spin-orbit energy of $E_\alpha = 44\,\mu\mathrm{eV}$. We let the induced superconducting gap be $200\,\mu\mathrm{eV} \approx 4.5E_\alpha$ and let the lead be connected to the left end, $x_0 = 0$. For simplicity we take the chemical potential to be zero, $\mu = 0$. We have typically calculated the conductance plots at a temperature of 20 mK which broadens and smoothens the peaks somewhat, and serves both to make the results closer to what one would obtain in an experiment which inevitably is done at finite temperature and it also better allows to resolve some very thin resonance peaks. We first calculate the differential conductance for various coupling strengths in the absence of an applied magnetic field with the results shown in Fig. 4.3. We first note that the induced superconducting gap is a clear feature of the conductance plot and thus measuring the conductance at zero Zeeman field can serve as an experimental method of determining the induced gap and thus the wire-SC coupling. Furthermore we note that stronger coupling leads to an increase of the conductance within the induced gap which, as expected, is a result of Andreev reflections. Next we turn on a magnetic field of strength 0.15 T along the wire direction equivalent to a Zeeman field of strength $5E_\alpha$ which should satisfy the topological phase condition $V > \Delta$. As a result, see Fig. 4.4, we see that the conductance plot develops a pronounced zero bias peak due the existence of a Majorana bound state. In the simple picture ignoring bulk states, see Fig. (4.2), we predicted a peak height of $2\frac{e^2}{h}$, but this seems not to be the case here. For weak couplings the zero bias peak height can be much smaller than $2\frac{e^2}{h}$, which is due to the temperature broadening, but for strong couplings the peak height can also be larger than this value.

To investigate how the bulk spectrum and the Majorana zero bias peak changes under the transition from the topologically trivial phase with $V = 0$ to the topologically non-trivial phase where $V > \Delta$, we calculate the conductance for a range of Zeeman field values and the result can be seen in Fig. 4.5. From the plot we clearly see how the minimum gap closes for increasing Zeeman field values until the critical field is reached where a zero bias peak appears and the minimum gap opens again as expected. One interesting thing we note is that the lowest bulk states inside the induced gap

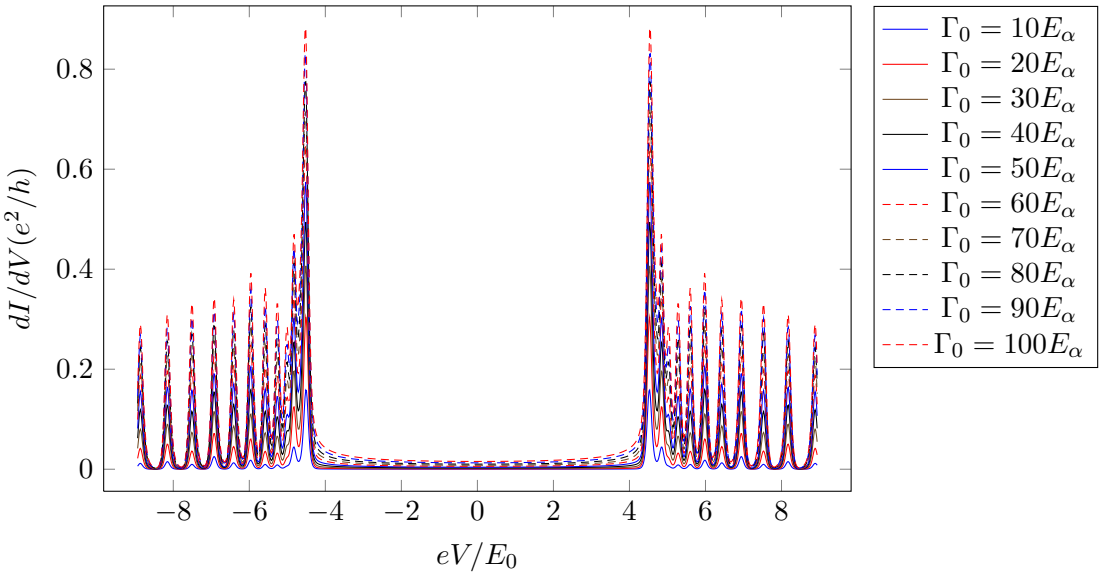

Figure 4.3: Differential conductance for the nanowire when no external magnetic field is applied for various values of the tunnel coefficients $\tilde{t} = \sqrt{\rho_0}t$. The induced superconducting gap of $\sim 4.5E_\alpha$, where $E_\alpha = 44\,\mu\text{eV}$, is clearly observed. A temperature of 20 mK has been used, which has smoothened the peaks somewhat.

$\sim 4.5E_\alpha$ have very small and broadened conductance peaks. As we saw in Fig. 3.10 the lowest bulk states are somewhat localized in the center of the wire and since tunnelling coefficient decays rapidly into the wire, the tunnel matrix elements for these states can be extremely small leading to very sharp conductance peaks which are heavily suppressed by temperature. We can compare this plot with a similar plot obtained in an experiment by the group of Leo Kouwenhoven [30] which is shown in Fig. 4.6.

4.4 Tunnelling into nanowire through a quantum dot

Motivated by a proposal by Flensberg and Leijnse [22] for a way to determine the life-time of a Majorana bound state, we will now consider a normal metal-quantum dot-nanowire junction or N-QD-NW in short. It has already been shown that conductance measurements in this type of setup can be used to exploit the zero-energy nature of the MBS as zero bias peak as in the N-NW case [22, 24, 13], but these considerations have however typically simplified the nanowire system by completely ignoring the the bulk states. Using the numerical methods used so far we can instead calculate the conductance through a quantum dot connected to a nanowire in the more realistic case where bulk states are also taken into account.

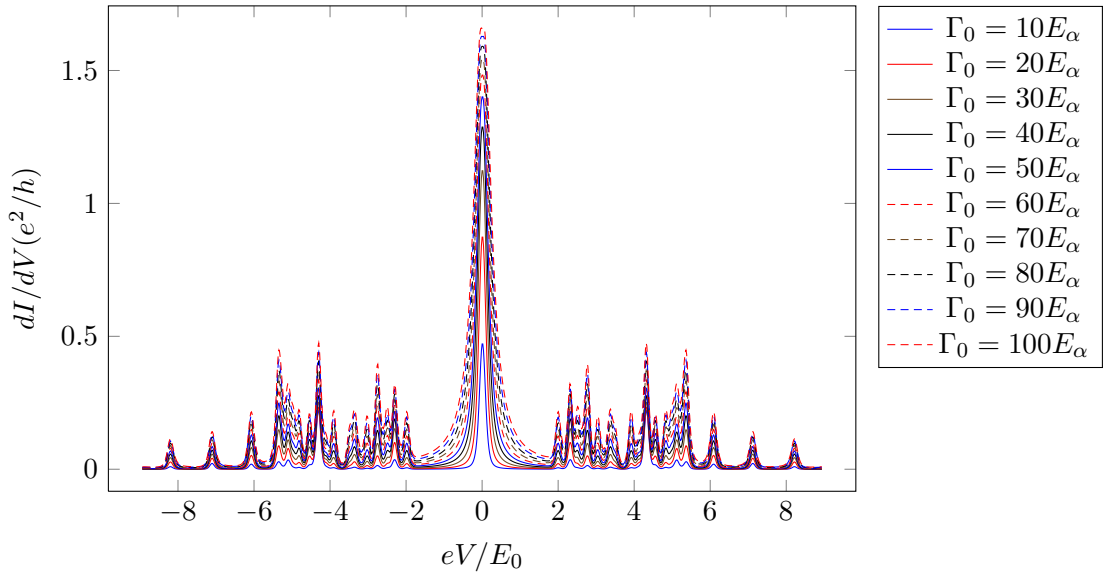

Figure 4.4: A plot of the differential conductance dI/dV of tunnelling into the end of the wire.

4.4.1 Single level connected to quantum dot

As a preliminary we are first going to study a much simpler system, where a quantum dot with a single level is connected to another single level i the nanowire. This is perhaps an oversimplification, but it can be solved analytically and gives a good intuition of what goes on the much more complicated case. The Hamiltonian of the quantum dot-nanowire system is

$$H = H_{\text{qd}} + H_{\text{w}} + H_{\text{qd-w}}, \tag{4.105}$$

where H_{qd} is the Hamiltonian for the quantum dot, H_{w} is the wire Hamiltonian and $H_{\text{qd-w}}$ descibes the tunnelling between the quantum dot and the wire. For simplicity we will assume that the dot is very small so that the level spacing is big and if a strong magnetic field is applied we can effectively describe the quantum dot by a single electronic level coupled capacitatively to the metallic lead, and thus we also disregard the coulombic interactions between the electrons on the dot. The Hamiltonian may thus be written

$$H_{\text{qd}} = (\varepsilon_{\text{qd}} - \mu - \alpha V_{\text{g}} - \beta V_{\text{l}})\, d^\dagger d, \tag{4.106}$$

where ε_{qd} is the level energy, α and β are constants that depend on the capacitance and V_{g} and V_{l} are the voltages of the gate and lead respectively. When measuring the conductance the gate voltage is held constant, so both the dot level and the capacitative energy due to the gate may be included in an effective potential $U_{\text{qd}} = \varepsilon_{\text{qd}} - \mu - \alpha V_{\text{g}}$. We will ignore the bulk states of the nanowire and it can therefore also be approximated by a single fermionic level:

$$H_{\text{w}} = \varepsilon_{\text{w}} a^\dagger a, \tag{4.107}$$

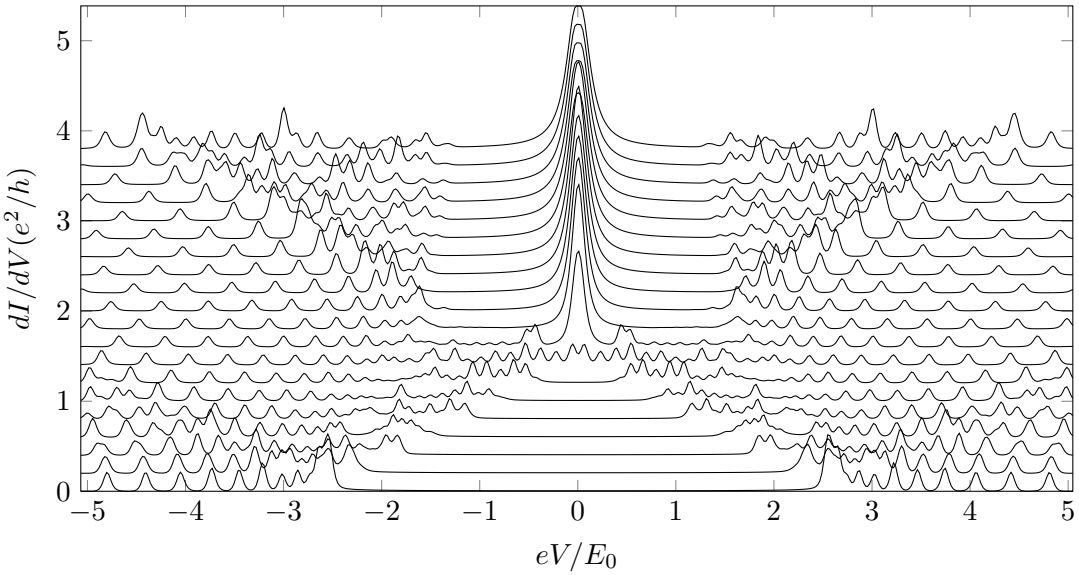

Figure 4.5: A plot of the differential conductance dI/dV of tunnelling into the end of the wire. The tunnel coupling is exponentially decreasing into the wire with peak value of $t_0 = 10E_0$ at the end. Each curve has been offset an amount of 0.1 and represent a different value of the Zeeman field with $V_{\rm zm} = 0$ for the lowest curve and increasing with $?E_0$ upwards. In the calculations a temperature of 20 K has been used.

where a is a Bogoliubov quasiparticle operator. Since the nanowire is effectively superconducting, we must allow for anormalous tunnelling and the tunnelling Hamiltonian therefore takes the form

$$H_{\rm qd-w} = tud^\dagger a + tvd^\dagger a^\dagger + \text{h.c.}, \tag{4.108}$$

where t is the electron tunnelling amplitude and u and v are the electron and hole components of the quasiparticle and satisfy $1 = u^2 + v^2$. Introducing combined Nambu spinors $\Psi = (d, d^\dagger, a, a^\dagger)$ the total Hamiltonian may be written

$$H = \frac{1}{2}\Psi^\dagger H_{\rm BdG}\Psi, \tag{4.109}$$

with the BdG Hamiltonian given by

$$H_{\rm BdG} = \begin{pmatrix} E_{\rm qd} & 0 & tu & tv \\ 0 & -E_{\rm qd} & -tv & -tu \\ tu & -tv & \varepsilon_{\rm w} & 0 \\ tv & -tu & 0 & -\varepsilon_{\rm w} \end{pmatrix} \tag{4.110}$$

where $E_{\rm qd} = U_{\rm qd} - \beta V_{\rm l}$. The coupling between the quantum dot and wire mode causes the the energy levels to shift and to investigate how the shifts depend on the coupling anf the nature of the wire level we solve the BdG Hamiltonian and show the eigenenergies

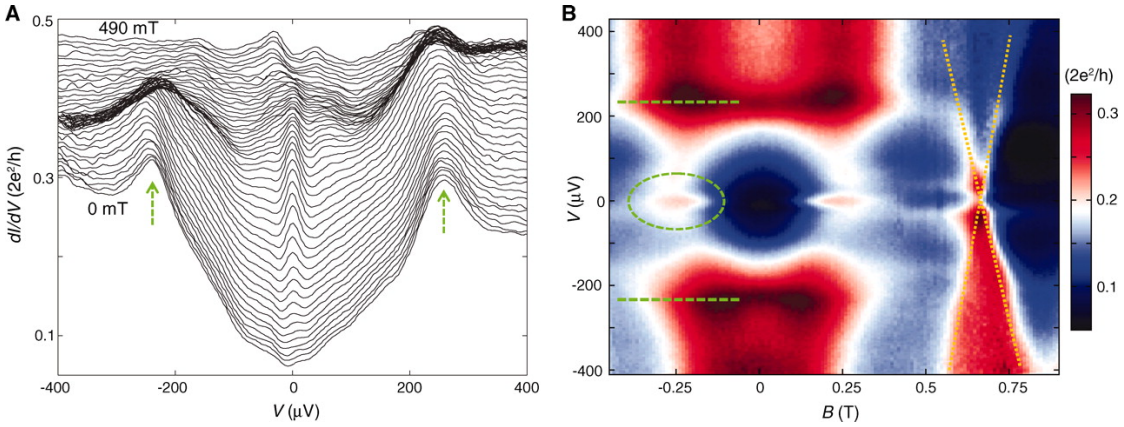

Figure 4.6: Differential conductance for several values of the applied magnetic field obtained in experiment. Image taken from Ref. 30.

as a function of the coupling $\Gamma_w = t^2$ in Fig. 4.7. We see that if the wire is non-superconducting and the level thus is normal fermionic with $u = 1$ and $v = 0$, its energy will decrease to exact zero energy for the coupling strength $\Gamma_w = \varepsilon_w$ are for stronger couplings it will again increase. On the other hand, if the level is chargeless $u = v = \frac{1}{\sqrt{2}}$ the coupling will only force the level towards xero energy. We thus expect that a zero bias conductance peak due to a Majorana mode will stay put for large couplings while that of a normal fermionic mode will split, a phenomenon which potentially can be used to detect Majoranas.

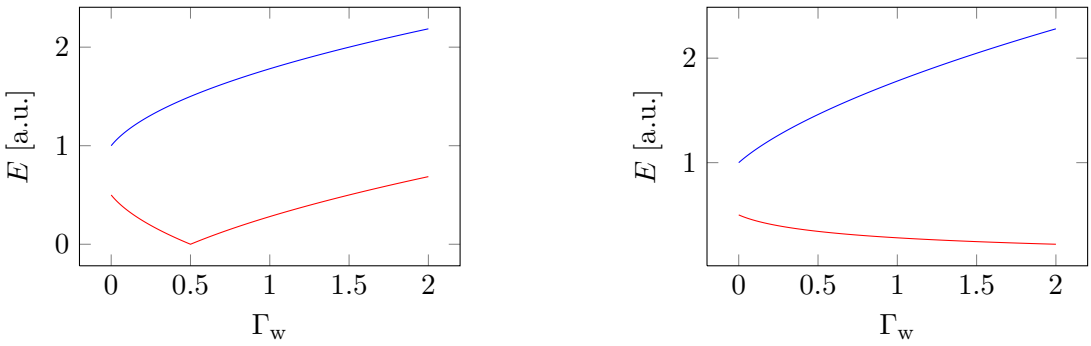

(a) Normal fermion: $u = 1, v = 0$.

(b) Majorana fermion: $u = \frac{1}{\sqrt{2}}, v = \frac{1}{\sqrt{2}}$

Figure 4.7: Energy shifts of the quantum dot and wire level as a function of the tunnel coupling Γ_w when the wire level is either a (a) normal fermion or (b) a Majorana fermion. The wire level has energy ε_w and the quantum dot level is at $\varepsilon_{qd} = 0.5$ in arbitrary unit.

The coupling of the metallic lead and the quantum dot can be described by the

Hamiltonian

$$H_{\mathrm{l-qd}} = \sum_k \left(\nu c_{\alpha k}^\dagger d + \nu d^\dagger c_{\alpha k}\right) = \sum_k \begin{pmatrix} c_{\alpha k}^\dagger & c_{\alpha k} \end{pmatrix} \begin{pmatrix} \nu & 0 & 0 & 0 \\ 0 & -\nu & 0 & 0 \end{pmatrix} \begin{pmatrix} d \\ d^\dagger \\ \gamma \\ \gamma^\dagger \end{pmatrix}. \tag{4.111}$$

We thus see that the electron and hole coupling are given by

$$\mathbf{\Gamma}^{\mathrm{e}} = 2\pi\rho_{\mathrm{l}} \begin{pmatrix} \nu & 0 \\ 0 & -\nu \\ 0 & 0 \\ 0 & 0 \end{pmatrix} \begin{pmatrix} 1 & 0 \\ 0 & 0 \end{pmatrix} \begin{pmatrix} \nu & 0 & 0 & 0 \\ 0 & -\nu & 0 & 0 \end{pmatrix} = \Gamma_0 \begin{pmatrix} 1 & 0 & 0 & 0 \\ 0 & 0 & 0 & 0 \\ 0 & 0 & 0 & 0 \\ 0 & 0 & 0 & 0 \end{pmatrix} \tag{4.112}$$

$$\mathbf{\Gamma}^{\mathrm{h}} = 2\pi\rho_{\mathrm{l}} \begin{pmatrix} \nu & 0 \\ 0 & -\nu \\ 0 & 0 \\ 0 & 0 \end{pmatrix} \begin{pmatrix} 0 & 0 \\ 0 & 1 \end{pmatrix} \begin{pmatrix} \nu & 0 & 0 & 0 \\ 0 & -\nu & 0 & 0 \end{pmatrix} = \Gamma_0 \begin{pmatrix} 0 & 0 & 0 & 0 \\ 0 & 1 & 0 & 0 \\ 0 & 0 & 0 & 0 \\ 0 & 0 & 0 & 0 \end{pmatrix}, \tag{4.113}$$

where we have set $\Gamma_0 = 2\pi\rho_{\mathrm{l}}\nu^2$ with ρ_{l} being the density of states in the lead which is assumed constant. The retarted tunnelling self-energy of the QD-NW system due to the metallic lead is

$$\mathbf{\Sigma}^{\mathrm{r}} = -\frac{\mathrm{i}}{2}\mathbf{\Gamma} = -\frac{\mathrm{i}}{2}(\mathbf{\Gamma}^{\mathrm{e}} + \mathbf{\Gamma}^{\mathrm{h}}) \tag{4.114}$$

and the retarded Nambu space Greens function is given by

$$\mathbf{G}^{\mathrm{r}}(\omega) = (\omega - \mathbf{H}_{\mathrm{BdG}} + \mathbf{\Sigma}^{\mathrm{r}})^{-1} = \left(\omega - \mathbf{H}_{\mathrm{BdG}} - \mathrm{i}\frac{1}{2}\mathbf{\Gamma}\right)^{-1}. \tag{4.115}$$

The matrix inversion can be performed but the general expression, even in this simple case, is rather long so we do not write it here. Inserting the expression for Γ^{e} and the Green's function in the expression for the transmission, Eq. (4.78), we obtain

$$M(\omega) = \mathrm{tr}(\mathbf{G}^{\mathrm{r}}(\omega)\mathbf{\Gamma}^{\mathrm{e}}\mathbf{G}^{\mathrm{a}}(\omega)\mathbf{\Gamma}^{\mathrm{h}}) = \frac{4t^2u^2v^2\Gamma_0^2\omega^2}{|\kappa(\omega)|^2}, \tag{4.116}$$

where

$$\begin{aligned} \kappa(\omega) = &\left(\omega^2 - E_{\mathrm{qd}}^2 - \frac{1}{4}\Gamma_0^2 - \mathrm{i}\omega\Gamma_0\right)(\omega^2 - \varepsilon_{\mathrm{w}}^2) \\ &- t^2(2\omega - \mathrm{i}\omega\Gamma_0) - 2t^2E_{\mathrm{qd}}\varepsilon_{\mathrm{w}}(u^2 - v^2) \end{aligned}. \tag{4.117}$$

The expression (4.116) can now be used to evaluate the current Eq. (4.82) and determine the conductance dI/dV. We first consider the case where both the wire level is situated at some small finite energy $\varepsilon_{\mathrm{w}} = 0$ and take $\epsilon_{\mathrm{qd}} = 0$, $\alpha = \frac{1}{2}$ and $\Gamma_{\mathrm{l}} = \Gamma_{\mathrm{w}} = \frac{1}{2}$. In Fig. 4.8 we see that the conductance has a slightly split zero bias peak corresponding to the superconducting level that stays fixed for all gate voltages. The peak-dip line through the diagram corresponds to the quansum dot level which naturally shows this structure due to its capacitative coupling to the lead. The different level splitting of the Majorna ($u = \sqrt{1/2}$) and other quasiparticle ($u \neq \sqrt{1/2}$) level seen in Fig. 4.7 can be observed in Fig. 4.8b where it leads to an asymmetry in the zero-bias peak along the gate voltage axis.

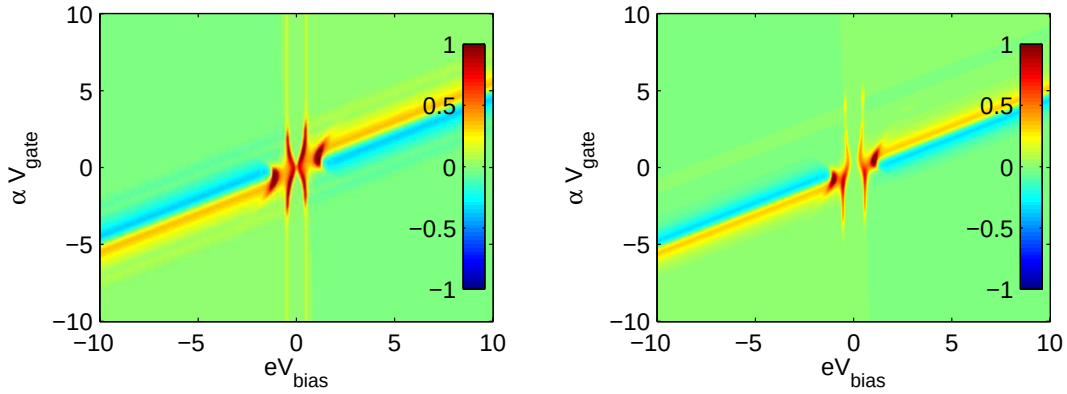

(a) Majorana level $u = \sqrt{1/2}$

(b) Other level $u = \sqrt{7/8}$

Figure 4.8: Tunnelling conductance into a quantum dot connected to a superconducting level as a function of bias and gate voltage. In (a) we have $u = \sqrt{1/2}$ corresponding to a Majorana level and in (b) we have $u = \sqrt{7/8}$. The units of the conductance is e^2/h and energies are measured in arbitrary unit.

4.4.2 Full nanowire system coupled to quantum dot

We now calculate the current through a wire and quantum dot system in a system similar to the one treated above, where the wire however only had a single level. Again we take the dot level to be at zero energy since this only the relative energy between the dot and wire is of importance and this is controlled by the gate voltage. This time we include a Zeeman splitting on the dot since it is situated in a magnetic field. We take the effective Landé g-factor to be that of free electrons, so the Zeeman splitting will be quite small, of order $\sim 1\,\mu\text{eV}$. We take the capacitative coupling of the lead to be $\beta = 2$ and the lead to dot coupling to be $\Gamma_{\text{l-qd}} = E_\alpha$ and the dot to wire coupling to be given by the usual exponentially decaying tunnelling coefficients of initial height $t_0 = 30\sqrt{E_a}$. All other parameters are kept as the ones used previously, ie. $E_\alpha = 44\,\mu\text{eV}$ and an induced gap of $\Delta = 200\,\mu\text{eV} = 4.5E_\alpha$. The results are shown in Fig. 4.9 and we see that qualitatively the conductance is spectrum is not changed much from the single level case. We note that a zero-bias peak is still the most dominant feature and the conductance from bulk states is heavily suppressed. One thing to note is that the height of the zero-bias peak is no longer $2e^2/h$, but in fact far less. This is of course not surprisisng since all current is carried by two tunnelling processes, first from the lead to the dot and then from the dot to the wire and the conductance is thus very sensitive to the two tunnel coupling strengths.

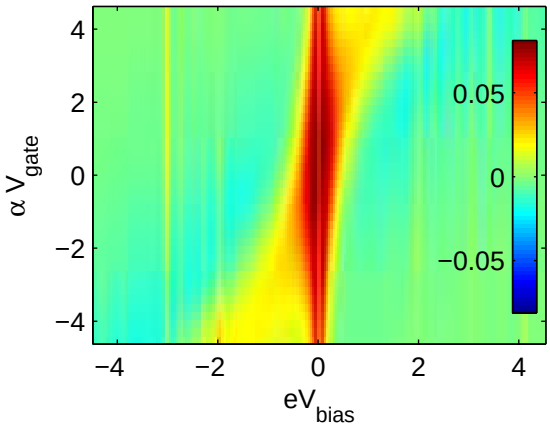

ht

Figure 4.9: Differential conductance through a quantum dot coupled to a nanowire.

Chapter 5

Conclusion

In this thesis we have carried out a theoretical investigation of the special condensed matter phenomenon known as Majorana bound states, that are believed to be useful for realizing robust qubit systems in a solid state quantum computer. As many are interested in the development of a quantum computer this research into Majorana bound states has recieved much interest lately. To understand how this phenomenon can be used to construct a quantum computer, the basics of quantum computing was first reviewed. From that we concluded that it is possible to carry out computations on a quantum system consisting of a set of qubits if one can perform quantum gates, which are elementary unitary transformations on a subset of the qubit states. However, quantum information decohere over time due to the interaction between the qubits and the environment, so in order for quantum computation to be feasible, one has to minimize this interaction.

Secondly we introduced the concept of anyons, which are particles living in a (2+1)-dimensional space-time whose wavefunction, contrary to the fundamental bosonic and fermionic particles, need not acquire a simple factor of ± 1 when two identical particles are physically interchanged. If a system has non-Abelian anyons the groundstate of the system is degenerate and interchanging two such particles may not even change the phase of the wavefunction but change the state within the groundstate manifold. It was noted that the general requirements for the existence of anyonic particles is that the excitations of the system has some non-vanishing gap and that parameters are such that a topological phase is favoured. In this topological phase, the system is said to have topological order, which cannot be characterized by a symmetrybreaking as in the case of normal phase transitions. The concept of anyons was first introduced to describe the Fractional Quantum Hall Effect, but it has been suggested that there are non-Abelian anyons bound to half-quantum vortices on the surface of p-wave superconductors. These quasiparticles would have the property that they are Majorana fermions, which are characterized by being its own antiparticle or hole. It was shown how one could construct qubit systems out of non-Abelian anyons and so also Majorana fermions, which are naturally protected from decoherence since the state of the qubit system is stored in a nonlocal way. Also these kinds of qubits would be less susceptible to unitary errors

introduced while performing quantum gate operations since many gates can be performed by braiding anyonic quasiparticles, which will perform an exact unitary operation on the qubit states. A system using non-Abelian quasiparticles such as Majorana fermions would thus be a strong candidate for a feasible quantum computer.

Next we focused on the concept of Majorana fermions and how they are envisioned to exist in one-dimensional solid-state system which have triplet-pairing superconductivity as first noted by Kitaev. We investigated how a realistic implementation of Kitaev's model could be engineered using heterostructures of semiconducting nanowires with strong Rashba spin-orbit coupling and a conventional s-wave superconductor subject to a sizeable Zeeman field. The low energy physics of this system could be mapped to that of spinless fermions with an effective p-wave pairing symmetry and thus it effectively simulates the Kitaev model. We found the spectrum for bulk excitations in the general case and saw that their gap closes when the parameters fulfilled a special relation. We attributed the gap-closing with a topological phase transition and showed that in the topological phase the system has a degenerate ground state characterized by the existence of Majorana fermions at each end of the wire. We also solved the system numerically in the case of a wire of finite length and we saw that the characteristics from the analytical investigation carried over into the general case, though the degeneracy of the ground state was slightly split.

It would be a remarkable milestone if Majorana fermions was experimentally observed. We studied one of the proposed methods for observing the features of Majorana fermions, namely tunnelling spectroscopy. Since Majorana fermions are a feature of superconducting systems, we needed a method for calculation of the electrical current into such systems, which was then developed using the methods of non-equilibrium Green's functions. We showed that a system with Majorana fermions is charactericed by having a conductance peak of height $\frac{2e^2}{h}$ at zero-bias due to the fact that the Majorana bound state is ensured to be localized at approximately zero energy. In a numerical study we saw that even in the general case the zero-bias peak is a robust feature which only occur when the system parameters satisfy the requirements for the topological phase. We compared the conductance spectrum with that obtained from recent experimental efforts to observe the Majorana bound state and generally remarked that the spectra had some similar features but the scales of the conductance peaks did not match. However we only studied a single band model and the peak height is very dependent on temperature and effective coupling to the level and thus it cannot be verified nor falsified that Majorana fermions has experimentally been observed. In general the existence of Majorana fermions cannot be verified by the observation of a zero-bias conductance peak alone, and the long term goal is to carry out a braid of two Majorana fermions and observe the changes to the system state.

Lastly we considered tunnelling into a Nanowire with Majorana fermions through a quantum dot, which is capacitatively coupled to the lead. We saw that this method should also be a viable way to observe the zero-bias conductance peak of a Majorana bound state. It can possibly also be used to distinguish true Majorana bound states from other states that are not an equal superposition of particles and holes. However,

due to the heavy calculations, a conductance spectrum for the full wire was not obtained by the finishing of this thesis.

We see that Majorana fermions may provide a feasible method for constructing a usable solid state quantum computer. While they can easily be shown to exist theoretically using only single-particle quantum mechanics, no conclusive experimental signature has yes been seen. One could also imagine that many-particle interactions may influence the existence of the Majorana bound state as well as lead to competing features in the conductance spectrum that might be misinterpreteted as signatures of the Majorana bound state, or suppress the real signatures so that they are hard to observe. Much reseach is currently going on to uncover these effects and hopefully many more experiments will soon give a better insight into the system.

Bibliography

[1] Jason Alicea, Yuval Oreg, Gil Refael, Felix von Oppen, and Matthew P. A. Fisher. Non-abelian statistics and topological quantum information processing in 1D wire networks. *Nature Physics*, 7(5):412–417, 2011.

[2] A. F. Andreev. Thermal conductivity of the intermediate state of superconductors. *Zh. Eksperim. i Teor. Fiz.*, 46, 1964.

[3] Daniel Arovas, J. R. Schrieffer, and Frank Wilczek. Fractional statistics and the quantum hall effect. *Physical Review Letters*, 53(7):722–723, August 1984.

[4] C. H. Bennett. Logical reversibility of computation. *IBM Journal of Research and Development*, 17(6):525 –532, November 1973.

[5] G. E. Blonder, M. Tinkham, and T. M. Klapwijk. Transition from metallic to tunneling regimes in superconducting microconstrictions: Excess current, charge imbalance, and supercurrent conversion. *Physical Review B*, 25(7):4515, April 1982.

[6] Henrik Bruus and Karsten Flensberg. *Many-Body Quantum Theory in Condensed Matter Physics: An Introduction*. OUP Oxford, September 2004.

[7] David J. Clarke, Jay D. Sau, and Sumanta Tewari. Majorana fermion exchange in quasi-one-dimensional networks. *Physical Review B*, 84(3):035120, July 2011.

[8] G. Dresselhaus. Spin-orbit coupling effects in zinc blende structures. *Physical Review*, 100(2):580–586, 1955.

[9] J. Eisert and M. M. Wolf. Quantum computing. *arXiv:quant-ph/0401019*, January 2004. In: "Handbook of Nature-Inspired and Innovative Computing" (Springer, New York, 2006).

[10] Karsten Flensberg. Tunneling characteristics of a chain of majorana bound states. *Physical Review B*, 82(18):180516, November 2010.

[11] Liang Fu and C. L. Kane. Superconducting proximity effect and majorana fermions at the surface of a topological insulator. *Physical Review Letters*, 100(9):096407, March 2008.

[12] Liang Fu and C. L. Kane. Josephson current and noise at a superconductor/quantum-spin-hall-insulator/superconductor junction. *Physical Review B*, 79(16):161408, April 2009.

[13] Anatoly Golub, Igor Kuzmenko, and Yshai Avishai. Metal-quantum dot-topological superconductor junction: Kondo correlations and majorana bound states. *arXiv:1105.0289*, May 2011.

[14] David J. Griffiths. *Introduction to Electrodynamics*. Pearson, 3 edition, February 1998.

[15] H. Haug and Antti-Pekka Jauho. *Quantum Kinetics in Transport and Optics of Semiconductors*. Springer-Verlag Berlin and Heidelberg GmbH & Co. K, illustrated edition edition, October 1996.

[16] D. A. Ivanov. Non-abelian statistics of half-quantum vortices in p-wave superconductors. *Physical Review Letters*, 86(2):268, January 2001.

[17] A Yu Kitaev. Unpaired majorana fermions in quantum wires. *Physics-Uspekhi*, 44:131–136, October 2001.

[18] A.Yu. Kitaev. Fault-tolerant quantum computation by anyons. *Annals of Physics*, 303(1):2–30, January 2003. http://arxiv.org/abs/quant-ph/9707021.

[19] Yaacov E. Kraus, Assa Auerbach, H. A. Fertig, and Steven H. Simon. Majorana fermions of a two-dimensional p_x+ip_y superconductor. *Physical Review B*, 79(13):134515, April 2009.

[20] R. Landauer. Irreversibility and heat generation in the computing process. *IBM Journal of Research and Development*, 5(3):183 –191, July 1961.

[21] K. T. Law, Patrick A. Lee, and T. K. Ng. Majorana fermion induced resonant andreev reflection. *Physical Review Letters*, 103(23):237001, December 2009.

[22] Martin Leijnse and Karsten Flensberg. Scheme to measure majorana fermion lifetimes using a quantum dot. *Physical Review B*, 84(14):140501, 2011.

[23] Chien-Hung Lin, Jay D Sau, and S. Das Sarma. Zero bias conductance peak in majorana wires made of semiconductor-superconductor hybrid structures. *arXiv:1204.3085*, April 2012.

[24] Dong E Liu and Harold U Baranger. Detecting a majorana-fermion zero mode using a quantum dot. *arXiv:1107.4338*, July 2011.

[25] Roman M. Lutchyn, Jay D. Sau, and S. Das Sarma. Majorana fermions and a topological phase transition in semiconductor-superconductor heterostructures. *Physical Review Letters*, 105(7):077001, 2010.

[26] Roman M. Lutchyn, Tudor D. Stanescu, and S. Das Sarma. Search for majorana fermions in multiband semiconducting nanowires. *Physical Review Letters*, 106(12):127001, March 2011.

[27] Ettore Majorana. Teoria simmetrica dell'elettrone e del positrone. *Il Nuovo Cimento (1924-1942)*, 14(4):171–184, 1937.

[28] Yigal Meir and Ned S. Wingreen. Landauer formula for the current through an interacting electron region. *Physical Review Letters*, 68(16):2512, April 1992.

[29] Gregory Moore and Nicholas Read. Nonabelions in the fractional quantum hall effect. *Nuclear Physics B*, 360(2-3):362–396, August 1991.

[30] V. Mourik, K. Zuo, S. M Frolov, S. R Plissard, E. P. a. M Bakkers, and L. P Kouwenhoven. Signatures of majorana fermions in hybrid superconductor-semiconductor nanowire devices. *Science*, April 2012.

[31] Chetan Nayak, Steven H. Simon, Ady Stern, Michael Freedman, and Sankar Das Sarma. Non-abelian anyons and topological quantum computation. *Reviews of Modern Physics*, 80(3):1083, 2008.

[32] Yuval Oreg, Gil Refael, and Felix von Oppen. Helical liquids and majorana bound states in quantum wires. *Physical Review Letters*, 105(17):177002, 2010.

[33] Elsa Prada, Pablo San-Jose, and Ramon Aguado. Transport spectroscopy of NS nanowire junctions with majorana fermions. *arXiv:1203.4488*, March 2012.

[34] John Preskill. Fault-tolerant quantum computation. *arXiv:quant-ph/9712048*, December 1997.

[35] John Preskill. Lecture notes for the course on quantum information at caltech, 2004.

[36] N. Read and Dmitry Green. Paired states of fermions in two dimensions with breaking of parity and time-reversal symmetries and the fractional quantum hall effect. *Physical Review B*, 61(15):10267–10297, April 2000.

[37] Jay D. Sau, Roman M. Lutchyn, Sumanta Tewari, and S. Das Sarma. Generic new platform for topological quantum computation using semiconductor heterostructures. *Physical Review Letters*, 104(4):040502, January 2010.

[38] Peter W. Shor. Scheme for reducing decoherence in quantum computer memory. *Physical Review A*, 52(4):R2493–R2496, 1995.

[39] Tudor D. Stanescu, Roman M. Lutchyn, and S. Das Sarma. Majorana fermions in semiconductor nanowires. *Physical Review B*, 84(14):144522, 2011.

[40] Tudor D. Stanescu, Jay D. Sau, Roman M. Lutchyn, and S. Das Sarma. Proximity effect at the superconductor-topological insulator interface. *Physical Review B*, 81(24):241310, June 2010.

[41] Ady Stern. Anyons and the quantum hall effect—A pedagogical review. *Annals of Physics*, 323(1):204–249, January 2008.

[42] Michael Tinkham. *Introduction to Superconductivity*. Dover Publications Inc., 2nd revised edition edition, June 2004.

[43] Xiao-Gang Wen. *Quantum Field Theory of Many-Body Systems: From the Origin of Sound to an Origin of Light and Electrons*. OUP Oxford, reissue edition, September 2007.

[44] Frank Wilczek. Quantum mechanics of fractional-spin particles. *Physical Review Letters*, 49(14):957–959, 1982.

[45] Frank Wilczek. *Fractional Statistics and Anyon Superconductivity*. World Scientific, 1990.

[46] Frank Wilczek. Majorana returns. *Nature Physics*, 5(9):614–618, 2009.

[47] Roland Winkler. *Spin-orbit Coupling Effects in Two-Dimensional Electron and Hole Systems*. Springer, softcover reprint of hardcover 1st ed. 2003 edition, December 2010.

Appendix A

Simplification of expression for the current

In this Appendix the simplification of the expression for the current in (**??**) will proven. We note that the expression contains four terms of the form

$$M^{(\mathrm{e/h})(\mathrm{e/h})}(\omega) = \mathrm{tr}\,\mathbf{G}^{\mathrm{R}}_{\omega}\mathbf{\Gamma}^{\mathrm{e/h}}_{\omega}\mathbf{G}^{\mathrm{A}}_{\omega}\mathbf{\Gamma}^{\mathrm{e/h}}_{\omega}. \tag{A.1}$$

We are now going to show that these terms can be related to one of the other thereby reducing the expression for the current. First we consider the term $M^{\mathrm{ee}}(\omega)$ and using the expression for the linewidth given in (4.51) we see that we have

$$\begin{aligned} M^{\mathrm{ee}}(\omega) &= (2\pi\rho_{\omega})^2\,\mathrm{tr}\,\mathbf{G}^{\mathrm{R}}_{\omega}\mathbf{\Omega}^{\mathrm{e}}_{\omega}\mathbf{G}^{\mathrm{A}}_{\omega}\mathbf{\Omega}^{\mathrm{e}}_{\omega} \\ &= (2\pi\rho_{\omega})^2\,\mathrm{tr}\,\mathbf{G}^{\mathrm{R}}_{\omega}\mathbf{T}^{\dagger}_{\omega}\mathbf{\Pi}^{\mathrm{e}}\mathbf{T}_{\omega}\mathbf{G}^{\mathrm{A}}_{\omega}\mathbf{T}^{\dagger}_{\omega}\mathbf{\Pi}^{\mathrm{e}}\mathbf{T}_{\omega} \\ &= (2\pi\rho_{\omega})^2\,\mathrm{tr}\,\mathbf{T}_{\omega}\mathbf{G}^{\mathrm{R}}_{\omega}\mathbf{T}^{\dagger}_{\omega}\mathbf{\Pi}^{\mathrm{e}}\mathbf{T}_{\omega}\mathbf{G}^{\mathrm{A}}_{\omega}\mathbf{T}^{\dagger}_{\omega}\mathbf{\Pi}^{\mathrm{e}}, \end{aligned} \tag{A.2}$$

where $\Pi^{\mathrm{e}} = \left(\begin{smallmatrix}1&0\\0&0\end{smallmatrix}\right)$ and we have used that the trace is cyclic to move the last $\mathbf{T}_{\omega}$ to the front in the last step. We now let

$$\mathbf{K}_{\omega\pm\pm} = \begin{pmatrix} P_{\omega\pm\pm} & \bar{Q}_{\omega\pm\pm} \\ Q_{\omega\pm\pm} & \bar{P}_{\omega\pm\pm} \end{pmatrix} = \sum_{\mu\nu}\mathbf{T}_{\pm\omega\mu}\mathbf{G}_{\omega\mu\nu}\mathbf{T}^{\dagger}_{\pm\omega\nu}, \tag{A.3}$$

where the $\pm$-subscripts on $\mathbf{K}_{\omega\pm\pm}$ determines the sign of ω on the $\mathbf{T}_{\pm\omega}$ matrices. We see that we then may write

$$\begin{aligned} M^{\mathrm{ee}}(\omega) &= (2\pi\rho_{\omega})^2\,\mathrm{tr}\,\mathbf{K}^{\mathrm{R}}_{\omega++}\mathbf{\Pi}^{\mathrm{e}}\mathbf{K}^{\mathrm{A}}_{\omega++}\mathbf{\Pi}^{\mathrm{e}} \\ &= (2\pi\rho_{\omega})^2\,\mathrm{tr}\left\{\begin{pmatrix} P^{\mathrm{R}}_{\omega++} & \bar{Q}^{\mathrm{R}}_{\omega++} \\ Q^{\mathrm{R}}_{\omega++} & \bar{P}^{\mathrm{R}}_{\omega++} \end{pmatrix}\begin{pmatrix}1&0\\0&0\end{pmatrix}\begin{pmatrix} P^{\mathrm{A}}_{\omega++} & \bar{Q}^{\mathrm{A}}_{\omega++} \\ Q^{\mathrm{A}}_{\omega++} & \bar{P}^{\mathrm{A}}_{\omega++} \end{pmatrix}\begin{pmatrix}1&0\\0&0\end{pmatrix}\right\} \\ &= (2\pi\rho_{\omega})^2 P^{\mathrm{R}}_{\omega++}P^{\mathrm{A}}_{\omega++} \end{aligned} \tag{A.4}$$

Similarly if we insert the expression for the hole linewidth from (4.52) in the expression for the term $M^{\mathrm{hh}}(\omega)$ we get

$$M^{\mathrm{hh}}(\omega) = (2\pi\rho_{-\omega})^2\,\mathrm{tr}\,\mathbf{T}_{-\omega}\mathbf{G}^{\mathrm{R}}_{\omega}\mathbf{T}^{\dagger}_{-\omega}\mathbf{\Pi}^{\mathrm{h}}\mathbf{T}_{-\omega}\mathbf{G}^{\mathrm{A}}_{\omega}\mathbf{T}^{\dagger}_{-\omega}\mathbf{\Pi}^{\mathrm{h}}, \tag{A.5}$$

where $\mathbf{\Pi} = \left(\begin{smallmatrix}0&0\\0&1\end{smallmatrix}\right)$. If we use the above definition of $\mathbf{K}_{\omega\pm\pm}$ we may write

$$\begin{aligned} M^{\mathrm{hh}}(\omega) &= (2\pi\rho_{-\omega})^2\,\mathrm{tr}\,\mathbf{K}^{\mathrm{R}}_{\omega--}\mathbf{\Pi}^{\mathrm{h}}\mathbf{K}^{\mathrm{A}}_{\omega--}\mathbf{\Pi}^{\mathrm{h}} \\ &= (2\pi\rho_{-\omega})^2\,\mathrm{tr}\left\{\begin{pmatrix} P^{\mathrm{R}}_{\omega--} & \bar{Q}^{\mathrm{R}}_{\omega--} \\ Q^{\mathrm{R}}_{\omega--} & \bar{P}^{\mathrm{R}}_{\omega--} \end{pmatrix}\begin{pmatrix}0&0\\0&1\end{pmatrix}\begin{pmatrix} P^{\mathrm{A}}_{\omega--} & \bar{Q}^{\mathrm{A}}_{\omega--} \\ Q^{\mathrm{A}}_{\omega--} & \bar{P}^{\mathrm{A}}_{\omega--} \end{pmatrix}\begin{pmatrix}0&0\\0&1\end{pmatrix}\right\} \\ &= (2\pi\rho_{-\omega})^2 \bar{P}^{\mathrm{R}}_{\omega--}\bar{P}^{\mathrm{A}}_{\omega--} \end{aligned} \tag{A.6}$$

Similarly we find that the other two term are given by

$$\begin{aligned} M^{\mathrm{eh}}(\omega) &= (2\pi)^2 \rho_\omega \rho_{-\omega} \operatorname{tr} \mathbf{K}^{\mathrm{R}}_{\omega -+} \mathbf{\Pi}^{\mathrm{e}} \mathbf{K}^{\mathrm{A}}_{\omega +-} \mathbf{\Pi}^{\mathrm{h}} \\ &= (2\pi)^2 \rho_\omega \rho_{-\omega} \operatorname{tr} \left\{ \begin{pmatrix} P^{\mathrm{R}}_{\omega -+} & \bar{Q}^{\mathrm{R}}_{\omega -+} \\ Q^{\mathrm{R}}_{\omega -+} & \bar{P}^{\mathrm{R}}_{\omega -+} \end{pmatrix} \begin{pmatrix} 1 & 0 \\ 0 & 0 \end{pmatrix} \begin{pmatrix} P^{\mathrm{A}}_{\omega +-} & \bar{Q}^{\mathrm{A}}_{\omega +-} \\ Q^{\mathrm{A}}_{\omega +-} & \bar{P}^{\mathrm{A}}_{\omega +-} \end{pmatrix} \begin{pmatrix} 0 & 0 \\ 0 & 1 \end{pmatrix} \right\} \\ &= (2\pi)^2 \rho_\omega \rho_{-\omega} Q^{\mathrm{R}}_{\omega -+} \bar{Q}^{\mathrm{A}}_{\omega +-} \end{aligned} \tag{A.7}$$

and

$$\begin{aligned} M^{\mathrm{eh}}(\omega) &= (2\pi)^2 \rho_\omega \rho_{-\omega} \operatorname{tr} \mathbf{K}^{\mathrm{R}}_{\omega +-} \mathbf{\Pi}^{\mathrm{h}} \mathbf{K}^{\mathrm{A}}_{\omega -+} \mathbf{\Pi}^{\mathrm{e}} \\ &= (2\pi)^2 \rho_\omega \rho_{-\omega} \operatorname{tr} \left\{ \begin{pmatrix} P^{\mathrm{R}}_{\omega +-} & \bar{Q}^{\mathrm{R}}_{\omega +-} \\ Q^{\mathrm{R}}_{\omega +-} & \bar{P}^{\mathrm{R}}_{\omega +-} \end{pmatrix} \begin{pmatrix} 0 & 0 \\ 0 & 1 \end{pmatrix} \begin{pmatrix} P^{\mathrm{A}}_{\omega -+} & \bar{Q}^{\mathrm{A}}_{\omega -+} \\ Q^{\mathrm{A}}_{\omega -+} & \bar{P}^{\mathrm{A}}_{\omega -+} \end{pmatrix} \begin{pmatrix} 1 & 0 \\ 0 & 0 \end{pmatrix} \right\} \\ &= (2\pi)^2 \rho_\omega \rho_{-\omega} \bar{Q}^{\mathrm{R}}_{\omega +-} Q^{\mathrm{A}}_{\omega -+}. \end{aligned} \tag{A.8}$$

Inserting the expressions for $\mathbf{T}_{\omega,\mu}$ given in Eq. (4.13) in the definition of $\mathbf{K}_{\omega\pm\pm}$ in Eq. (A.3) we see that we have

$$P_{\omega\pm\pm} = \sum_{\mu\nu} \left[t_{\pm\omega\mu} G_{\omega\mu\nu} t^*_{\pm\omega\nu} + t_{\pm\omega\mu} \bar{F}_{\omega\mu\nu} w^*_{\pm\omega\nu} + w_{\pm\omega\mu} F_{\omega\mu\nu} t^*_{\pm\omega\nu} + w_{\pm\omega\mu} \bar{G}_{\omega\mu\nu} w^*_{\pm\omega\nu} \right] \tag{A.9a}$$

$$\bar{P}_{\omega\pm\pm} = \sum_{\mu\nu} \left[w^*_{\pm\omega\mu} G_{\omega\mu\nu} w_{\pm\omega\nu} + w^*_{\pm\omega\mu} \bar{F}_{\omega\mu\nu} t^*_{\pm\omega\nu} + t^*_{\pm\omega\mu} F_{\omega\mu\nu} w_{\pm\omega\nu} + t^*_{\pm\omega\mu} \bar{G}_{\omega\mu\nu} t_{\pm\omega\nu} \right] \tag{A.9b}$$

$$Q_{\omega\pm\pm} = \sum_{\mu\nu} \left[-w^*_{\pm\omega\mu} G_{\omega\mu\nu} t^*_{\pm\omega\nu} - w^*_{\pm\omega\mu} \bar{F}_{\omega\mu\nu} w^*_{\pm\omega\nu} - t^*_{\pm\omega\mu} F_{\omega\mu\nu} t^*_{\pm\omega\nu} - t^*_{\pm\omega\mu} \bar{G}_{\omega\mu\nu} w^*_{\pm\omega\nu} \right] \tag{A.9c}$$

$$\overline{Q}_{\omega\pm\pm} = \sum_{\mu\nu} \left[-t_{\pm\omega\mu} G_{\omega\mu\nu} w_{\pm\omega\nu} - t_{\pm\omega\mu} \bar{F}_{\omega\mu\nu} t_{\pm\omega\nu} - w_{\pm\omega\mu} F_{\omega\mu\nu} w_{\pm\omega\nu} - w_{\pm\omega\mu} \bar{G}_{\omega\mu\nu} t_{\pm\omega\nu} \right]. \tag{A.9d}$$

From the definition of the retarded and advanced Green's function we easily see that

$$G_{\mu\nu}(t,t')^{\mathrm{R}} = -i\theta(t-t')\langle\{d_\mu(t), d^\dagger_\nu(t')\}\rangle = -i\theta(t-t')\langle\{d^\dagger_\nu(t'), d_\mu(t)\}\rangle = -\bar{G}^{\mathrm{A}}_{\nu\mu}(t',t), \tag{A.10}$$

from which it then follows that $G^{\mathrm{R}}_{\mu\nu}(\omega) = -\bar{G}^{(}_{\nu\mu} - \omega)$ and $F^{\mathrm{R}}_{\mu\nu}(\omega) = -F^{\mathrm{A}}_{\nu\mu}(-\omega)$. Similar relations hold for the corresponding hole Green's functions and we then see that for e.g. $P^{\mathrm{R}}_{\omega++}$ we have

$$\begin{aligned} P^{\mathrm{R}}_{\omega++} = &\sum_{\mu\nu} \left[t_{\omega\mu}(-\bar{G}^{\mathrm{A}}_{-\omega\nu\mu}) t^*_{\omega\nu} + t_{\omega\mu}(-\bar{F}^{\mathrm{A}}_{-\omega\nu\mu}) w^*_{\omega\nu} \right. \\ &\left. + w_{\omega\mu}(-F^{\mathrm{A}}_{-\omega\nu\mu}) t^*_{\omega\nu} + w_{\omega\mu}(-G^{\mathrm{A}}_{-\omega\nu\mu}) w^*_{\omega\nu} \right] \\ = &\bar{P}^{\mathrm{A}}_{-\omega++}. \end{aligned} \tag{A.11}$$

One can easily convince one-self that the following general relations hold true,

$$P^{\mathrm{R/A}}_{\omega\pm_1\pm_2} = -\bar{P}^{\mathrm{A/R}}_{-\omega\pm_2\pm_1}, \qquad Q^{\mathrm{R/A}}_{\omega\pm_1\pm_2} = -Q^{\mathrm{A/R}}_{\omega\pm_2\pm_1} \tag{A.12}$$

where the numbers on the subscript $\pm$-indices denote the order of the signs to clarify that these are interchanged. Similar relations also hold for the corresponding hole versions. Using the in the expression for $M^{\mathrm{he}}(\omega)$ in (A.8) we see that we have

$$M^{\mathrm{he}}(\omega) = (2\pi)^2 \rho_\omega \rho_{-\omega} Q^{\mathrm{R}}_{-\omega+-} \bar{Q}^{\mathrm{A}}_{-\omega-+} = M^{\mathrm{eh}}(-\omega), \tag{A.13}$$

where we have used that an overall change of sign on ω also changes the sign of the sign subindices. Taking a look back on the expression for $M^{\mathrm{hh}}(\omega)$ in Eq. (A.6) we note that this may be written

$$M^{\mathrm{hh}}(\omega) = (2\pi\rho_{-\omega})^2 P^{\mathrm{R}}_{-\omega--} P^{\mathrm{A}}_{-\omega--} = M^{\mathrm{ee}}(-\omega) \tag{A.14}$$